PHYTOPLANKTON DYNAMICS IN AN URBANIZING SOUTH TEXAS ESTUARY, CORPUS CHRISTI BAY, TEXAS

A Dissertation

by

SARAH A TOMINACK

BA, University of North Alabama, 2011
MS, The University of West Florida, 2014

Submitted in Partial Fulfillment of the Requirements for the Degree of

DOCTOR OF PHILOSOPHY

in

MARINE BIOLOGY

Texas A&M University-Corpus Christi
Corpus Christi, Texas

December 2021

December 2021

PHYTOPLANKTON DYNAMICS IN AN URBANIZING SOUTH TEXAS ESTUARY, CORPUS CHRISTI BAY, TEXAS

A Dissertation

by

SARAH TOMINACK

This dissertation meets the standards for scope and quality of
Texas A&M University-Corpus Christi and is hereby approved.

Michael S. Wetz, Ph.D.
Chair

Brandi K. Reese, Ph.D.
Committee Member

Kyeong Park, Ph.D.
Committee Member

Antonietta Quigg, Ph.D.
Committee Member

Jim Lee, Ph.D.
Graduate Faculty Representative

December 2021

ABSTRACT

Low inflow estuaries are thought to be susceptible to cultural eutrophication due to lack of flushing and increased residence times, allowing for accumulation of phytoplankton. Corpus Christi Bay is a low inflow estuary located on the south Texas coast that has a rapidly urbanizing watershed and is subject to near annual occurrence of *K. brevis* red tides. Increasing demands for freshwater and a shift to a warmer and drier climate predicted for this region have the potential to further decrease freshwater inflows to the estuary, resulting in decreased nutrient inputs, increased salinity, and increased water residence time. To date, however, there has been little work to quantify patterns in phytoplankton biovolume, community composition, or their environmental drivers. This dissertation provides an assessment of phytoplankton dynamics in Corpus Christi Bay and furthers our understanding of how urbanization and global climate change are likely to impact the estuary.

Results of a two-year field study indicate that phytoplankton biomass in Corpus Christi Bay displayed relationships with nutrients, precipitation, and temperature. Accumulation of phytoplankton biovolume during the spring and summer were limited by the availability of nutrients, whereas hydraulic flushing and decreased temperatures were also important during the fall and winter, respectively. A site located in a man-made canal system demonstrated relatively high phytoplankton biovolume and the occurrence of high biovolume blooms following precipitation-derived nutrient inputs. In contrast, regions closer to freshwater sources demonstrated lower overall phytoplankton biovolume despite relatively high concentrations of precipitation-derived nutrients, likely due to flushing effects. This indicates that projected decreases in precipitation and increases in temperature may create an environment more

susceptible to phytoplankton blooms and earlier timing of the spring bloom. Phytoplankton community composition also varied in relation to nutrients, precipitation, and temperature. Diatoms were dominant during periods of cooler temperatures and higher nutrients, followed by a shift to dinoflagellate and picocyanobacteria dominance as temperatures warmed and nutrients were depleted. Dinoflagellates and picocyanobacteria were also dominant in the man-made canal site, where higher residence times and recycled nutrients were important factors supporting dominance of these groups. Given projections for a drier, warmer climate and increased water residence times, these findings indicate that there is potential for a prolonged increase in mean phytoplankton standing crops and a potential shift to more persistent dominance by dinoflagellates and picocyanobacteria in Corpus Christi Bay.

Nutrient addition bioassays showed that nitrogen was the primary limiting nutrient. In spring, summer, and fall, phytoplankton growth rates increased with nitrogen additions indicating that future increases in the availability of nitrogen due to increased urbanization will influence the accumulation of phytoplankton in Corpus Christi Bay. The short duration of the experiments tended to favor diatoms in comparison to other taxonomic groups. This may indicate that when nutrients are pulsed, as is common in this region due to the flashy nature of rainfall, the Corpus Christi Bay system is buffered against negative impacts of nutrient loading on community composition (i.e., dominance of dinoflagellates and HABs) that have been observed elsewhere.

Lastly, this study quantified *K. brevis* red tide frequency, duration, and environmental drivers. Results show a long-term increase in *K. brevis* frequency in the Nueces Estuary, which correlated with increased salinity and decreased precipitation during non-El Niño periods and the negative phase of the North Atlantic Oscillation. Additionally, duration was inversely related to temperature and wind speed, with fall-like temperatures and calm water conditions conducive to

prolonging red tides. Given projections for warmer and drier conditions in south Texas, these results indicate the potential for continued increases in the occurrence of red tides, a potential shift to occurrence later in the year, and the potential for blooms to extend longer into winter months.

Together, this research improves our understanding of factors driving phytoplankton dynamics in a rapidly urbanizing, low-inflow estuary. Results suggest that Corpus Christi Bay may currently be buffered against the occurrence of large, nutrient-driven phytoplankton blooms due to the opposing influences of nutrient availability and increased flushing (during rain events). Evidence presented here suggests that future changes in climate patterns, such as overall decreased precipitation and warmer temperatures, are likely to result in changes in both the frequency, timing and composition of phytoplankton blooms, and this study provides the basis for additional hypothesis-based studies to address these issues.

DEDICATION

This dissertation is dedicated to my husband who has supported me in innumerable ways on this journey.

TABLE OF CONTENTS

Page

ABSTRACT iv

DEDICATION vii

TABLE OF CONTENTS viii

LIST OF FIGURES xiii

LIST OF TABLES xvi

INTRODUCTION 1

References 10

CHAPTER I: VARIABILITY IN PHYTOPLANKTON BIOVOLUME AND COMMUNITY COMPOSITION IN CORPUS CHRISTI BAY, CORPUS CHRISTI, TX, USA 23

Abstract 23

Introduction 24

Methods 28

Study Area 28

Sampling Sites 29

Field Sampling 29

Laboratory Processing 30

Phytoplankton Enumeration 31

Nutrients 31

Accessory Data Collection 32
Data Analysis 33
Results 36
Environmental Dynamics 36
Phytoplankton Population Dynamics 40
Environmental Drivers of Phytoplankton Dynamics 43
Phytoplankton Biovolume 43
Phytoplankton Community Composition 43
Discussion 43
Environmental Dynamics 45
Phytoplankton Biovolume and Community Composition 46
Future Implications 52
Conclusion 54
References 55
CHAPTER II: PHYTOPLANKTON RESPONSE TO PULSED NITROGEN ADDITIONS FROM NATURAL AND ANTHROPOGENIC SOURCES IN A RAPIDLY URBANIZING, LOW INFLOW ESTUARY (CORPUS CHRISTI BAY, TX, USA) 80
Abstract 80
Introduction 81
Methods 85

Study Site 85
Data Collection 85
Nutrient Source Collection 85
Corpus Christi Bay Water Collection 86
Experimental Design 87
Laboratory Processing 88
Phytoplankton Enumeration 88
Chlorophyll *a* and Nutrient Quantification 89
Data Analysis 90
Growth Rate Calculations 90
Statistical Analyses 90
Results 92
Whole Community Growth Rate Response 95
Treatment Comparisons 95
Major Taxonomic Group Growth Rate Response 97
Summer 97
Fall 97
Winter 98
Spring 98
Discussion 98

Whole Community Growth Rates 99

Major Taxonomic Group Growth Rates 104

Influence of N Sources 109

Conclusion 112

References 113

CHAPTER III: AN ASSESSMENT OF TRENDS IN THE FREQUENCY AND DURATION OF *KARENIA BREVIS* RED TIDE BLOOMS ON THE SOUTH TEXAS COAST 137

Abstract 137

Introduction 138

Methods 141

Accessory Data Collection 141

Statistical Analysis 142

Trends in Bloom Presence/Absence & Relationship with Environmental Factors 142

Trends in bloom duration & relationship with environmental factors 144

Environmental conditions associated with bloom stages 144

Results 145

Validation of the Corpus Christi Caller Times Dataset 145

Trends in bloom presence/absence 147

Trends in bloom duration 148

Environmental conditions associated with bloom stages 148

Discussion 149

Conclusion 155

References 157

CONCLUDING SUMMARY 180

APPENDIX 1 184

LIST OF FIGURES

Page

Figure 1.1: Location of sampling sites throughout Corpus Christi Bay. Corpus Christi is denoted with a star in the inset map. 70

Figure 1.2: PCA plot with sampling events coded by sampling site. Variable abbreviations are as follows, temperature (temp), dissolved oxygen (dox), dissolved organic nitrogen (don), and nitrate + nitrite (nox), phosphate (phos). All other variables are as displayed. 71

Figure 1.3: Principal component scores plotted over time and coded by site to better resolve the spatial variability associated with stochasticity and seasonality.....72

Figure 1.4: Plots of ammonium, NOx, silicate, phosphate, and DON plotted against salinity (a - e) and temperature (f - j) coded by site. 73

Figure 1.5: Boxplots of phytoplankton biovolume (μm^3 mL^{-1}) across sites (a) and seasons (b). Thick line represents median values and outliers are represented by (+). There is a single outlier not shown on these graphs that occurred at Cole Park during the fall of 2016 (10/14/2016) associated with a *K. brevis* red tide. The total biovolume of that event was 1.94 x 10^8 μm^3 mL^{-1}. 74

Figure 1.6: Stacked bar graphs of median phytoplankton biovolume (μm^3 mL^{-1}) coded by major taxonomic group. Panels a and b represent season and site-specific medians. Panel c is site medians across seasons. 74

Figure 1.7: Temporal variability in phytoplankton biovolume (μm^3 mL^{-1}) and major group contribution at all sites studied. Black line represents salinity. At Cole Park, the sampling event with phytoplankton biovolume greater than the scale of the plot was on 10/14/2016 associated with a *K. brevis* red tide. The total biovolume was 1.94 x 10^8 μm^3 mL^{-1}.....75

Figure 2.1: Relative position of Corpus Christi Bay on the Texas coast (a), full view of the Corpus Christi Bay system (b). Site of water collection for bioassays (white square), *in situ* incubation (red square), and locations of nutrient source collections (yellow stars).....125

Figure 2.2: Inorganic nutrient concentrations and ratios over the course of the summer experiment.....126

Figure 2.3: Inorganic nutrient concentrations and ratios over the course of the fall experiment. 127

Figure 2.4: Inorganic nutrient concentrations and ratios over the course of the winter experiment. 128

Figure 2.5: Inorganic nutrient concentrations and ratios over the course of the spring experiment. 129

Figure 2.6: Growth rates calculated from T0 to T48 using community biovolume (μm^3 mL^{-1}) as the response metric. Lowercase letters indicate results from multiple comparison procedures with treatments with different letters indicating significant differences.....130

Figure 2.7: Growth rates calculated from T0 to T48 during the summer bioassay for each major taxonomic group using biovolume (μm^3 mL^{-1}) as the response metric. 130

Figure 2.8: Growth rates calculated from T0 to T48 during the fall bioassay for each major taxonomic group using biovolume (μm^3 mL^{-1}) as the response metric. 131

Figure 2.9: Growth rates calculated from T0 to T48 during the winter bioassay for each major taxonomic group using biovolume (μm^3 mL^{-1}) as the response metric. 131

Figure 2.10: Growth rates calculated from T0 to T48 during the spring bioassay for each major taxonomic group using biovolume (μm^3 mL^{-1}) as the response metric. The runoff treatment was not applied during the spring bioassay.....132

Figure 2.11: Hierarchical clustering (group-average) analysis with biovolume-based community composition across all seasons. Red lines indicate no significant difference between communities (SIMPROF, Primer v7). 132

Figure 3.1: Map of study areas on Texas Gulf of Mexico coastline. (A) location of Nueces Estuary in the Gulf of Mexico (red circle), (B) zoomed in view of the Nueces Estuary and the location of Naval Air Station Corpus Christi (yellow circle), and (C) location of the Nueces Estuary relative to the adjacent coastal zone. The coastal zone segment (purple) extends from the Land Cut in the south to Port O'Connor in the north. 167

Figure 3.2: Comparison of air and water temperature (°C) at Packery Channel in the Nueces Estuary. Data were obtained from https://tidesandcurrents.noaa.gov, station number 8775792, for the time period of August 2012 thru October 2018. 168

Figure 3.3: Red tide duration in the Nueces Estuary plotted against average Fall temperatures (°C). Fall temperatures were calculated as the average of all temperatures recorded in the Texas Parks and Wildlife trawl dataset in the Nueces Estuary from August through November of each year (1982-2015). The red line represents the linear regression model fit. 169

LIST OF TABLES

Page

Table 1.1: Mean and (standard deviation) of salinity and selected nutrient parameters across sites and seasons. Parameters denoted with an asterisk (*) demonstrated a significant interaction between site and season. Superscript letters indicate the results of a one-way ANOVA, with a > b > c > d > e. 76

Table 1.2: Median and (range) of biovolume ($\mu m^3 L^{-1} \times 10^5$) of the four most abundant major taxonomic groups across sites and seasons. Results of one-way Kruskal-Wallis ANOVAs comparing differences among sites and seasons denoted by superscript letters, with the order a > b > c > d. 77

Table 1.3: Environmental variables found to be significantly ($p < 0.05$) related to phytoplankton biovolume based on pairwise Kendall's Tau correlations. Days since rainfall > 0.1 in. is abbreviated as DSR. 78

Table 1.4: Environmental variables found to be significantly ($p < 0.05$) related to diatom, dinoflagellate, picocyanobacteria, and picoeukaryote biovolume based on pairwise Kendall's Tau correlations. Days since rainfall > 0.1 in. is abbreviated as DSR and dissolved oxygen is abbreviated DOx. Italicized rows indicate relatively weak correlations. 79

Table 2.1: Site conditions at time of collection. 133

Table 2.2: Nutrient concentrations at T0 following nutrient additions. NH_4^+ and NOx represent ammonium and nitrate plus nitrite, DIN in the sum of NH_4^+ and NOx, DIP is orthophosphate (PO_4), Si is silicate, and all are in $\mu mol\ L^{-1}$. N added was calculated by mean T0 TDN - mean Initial TDN for each treatment individually. 134

Table 2.3: Initial phytoplankton biovolume ($\mu m^3 L^{-1} \times 10^6$) and (percent contribution) of each major taxonomic group counted. The (-) indicates non-detect. 136
Table 3.1: Fall seasonal average water temperature (°C) ± standard deviation, salinity ± standard deviation, and number of observations for Texas Parks and Wildlife trawl dataset. Seasonal averages are comprised of values from August thru November of each year. 170
Table 3.2: Comparison of red tide duration (days) from newspaper reports with cell counts data from the Texas Health Department (TXHD) and NOAA Harmful Algal Bloom Observation Study (HABSOS) (NOAA National Centers for Environmental Information 2014). A 2000 red tide in the Coastal Zone during the same period as in the newspaper accounts was confirmed by Magaña et al. (2003) and Cheng et al. (2005).....172
Table 3.3: Summary of *Corpus Christi Caller Times* articles. References for published work that corroborates occurrence of red tides prior to 1996 appear in the 'Notes' column along with any unique features of the reporting. 174
Table 3.4: Summary information for the logistic regression of red tide occurrence vs year (year-only model) for each region. 178
Table 3.5: Results of change point analysis (Pettitt's Test), where $p \leq 0.5$ is significant. 178
Table 3.6: Results from final logistic regression model explaining red tide occurrence chosen for the Nueces Estuary.....178
Table 3.7: Summary information for the final three logistic regression models chosen to explain daily presence/absence of *K. brevis* red tides in Nueces Estuary. 179

INTRODUCTION

Estuaries provide important services to local and regional ecosystems and economies, including but not limited to commercial and recreational fisheries and shellfishes, nursery habitat for juveniles of marine species, habitat and food resources for resident and migratory birds, and finally tourism, recreation, human wellbeing and sense of place (Cloern 2001; Barbier et al. 2011). During the past half-century however, urbanization and agriculturalization have increased in coastal watersheds. These land use and land cover changes are often associated with alteration of freshwater inflows, increased nutrient inputs, and changes in nutrient composition (Gillanders and Kingsford 2002; Jordan et al. 2018). These changes, individually or in concert, can lead to degradation of water quality and potential loss of any number of ecosystem services initially provided (Crain et al. 2008; Paerl et al. 2018; Nohe et al. 2020).

Symptoms of declining coastal water quality are often closely related to cultural eutrophication. Eutrophication is defined as an increase in the organic matter supplied to a system (Nixon 1995) whereas the term cultural eutrophication is used here and elsewhere (Hasler 1975; Yamamoto 2003; Burkholder et al. 2008; Smayda 2008; Anderson et al. 2012; Paerl et al. 2018) to make explicit the role of anthropogenic activities, specifically increased nutrient inputs, in the processes driving increased organic matter accumulation. Often the first symptom of cultural eutrophication is an increase in phytoplankton biomass as chlorophyll *a* (Cloern 1999; Paerl 2006; Spatharis et al. 2007; Bricker et al. 2008).

Phytoplankton growth is regulated from the bottom-up by availability of light, macronutrients, and trace elements, and from the top-down by predation, grazing, and viral lysis (Alpine and Cloern 1992; Brussaard 2004; Örnólfsdóttir et al. 2004). For macronutrients, the form that is delivered (i.e., organic vs inorganic), in addition to overall quantity, is important in

determining the magnitude and direction of change in total phytoplankton biomass and taxa-specific biomass (Glibert et al. 2005; Phlips et al. 2011; Cira et al. 2016; van Meerssche and Pinckney 2019). In addition, physical-chemical factors (i.e. temperature, salinity, turbulence, residence time) act to further regulate phytoplankton biomass accumulation (Ferreira et al. 2005; Cloern and Jassby 2008; Paerl and Justić 2013; Cloern 2018). These biotic and abiotic factors, combined with the evolutionary adaptations of different taxa, control phytoplankton biomass and influence the structure of the phytoplankton community (Paerl 1997; Cloern 1999; Ferreira et al. 2005; Paerl et al. 2010).

Many aquatic systems exhibit seasonal fluctuations in phytoplankton biomass with spring blooms being the most common and winter blooms being the least common (Cloern and Jassby 2008). These seasonal patterns in phytoplankton biomass tend to be the most pronounced in regions where seasonal changes in solar insolation, temperature, and rainfall are strong (Gilabert 2001; Cloern and Dufford 2005; Cloern and Jassby 2008; Baek et al. 2015), whereas regions with less variability in these factors (e.g., tropics) are less likely to conform to the stereotypical seasonal patterns (Flint 1984; Bonilla et al. 2005; Phlips et al. 2011). On interannual, decadal, and multi-decadal time scales, phytoplankton biomass can be altered by large-scale climate variability that regulates temperature and/or rainfall such as the El Niño-Southern Oscillation (ENSO), North Atlantic Oscillation (NAO), Atlantic Multi-Decadal Oscillation (AMO), and the Pacific Decadal Oscillation (PDO) among others (Breton et al. 2006; Cloern and Jassby 2010; Paerl et al. 2010; Alheit et al. 2019; Gomez et al. 2019; Phlips et al. 2020). Lastly, the rapid growth of phytoplankton allows them to respond to climatological fluctuations that act at hourly to daily time scales (Cloern and Nichols 1985; Dustan and Pinckney 1989; Odebrecht et al. 2015; Geyer et al. 2018), though the lower frequency of many monitoring studies leaves us with a

limited understanding at this temporal resolution (Glasgow and Burkholder 2000; Zingone et al. 2010; Contreras and Polo 2014; Harvey et al. 2015).

When considering the interactions among factors influencing estuarine phytoplankton growth and biomass, it is important to recognize not only how these factors may influence overall phytoplankton biomass, but how they can affect the structure of phytoplankton communities at different levels of taxonomic resolution as well. Turbulence (stratification), light availability, nutrient quantity and form, and grazing can select for, or against, phytoplankton taxa. Diatoms tend to be favored in cooler environments, well-mixed water columns, and moderate to high nutrient conditions, especially when the dominant form of nitrogen is nitrate (Bonilla et al. 2005; Cloern and Dufford 2005; Suggett et al. 2009; Baek et al. 2015). Diatoms can respond rapidly to increased nutrient and light conditions due to fast growth rates (doubling times < 1 day) and often form spring blooms (Cloern and Dufford 2005; Maier et al. 2012). Dinoflagellates often tend to be favored in warm, stratified waters where motility allows access to both light (surface) and nutrients (lower water column) (de Souza et al. 2014; Nohe et al. 2020). Dinoflagellates prefer reduced nitrogen forms (organic and/or ammonium) and some taxa can sequester phosphorus under replete conditions, though relatively slow growth rates mean that they do not respond to favorable conditions as rapidly as diatoms (Bricker et al. 2008; Paerl and Justić 2013; Glibert et al. 2016; Nohe et al. 2020). Cyanobacteria are favored under warm, calm conditions (Paerl 1988; Paerl and Huisman 2008). Both nitrogen and phosphorus limitation can favor certain groups of cyanobacteria. Some taxa overcome nitrogen limitation through the fixation of atmospheric nitrogen while others can regulate buoyancy and position in the water column for nutrient acquisition (Glibert and Burkholder 2011). Additionally, the small size of the picocyanobacteria such as *Synechoccocus* allows them to utilize nutrients more efficiently at low

ambient concentrations (Paerl 1988; Paerl and Paul 2012; Paerl and Justić 2013). The picocyanobacteria also tend to be inversely correlated with nitrate concentrations (Agawin et al. 2000; Cloern and Jassby 2008; Gaulke et al. 2010; de Souza et al. 2014), indicating that they may be favored by reduced nitrogen forms like dinoflagellates (Glibert et al. 2005; Glibert and Burkholder 2011; Altman and Paerl 2012). Cryptophytes and chlorophytes are also favored by high nutrient conditions like diatoms but prefer reduced forms of nitrogen like dinoflagellates (Cloern and Dufford 2005; Paerl and Justić 2013). These small flagellate groups are capable of exceptionally high growth and can form blooms under high inflow (rapid flushing) conditions, though they are also favored under calm (stratified) conditions (Paerl 2006; Suggett et al. 2009; Paerl and Justić 2013; Baek et al. 2015).

The different environmental and nutrient conditions favoring each of these major groups leads to seasonal succession in many environments, though the actual pattern is specific to the environment type (i.e., river dominated vs lagoonal) as well as location (i.e., high vs low vs mid latitudes) (Cloern 1999; Örnólfsdóttir et al. 2004; Cloern and Jassby 2008; Cloern and Jassby 2010). Chronic (urbanization, nutrient pollution, climate change, etc.) and acute (hurricanes, droughts, chemical spills, etc.) ecosystem perturbations that alter the biotic and abiotic conditions described above can cause shifts in the timing and magnitude of peak biomass and alter patterns of community composition (Piehler et al. 2004; Cloern and Jassby 2010; Paerl et al. 2010; Zingone et al. 2010; Shangguan et al. 2017; Phlips et al. 2020). These perturbations can also result in the occurrence of harmful algal bloom (HAB)-forming taxa that can create an ecosystem-wide cascade of deleterious effects (Piehler et al. 2004; Ferreira et al. 2005; Irigoien et al. 2005; Paerl 2006; Bricker et al. 2008; Smayda 2008; Davidson et al. 2014; Barroso et al. 2018).

Increased nutrient concentrations, altered nutrient form, and altered nutrient ratios are often cited as a major factor in the global proliferation of HABs (Anderson et al. 2002; Anderson et al. 2012; Davidson et al. 2014; Nohe et al. 2020), with HABs considered an important indicator of eutrophication. In some systems the relationship between HABs and eutrophication is clear and direct, though this is not always the case (Anderson et al. 2012). For example, Breton et al. (2006) demonstrated that local climatological effects of the North Atlantic Oscillation played a large role in the distribution of nutrients, nitrate in particular, and subsequent blooms of the HAB former *Phaeocystis* in Belgian coastal waters. In Loch Creran, Scotland, *Alexandrium* blooms occur with no known linkage to anthropogenic activities, as the magnitude of blooms vary across years with no observed variability in nutrient inputs (Davidson et al. 2014). A third example is the consistent lack of a relationship between nutrient concentrations and *Karenia brevis* red tides on the West Florida Shelf (Dixon et al. 2014; Heil et al. 2014). In this instance, Gulf of Mexico circulation patterns have been found to play a large role in the initiation and shoreward transport of these blooms. HAB occurrence without direct linkages to nutrient inputs can be found in other locations and can be linked to many different factors such as the occurrence of tropical storms, changing climate, or transport of HAB cells through ship ballast water (Phlips 2011; Anderson et al. 2012). This lack of a universal relationship between nutrients and HABs supports the need for place-based studies of HAB dynamics and the physical, chemical, and biological factors (other than nutrient availability) influencing bloom initiation, maintenance, and decline.

K. brevis red tides are an ecological and economic concern, causing fish kills, shellfisheries closures, marine mammal and seabird mortality, and respiratory and digestive distress in humans (Aldrich and Wilson 1960; Magaña and Villareal 2006; Maier Brown et al.

2006). Historically, the west coast of Florida experienced more frequent blooms (prior to the mid-1980s) than Texas and as such, most of the initial research has focused on strains isolated there and on associated local environmental conditions. Early studies indicated that low salinity water (< 24) may provide a barrier to red tide dispersal and survival (Rounsefell and Nelson 1966; Steidinger and Ingle 1972; Steidinger 2009). This salinity barrier has been cited for the exclusion of *K. brevis* red tides from Florida estuaries, with prolonged red tides only affecting the estuarine environment under drought conditions (Trebatoski 1988; Buskey 1996). The research focus on the West Florida Shelf has left us with limited understanding of *K. brevis* ecology in coastal bays, where proximity to human population centers as well as nutrient sources are most pronounced. Blooms of *K. brevis* along the Texas coast can enter estuaries from Galveston Bay (Galveston) to South Bay (Brownsville) and maintain biomass for extended periods (Trebatoski 1988; Buskey 1996). Understanding how red tide dynamics in an estuarine setting compared to what is known for open ocean and coastal zone environments will be critical for developing mitigation techniques and/or predictive models for resource managers at the local level.

This dissertation is comprised of three chapters aimed at understanding phytoplankton community dynamics in Corpus Christi Bay, Texas. Corpus Christi Bay is a shallow (~ 3 m, ship channel ~ 15 m), microtidal (~ 0.3 m range), wind-driven (~ 18 kph yearly average) system (Ritter and Montagna 1999; Islam et al. 2014) and comprises the largest portion of the Nueces Estuary. Corpus Christi Bay is located on the semi-arid South Texas coast and is separated from the Gulf of Mexico by Padre Island, with two narrow inlets for water exchange (Packery Channel and Aransas Pass). Corpus Christi Bay hydrodynamics are further influenced by freshwater inflows from the extensively altered Nueces River, with very little riverine inflow reaching the

bay compared to historic conditions. This leads to a relatively long residence time (> 5 mo. – 1 year), pulsed rather than constant nutrient inputs, and a generally well-mixed water column (Ritter and Montagna 1999). The bay is directly bordered by large urban areas in the cities of Corpus Christi, Portland, and Ingleside though much of the watershed is dominated by agriculture (47% cultivated crops). Lastly, Corpus Christi Bay is also susceptible to seasonal hypoxia (Ritter and Montagna 1999; Applebaum et al. 2005) and *Karenia brevis* red tides (Buskey 1996).

Chapter I of this dissertation was designed to characterize spatial and temporal variability in phytoplankton biomass and community structure along an estuarine-nutrient gradient. It was hypothesized that both phytoplankton biomass and community structure would display spatial variability in response to different levels of anthropogenic nutrient inputs. Specifically, regions of greatest nutrient input would support the highest overall biomass (Flint 1984) and a greater proportion of community biovolume attributed to dinoflagellate and cryptophyte taxa (Cloern and Dufford 2005; Burkholder et al. 2008; Davidson et al. 2014). Seasonal fluctuations in temperature, rainfall, and wind were also hypothesized to be important factors influencing phytoplankton biomass, with biomass maxima expected in summer months (Flint 1984; Pennock et al. 1999). These factors, along with nutrient availability, were hypothesized to play a role in seasonal variation in phytoplankton community structure with diatoms playing a large role year-round, and flagellated taxa increasing in abundance in the fall (Holland et al. 1975). To test these hypotheses, a field-based monitoring study was conducted over two years at six different sites. Each of the six sites represent different levels of anthropogenic impact as well as regions within Corpus Christi Bay representing different levels of connectivity with freshwater inflows and the Gulf of Mexico. During the two years of sampling this study captured periods of low and high

riverine inflow, one brief *K. brevis* red tide, and multiple precipitation events with appreciable stormwater runoff. This study is the first in nearly 40 years to explicitly address the variability in phytoplankton biomass, community structure, and driving environmental factors in the Corpus Christi Bay system.

Chapter II of this dissertation builds on Chapter I to quantify the influence of natural and anthropogenic nutrient sources likely available to phytoplankton in Corpus Christi Bay. It was hypothesized that nitrogen additions would increase phytoplankton growth rates relative to a control due to the oligo-mesotrophic status of Corpus Christi Bay and the strong reliance on sporadic inputs of "new" nutrients (Flint 1984). The short duration of experiments combined with the pulsed nutrient delivery would favor faster growing taxa (i.e. diatoms) over slower growing taxa (i.e. dinoflagellates). Additionally, the form of nitrogen present in the different nutrient sources was hypothesized to favor different taxa based on preferences for oxidized (i.e. diatoms) or reduced (i.e. dinoflagellates) forms of nitrogen. Finally, for both whole community and taxa specific responses, it was hypothesized that the initial phytoplankton community would play a role in the responses predicted above. Understanding the magnitude and timing of phytoplankton responses to nutrient inputs throughout the year will lay the groundwork for understanding how estuarine phytoplankton in low inflow systems such as Corpus Christi Bay may be affected under projected nutrient increases resulting from population growth and climate change scenarios.

Chapter III of this dissertation quantified trends in the frequency of occurrence of *K. brevis* red tides and identified factors driving their occurrence as well as duration of blooms on the Texas coast. It was hypothesized that *K. brevis* red tide frequency on the Texas coast has increased due to large-scale environmental changes. Based on what is known about the salinity

preference of *K. brevis* (20-40) (Aldrich and Wilson 1960; Magaña and Villareal 2006; Steidinger 2009; Dixon et al. 2014) and the strong relationships between rainfall and climate oscillations (ENSO, NAO, and PDO) on the Texas coast (Kurtzman and Scanlon 2007; Tolan 2007; Parazoo et al. 2015) it was hypothesized that there would be significant evidence of an association between salinity, one or more climate oscillation indices, and the occurrence of red tides. Further support for this hypothesis can be found in Bugica et al. (2020), where the authors reported evidence of a long-term increase in salinity in the Nueces Estuary. Anecdotal evidence suggests that *K. brevis* red tide demise coincides with frontal passages (Tester and Steidinger 1997; Magaña and Villareal 2006; Vargo 2009). Thus, it was hypothesized that decreased temperature and increased wind speed would be significant explanatory factors of red tide duration and the transition from bloom period to post-bloom period.

These chapters combined fill a knowledge gap in the Corpus Christi Bay system that is a crucial part of defining water quality and freshwater inflow management targets for current and future Coastal Bend communities. Chapter I provides information about the environmental drivers of phytoplankton biovolume and community composition, furthering our understanding of phytoplankton dynamics in urbanizing, low inflow estuaries. This is critical for the assessment of freshwater inflow and nutrient management strategies that may be needed given projections of a warmer, drier climate and continued population growth and urbanization. Chapter II further resolves the role of nutrient source (new vs. internal) and delivery (pulsed vs. chronic) in driving phytoplankton biovolume and community composition. The results here lay the groundwork for future, more targeted, studies aimed at assessing the role of anthropogenic nutrient pollution in driving phytoplankton dynamics. Lastly, Chapter III provides information on the role of freshwater inflows in creating a habitat suitable for *K. brevis* red tides. The findings here indicate

that projected drier conditions may favor an increased occurrence of *K. brevis* red tides and freshwater management plans should include habitat suitability for *K. brevis* in determining minimum inflow guidelines.

References

Agawin, N. S. R., C. M. Duarte, and S. Agustí. 2000. Nutrient and temperature control of the contribution of picoplankton to phytoplankton biomass and production. *Limnology and Oceanography* 45. American Society of Limnology and Oceanography Inc.: 591–600. doi: 10.4319/lo.2000.45.3.0591.

Aldrich, D. v, and W. B. Wilson. 1960. The effect of salinity on growth of Gymnodinium breve Davis. *The Biological Bulletin* 119: 57–64.

Alheit, J., J. Gröger, P. Licandro, I. H. McQuinn, T. Pohlmann, and A. C. Tsikliras. 2019. What happened in the mid-1990s? The coupled ocean-atmosphere processes behind climate-induced ecosystem changes in the Northeast Atlantic and the Mediterranean. *Deep-Sea Research Part II: Topical Studies in Oceanography* 159. Elsevier Ltd: 130–142. doi: 10.1016/j.dsr2.2018.11.011.

Alpine, A. E., and J. E. Cloern. 1992. Trophic interactions and direct physical effects control phytoplankton biomass and production in an estuary. *Limnology and Oceanography* 37: 946–955. doi: 10.4319/lo.1992.37.5.0946.

Altman, J. C., and H. W. Paerl. 2012. Composition of inorganic and organic nutrient sources influences phytoplankton community structure in the New River Estuary, North Carolina. *Aquatic Ecology* 46: 269–282. doi: 10.1007/s10452-012-9398-8.

Anderson, D. M., A. D. Cembella, and G. M. Hallegraeff. 2012. Progress in understanding harmful algal blooms: Paradigm shifts and new technologies for research, monitoring,

and management. *Annual Review of Marine Science*. doi: 10.1146/annurev-marine-120308-081121.

Anderson, D. M., P. M. Glibert, and J. M. Burkholder. 2002. Harmful algal blooms and eutrophication: Nutrient Sources, Composition, and Consequences. *Estuaries* 25: 704–726.

Applebaum, S., P. A. Montagna, and C. Ritter. 2005. Status and trends of dissolved oxygen in Corpus Christi Bay, Texas, U.S.A. *Environmental Monitoring and Assessment* 107: 297–311. doi: 10.1007/s10661-005-3111-5.

Baek, S. H., D. Kim, M. Son, S. M. Yun, and Y. O. Kim. 2015. Seasonal distribution of phytoplankton assemblages and nutrient-enriched bioassays as indicators of nutrient limitation of phytoplankton growth in Gwangyang Bay, Korea. *Estuarine, Coastal and Shelf Science* 163. Academic Press: 265–278. doi: 10.1016/j.ecss.2014.12.035.

Barbier, E. B., S. D. Hacker, C. Kennedy, E. W. Koch, A. C. Stier, and B. R. Silliman. 2011. The value of estuarine and coastal ecosystem services. *Ecological Monographs* 81: 169–193. doi: 10.1890/10-1510.1.

Barroso, H. de S., T. C. L. Tavares, M. de O. Soares, T. M. Garcia, B. Rozendo, A. S. C. Vieira, P. B. Viana, et al. 2018. Intra-annual variability of phytoplankton biomass and nutrients in a tropical estuary during a severe drought. *Estuarine, Coastal and Shelf Science* 213. Academic Press: 283–293. doi: 10.1016/j.ecss.2018.08.023.

Bonilla, S., D. Conde, L. Aubriot, and M. D. C. Pérez. 2005. Influence of hydrology on phytoplankton species composition and life strategies in a subtropical coastal lagoon periodically connected with the Atlantic Ocean. *Estuaries* 28: 884–895. doi: 10.1007/BF02696017.

Breton, E., V. Rousseau, J. Y. Parent, J. Ozer, and C. Lancelot. 2006. Hydroclimatic modulation of diatom/Phaeocystis blooms in nutrient-enriched Belgian coastal waters (North Sea). *Limnology and Oceanography* 51: 1401–1409. doi: 10.4319/lo.2006.51.3.1401.

Bricker, S. B., B. Longstaff, W. Dennison, A. Jones, K. Boicourt, C. Wicks, and J. Woerner. 2008. Effects of nutrient enrichment in the nation's estuaries: A decade of change. *Harmful Algae* 8: 21–32. doi: 10.1016/j.hal.2008.08.028.

Brussaard, C. P. D. 2004. Viral Control of Phytoplankton Population--a Review. *Journal of Eukaryotic Microbiology* 51: 125–138. doi: 10.1111/j.1550-7408.2005.000vol-cont.x.

Bugica, K., B. Sterba-Boatwright, and M. S. Wetz. 2020. Water quality trends in Texas estuaries. *Marine Pollution Bulletin* 152. Elsevier Ltd. doi: 10.1016/j.marpolbul.2020.110903.

Burkholder, J. A. M., P. M. Glibert, and H. M. Skelton. 2008. Mixotrophy, a major mode of nutrition for harmful algal species in eutrophic waters. *Harmful Algae* 8: 77–93. doi: 10.1016/j.hal.2008.08.010.

Buskey, E. J. 1996. Current Status and Historical Trends of Brown Tide and Red Tide Phytoplankton Blooms in the Corpus Christi Bay National Estuary Program Study Area *Corpus Christi Bay National Estuary Program CCBNEP-07* •. Austin, Texas.

Cira, E. K., H. W. Paerl, and M. S. Wetz. 2016. Effects of nitrogen availability and form on phytoplankton growth in a eutrophied estuary (Neuse River Estuary, NC, USA). Edited by Christopher J. Gobler. *PLoS ONE* 11. Public Library of Science: e0160663. doi: 10.1371/journal.pone.0160663.

Cloern, J. E. 1999. The relative importance of light and nutrient limitation of phytoplankton growth: A simple index of coastal ecosystem sensitivity to nutrient enrichment. *Aquatic Ecology* 33: 3–19.

Cloern, J. E. 2001. Our evolving conceptual model of the coastal eutrophication problem. *Marine Ecology Progress Series* 210: 223–253. doi: 10.3354/meps210223.

Cloern, J. E. 2018. Why large cells dominate estuarine phytoplankton. *Limnology and Oceanography* 63: S392–S409. doi: 10.1002/lno.10749.

Cloern, J. E., and R. Dufford. 2005. Phytoplankton community ecology: Principles applied in San Francisco Bay. *Marine Ecology Progress Series* 285: 11–28. doi: 10.3354/meps285011.

Cloern, J. E., and A. D. Jassby. 2008. Complex seasonal patterns of primary producers at the land-sea interface. *Ecology Letters* 11: 1294–1303. doi: 10.1111/j.1461-0248.2008.01244.x.

Cloern, J. E., and A. D. Jassby. 2010. Patterns and scales of phytoplankton variability in estuarine-coastal ecosystems. *Estuaries and Coasts* 33: 230–241. doi: 10.1007/s12237-009-9195-3.

Cloern, J. E., and F. H. Nichols. 1985. Time scales and mechanisms of estuarine variability, a synthesis from studies of San Francisco Bay. *Hydrobiologia* 129. Kluwer Academic Publishers: 229–237. doi: 10.1007/BF00048697.

Contreras, E., and M. J. Polo. 2014. Measurement frequency and sampling spatial domains required to characterize turbidity and salinity events in the Guadalquivir estuary (Spain). *Nat. Hazards Earth Syst. Sci* 12: 2581–2589. doi: 10.5194/nhess-12-2581-2012.

Crain, C. M., K. Kroeker, and B. S. Halpern. 2008. Interactive and cumulative effects of multiple human stressors in marine systems. *Ecology Letters* 11: 1304–1315. doi: 10.1111/j.1461-0248.2008.01253.x.

Davidson, K., R. J. Gowen, P. J. Harrison, L. E. Fleming, P. Hoagland, and G. Moschonas. 2014. Anthropogenic nutrients and harmful algae in coastal waters. *Journal of Environmental Management* 146. Academic Press: 206–216. doi: 10.1016/j.jenvman.2014.07.002.

Dixon, L. K., G. J. Kirkpatrick, E. R. Hall, and A. Nissanka. 2014. Nitrogen, phosphorus and silica on the West Florida Shelf: Patterns and relationships with Karenia spp. occurrence. *Harmful Algae* 38. Elsevier: 8–19. doi: 10.1016/j.hal.2014.07.001.

Dustan, P., and J. L. Pinckney. 1989. Tidally induced estuarine phytoplankton patchiness. *Limnology and Oceanography* 34: 410–419. doi: 10.4319/lo.1989.34.2.0410.

Ferreira, J. G., W. J. Wolff, T. C. Simas, and S. B. Bricker. 2005. Does biodiversity of estuarine phytoplankton depend on hydrology? *Ecological Modelling* 187: 513–523. doi: 10.1016/j.ecolmodel.2005.03.013.

Flint, R. W. 1984. Phytoplankton production in the Corpus Christi Bay Estuary. *Contributions in Marine Science*.

Gaulke, A. K., M. S. Wetz, and H. W. Paerl. 2010. Picophytoplankton: A major contributor to planktonic biomass and primary production in a eutrophic, river-dominated estuary. *Estuarine, Coastal and Shelf Science* 90: 45–54. doi: 10.1016/j.ecss.2010.08.006.

Geyer, N. L., M. Huettel, and M. S. Wetz. 2018. Phytoplankton Spatial Variability in the River-Dominated Estuary, Apalachicola Bay, Florida. *Estuaries and Coasts* 41. Springer New York LLC: 2024–2038. doi: 10.1007/s12237-018-0402-y.

Gilabert, J. 2001. Seasonal plankton dynamics in a Mediterranean hypersaline coastal lagoon: The Mar Menor. *Journal of Plankton Research* 23: 207–217. doi: 10.1093/plankt/23.2.207.

Gillanders, B., and M. Kingsford. 2002. Impact of Changes in Flow of Freshwater on Estuarine and Open Coastal Habitats and the Associated Organisms. *Oceanography and marine biology and annual review* 40: 233–309. doi: 10.1201/9780203180594.ch5.

Glasgow, H. B., and J. M. Burkholder. 2000. Water quality trends and management implications from a five-year study of a eutrophic estuary. *Ecological Applications* 10. Wiley: 1024–1046. doi: 10.1890/1051-0761(2000)010[1024:wqtami]2.0.co;2.

Glibert, P. M., and J. A. M. Burkholder. 2011. Harmful algal blooms and eutrophication: "strategies" for nutrient uptake and growth outside the Redfield comfort zone. *Chinese Journal of Oceanology and Limnology* 29: 724–738. doi: 10.1007/s00343-011-0502-z.

Glibert, P. M., S. Seitzinger, C. A. Heil, J. M. Burkholder, M. W. Parrow, L. A. Codispoti, and V. Kelly. 2005. The role of eutrophication in the global proliferation of harmful algal blooms. *Oceanography* 18: 198–209. doi: 10.5670/oceanog.2005.54.

Glibert, P. M., F. P. Wilkerson, R. C. Dugdale, J. A. Raven, C. L. Dupont, P. R. Leavitt, A. E. Parker, J. M. Burkholder, and T. M. Kana. 2016. Pluses and minuses of ammonium and nitrate uptake and assimilation by phytoplankton and implications for productivity and community composition, with emphasis on nitrogen-enriched conditions. *Limnology and Oceanography* 61. John Wiley & Sons, Ltd: 165–197. doi: 10.1002/LNO.10203@10.1002/(ISSN)1939-5590.STABLE-ISOTOPES.

Gomez, F. A., S. K. Lee, F. J. Hernandez, L. M. Chiaverano, F. E. Muller-Karger, Y. Liu, and J. T. Lamkin. 2019. ENSO-induced co-variability of Salinity, Plankton Biomass and Coastal Currents in the Northern Gulf of Mexico. *Scientific Reports* 9. Nature Publishing Group. doi: 10.1038/s41598-018-36655-y.

Hasler, Arthur D. 1975. Man-Induced Eutrophication of Lakes. In The Changing Global Environment, 383–399. Springer Netherlands. doi: 10.1007/978-94-010-1729-9_24.

Harvey, E. T., S. Kratzer, and P. Philipson. 2015. Satellite-based water quality monitoring for improved spatial and temporal retrieval of chlorophyll-a in coastal waters. *Remote Sensing of Environment* 158. Elsevier Inc.: 417–430. doi: 10.1016/j.rse.2014.11.017.

Heil, C. A., L. K. Dixon, E. Hall, M. Garrett, J. M. Lenes, J. M. O'Neil, B. M. Walsh, et al. 2014. Blooms of Karenia brevis (Davis) G. Hansen & Ø. Moestrup on the West Florida Shelf: Nutrient sources and potential management strategies based on a multi-year regional study. *Harmful Algae* 38. Elsevier: 127–140. doi: 10.1016/j.hal.2014.07.016.

Holland, J., N. J. Maciolek, R. D. Kalke, L. Mullins, and C. H. Oppenheimer. *A Benthos and Plankton Study of the Corpus Christi, Copano and Aransas Bay Systems III. Report on Data Collected During the Period July 1974-May 1975 and Summary of the Three-year Project*.

Irigoien, X., K. J. Flynn, and R. P. Harris. 2005. Phytoplankton blooms: A "loophole" in microzooplankton grazing impact? *Journal of Plankton Research* 27: 313–321. doi: 10.1093/plankt/fbi011.

Islam, M. S., J. S. Bonner, B. L. Edge, and C. A. Page. 2014. Hydrodynamic characterization of Corpus Christi Bay through modeling and observation. *Environmental Monitoring and Assessment* 186. Kluwer Academic Publishers: 7863–7876. doi: 10.1007/s10661-014-3973-5.

Jordan, T. E., D. E. Weller, and C. E. Pelc. 2018. Effects of Local Watershed Land Use on Water Quality in Mid-Atlantic Coastal Bays and Subestuaries of the Chesapeake Bay. *Estuaries and Coasts* 41. Springer New York LLC: 38–53. doi: 10.1007/s12237-017-0303-5.

Kurtzman, D., and B. R. Scanlon. 2007. El Niño-Southern Oscillation and Pacific Decadal Oscillation impacts on precipitation in the southern and central United States: Evaluation of spatial distribution and predictions. *Water Resources Research* 43: 1–12. doi: 10.1029/2007WR005863.

Magaña, H. A., and T. A. Villareal. 2006. The effect of environmental factors on the growth rate of Karenia brevis (Davis) G. Hansen and Moestrup. *Harmful Algae* 5: 192–198. doi: 10.1016/j.hal.2005.07.003.

Maier Brown, A. F., Q. Dortch, F. M. V. Dolah, T. A. Leighfield, W. Morrison, A. E. Thessen, K. Steidinger, B. Richardson, C. A. Moncreiff, and J. R. Pennock. 2006. Effect of salinity on the distribution, growth, and toxicity of Karenia spp. *Harmful Algae* 5: 199–212. doi: 10.1016/j.hal.2005.07.004.

Maier, G., G. A. Glegg, A. D. Tappin, and P. J. Worsfold. 2012. A high resolution temporal study of phytoplankton bloom dynamics in the eutrophic Taw Estuary (SW England). *Science of the Total Environment* 434. Elsevier: 228–239. doi: 10.1016/j.scitotenv.2011.08.044.

van Meerssche, E., and J. L. Pinckney. 2019. Nutrient Loading Impacts on Estuarine Phytoplankton Size and Community Composition: Community-Based Indicators of Eutrophication. *Estuaries and Coasts* 42. Estuaries and Coasts: 504–512. doi: 10.1007/s12237-018-0470-z.

Nixon, Scott W. 1995. Coastal marine eutrophication: A definition, social causes, and future concerns. Ophelia 41: 199–219. doi: 10.1080/00785236.1995.10422044.

Nohe, A., A. Goffin, L. Tyberghein, R. Lagring, K. de Cauwer, W. Vyverman, and K. Sabbe. 2020. Marked changes in diatom and dinoflagellate biomass, composition and seasonality

in the Belgian Part of the North Sea between the 1970s and 2000s. *Science of the Total Environment* 716. Elsevier B.V. doi: 10.1016/j.scitotenv.2019.136316.

Odebrecht, C., P. C. Abreu, and J. Carstensen. 2015. Retention time generates short-term phytoplankton blooms in a shallow microtidal subtropical estuary. *Estuarine, Coastal and Shelf Science* 162. Academic Press: 35–44. doi: 10.1016/j.ecss.2015.03.004.

Örnólfsdóttir, E. B., S. E. Lumsden, and J. L. Pinckney. 2004. Nutrient pulsing as a regulator of phytoplankton abundance and community composition in Galveston Bay, Texas. *Journal of Experimental Marine Biology and Ecology* 303: 197–220. doi: 10.1016/j.jembe.2003.11.016.

Paerl, H. W. 1988. Nuisance phytoplankton blooms in coastal, estuarine, and inland waters1. *Limnology and Oceanography* 33: 823–843. doi: 10.4319/lo.1988.33.4part2.0823.

Paerl, H. W. 1997. Coastal eutrophication and harmful algal blooms: Importance of atmospheric deposition and groundwater as "new" nitrogen and other nutrient sources. *Limnology and Oceanography* 42: 1154–1165. doi: 10.4319/lo.1997.42.5_part_2.1154.

Paerl, H. W. 2006. Assessing and managing nutrient-enhanced eutrophication in estuarine and coastal waters: Interactive effects of human and climatic perturbations. *Ecological Engineering* 26: 40–54. doi: 10.1016/j.ecoleng.2005.09.006.

Paerl, H. W., and J. Huisman. 2008. Climate: Blooms like it hot. *Science*. American Association for the Advancement of Science. doi: 10.1126/science.1155398.

Paerl, H. W., and D. Justić. 2013. Estuarine phytoplankton. In *Estuarine ecology*, Second, 85–110. Wiley Online Library.

Paerl, H. W., T. G. Otten, and R. Kudela. 2018. Mitigating the Expansion of Harmful Algal Blooms Across the Freshwater-to-Marine Continuum. *Environmental Science and Technology* 52. American Chemical Society: 5519–5529. doi: 10.1021/acs.est.7b05950.

Paerl, H. W., and V. J. Paul. 2012. Climate change: Links to global expansion of harmful cyanobacteria. *Water Research* 46. Elsevier Ltd: 1349–1363. doi: 10.1016/j.watres.2011.08.002.

Paerl, H. W., K. L. Rossignol, S. N. Hall, B. L. Peierls, and M. S. Wetz. 2010. Phytoplankton community indicators of short- and long-term ecological change in the anthropogenically and climatically impacted neuse river estuary, North Carolina, USA. *Estuaries and Coasts* 33: 485–497. doi: 10.1007/s12237-009-9137-0.

Parazoo, N. C., E. Barnes, J. Worden, A. B. Harper, K. B. Bowman, C. Frankenberg, S. Wolf, M. Litvak, and T. F. Keenan. 2015. Global Biogeochemical Cycles in the Texas-northern Mexico region. *Global Biogeochemical Cycles* 29: 1–19. doi: 10.1002/2015GB005125.Received.

Pennock, J. R., J. N. Boyer, J. A. Herrera-Silveira, R. L. Iverson, T. E. Whitledge, B. Mortazavi, and F. A. Comin. 1999. Nutrient Behavior and Phytoplankton Production in Gulf of Mexico Estuaries. In *Biogeochemistry of Gulf of Mexico Estuaries*, ed. T. S. Bianchi, J. R. Pennock, and R. R. Twilley, 109–162. John Wiley and Sons, Inc.

Phlips, E. J., S. Badylak, M. Christman, J. Wolny, J. Brame, J. Garland, L. Hall, et al. 2011. Scales of temporal and spatial variability in the distribution of harmful algae species in the Indian River Lagoon, Florida, USA. *Harmful Algae* 10. Elsevier B.V.: 277–290. doi: 10.1016/j.hal.2010.11.001.

Phlips, E. J., S. Badylak, N. G. Nelson, and K. E. Havens. 2020. Hurricanes, El Niño and harmful algal blooms in two sub-tropical Florida estuaries: Direct and indirect impacts. *Scientific Reports* 10: 1–12. doi: 10.1038/s41598-020-58771-4.

Piehler, M. F., L. J. Twomey, N. S. Hall, and H. W. Paerl. 2004. Impacts of inorganic nutrient enrichment on phytoplankton community structure and function in Pamlico Sound, NC, USA. *Estuarine, Coastal and Shelf Science* 61: 197–209. doi: 10.1016/j.ecss.2004.05.001.

Ritter, C., and P. A. Montagna. 1999. Seasonal hypoxia and models of benthic response in a Texas Bay. *Estuaries* 22: 7–20. doi: 10.2307/1352922.

Rounsefell, G. A., and W. R. Nelson. 1967. *Red-Tide Research Summarized to 1964 Including an Annotated Bibliography*. Washington, D.C.

Shangguan, Y., P. M. Glibert, J. A. Alexander, C. J. Madden, and S. Murasko. 2017. Nutrients and phytoplankton in semienclosed lagoon systems in Florida Bay and their responses to changes in flow from Everglades restoration. *Limnology and Oceanography* 62: S327–S347. doi: 10.1002/lno.10599.

Smayda, T. J. 2008. Complexity in the eutrophication-harmful algal bloom relationship, with comment on the importance of grazing. *Harmful Algae* 8. Elsevier: 140–151. doi: 10.1016/j.hal.2008.08.018.

de Souza, K. B., T. Jephson, T. B. Hasper, and P. Carlsson. 2014. Species-specific dinoflagellate vertical distribution in temperature-stratified waters. *Marine Biology* 161. Springer Verlag: 1725–1734. doi: 10.1007/s00227-014-2446-2.

Spatharis, S., G. Tsirtsis, D. B. Danielidis, T. do Chi, and D. Mouillot. 2007. Effects of pulsed nutrient inputs on phytoplankton assemblage structure and blooms in an enclosed coastal area. *Estuarine, Coastal and Shelf Science* 73: 807–815. doi: 10.1016/j.ecss.2007.03.016.

Steidinger, K. A., and R. M. Ingle. 1972. Observations on the 1971 summer red tide in Tampa Bay, Florida. *Environmental Letters* 3: 271–278.

Steidinger, K. A. (2009). Historical perspective on Karenia brevis red tide research in the Gulf of Mexico. *Harmful Algae*, *8*(4), 549–561. https://doi.org/10.1016/j.hal.2008.11.009

Suggett, D. J., C. M. Moore, A. E. Hickman, and R. J. Geider. 2009. Interpretation of fast repetition rate (FRR) fluorescence: Signatures of phytoplankton community structure versus physiological state. *Marine Ecology Progress Series* 376: 1–19. doi: 10.3354/meps07830.

Tester, P. A., and K. A. Steidinger. 1997. Gymnodinium breve red tide blooms: Initiation, transport, and consequences of surface circulation. *Limnology and Oceanography* 42. Wiley-Blackwell: 1039–1051. doi: 10.4319/lo.1997.42.5_part_2.1039.

Tolan, J. M. 2007. El Niño-Southern Oscillation impacts translated to the watershed scale: Estuarine salinity patterns along the Texas Gulf Coast, 1982 to 2004. *Estuarine, Coastal and Shelf Science* 72: 247–260. doi: 10.1016/j.ecss.2006.10.018.

Trebatoski, B. 1988. Observations on the 1986-1987 Texas Red Tide (Ptychodiscus brevis). *Texas Water Comission*. Austin, Texas: Texas Water Commission .

Vargo, G. A. 2009. A brief summary of the physiology and ecology of Karenia brevis Davis (G. Hansen and Moestrup comb. nov.) red tides on the West Florida Shelf and of hypotheses posed for their initiation, growth, maintenance, and termination. *Harmful Algae* 8: 573–584. doi: 10.1016/j.hal.2008.11.002.

Yamamoto, T. 2003. The Seto Inland Sea - Eutrophic or oligotrophic? In *Marine Pollution Bulletin*, 47:37–42. Elsevier Ltd. doi: 10.1016/S0025-326X(02)00416-2.

Zingone, A., E. J. Phlips, and P. J. Harrison. 2010. Multiscale variability of twenty-two coastal phytoplankton time series: A global scale comparison. *Estuaries and Coasts* 33: 224–229. doi: 10.1007/s12237-009-9261-x.

CHAPTER I: VARIABILITY IN PHYTOPLANKTON BIOVOLUME AND COMMUNITY COMPOSITION IN CORPUS CHRISTI BAY, CORPUS CHRISTI, TX, USA

Abstract

Corpus Christi Bay is a shallow, wind-driven lagoon on the South Texas coast that has a rapidly urbanizing watershed. Here, a 27-month field study was undertaken to quantify phytoplankton biovolume, community composition, and relationships with environmental drivers. Phytoplankton biovolume varied unimodally with a peak in biovolume from spring through summer followed by a decline into fall and winter. Phytoplankton biovolume was limited nutrients during the spring and summer, though physical factors such as precipitation and temperature were important limiting factors during the fall and winter. Regions with more restricted circulation patterns (i.e., man-made canals) were found to support higher standing crops of phytoplankton and the occurrence of very high biovolume blooms. The composition of the phytoplankton community was also related to nutrients, precipitation, and temperature. Diatoms were dominant during the winter and spring, dinoflagellates were dominant during the summer and fall, and picophytoplankton groups were important during spring, summer, and fall. These general conditions were punctuated by precipitation-driven freshwater inflow/nutrient delivery events and the occurrence of a *K. brevis* red tide during fall months. Future projections indicate that this region will become warmer and drier and will support an increasing urban population. Understanding the role of restricted freshwater inflows, land use patterns, and nutrients in driving phytoplankton community dynamics in this system is therefore paramount in predicting future changes to this ecologically and economically important system.

Introduction

Phytoplankton are often the dominant primary producers in estuaries (Cloern and Dufford 2005; Paerl et al. 2010; Cloern et al. 2014), providing food resources for benthic and pelagic consumers as well as detritivores and the microbial loop (Azam et al. 1983; Mallin and Paerl 1994; Finkel et al. 2010; Caron and Hutchins 2013). Estuaries are highly dynamic systems at the confluence of rivers and the ocean and are subject to environmental fluctuations acting on multiple time scales (Cloern and Jassby 2010; Paerl et al. 2010; Zingone et al. 2010). On shorter time scales, event based, or stochastic, variability is driven by changes in environmental conditions on the order of hours to weeks and can be driven by factors such as tides, wind, storm events, and floods (Cloern and Nichols 1985; Peierls et al. 2003; Paerl et al. 2010). Due to relatively rapid growth rates of phytoplankton, they can respond to these environmental perturbations with increasing biomass and/or changes in community composition (Peierls et al. 2003; Yin et al. 2004; Hays et al. 2005; Cloern and Jassby 2008; Phlips et al. 2020). On annual time scales, water temperature, light and nutrient availability are often important drivers of seasonal changes in phytoplankton biomass, with the greatest proportion of high biomass events recorded during the spring and the lowest during the winter on a global scale (Cloern and Jassby 2008; Cloern and Jassby 2010). Additionally, the ecophysiology of different phytoplankton groups often results in predictable patterns of seasonal community succession, with diatoms tending to dominate in cooler and/or wetter seasons and dinoflagellates tending to dominate during warmer and/or drier seasons (Cloern 1999; Örnólfsdóttir et al. 2004; Cloern and Jassby 2008; Cloern and Jassby 2010).

In addition to experiencing temporal variability, spatial variability in environmental forcings can similarly influence phytoplankton dynamics. In river dominated estuaries for

example, the strength of freshwater inflows plays a large role in where peak phytoplankton biomass is observed and how community composition across the freshwater-marine continuum is structured (Paerl et al. 2010; Peierls et al. 2012; Roelke et al. 2013; Dorado et al. 2015). In regions where nutrients are higher and residence time is lower, such as the head of the estuary, taxa with relatively fast growth rates (i.e., diatoms, cryptophytes, chlorophytes) are more likely to be favored. In contrast, regions where nutrients are lower and residence time is higher, such as the mid- to lower estuary, tend to support slower growing taxa (i.e., dinoflagellates) (Cloern and Dufford 2005; Paerl et al. 2010).

Watershed land use at the local and regional scale also represents a factor influencing the spatial distribution of phytoplankton by influencing nutrient delivery. In the Indian River Lagoon, portions of the estuary with greater anthropogenic influence on watershed land use patterns demonstrated higher mean phytoplankton biovolume than regions with smaller and more pristine watersheds (Phlips et al. 2011). Deforestation coupled with increased urban and suburban development has been shown to increase nutrient loads and change the ratio of various nutrients delivered to estuaries (Paerl et al. 2014; Jordan et al. 2018). For example, wastewater treatment plant (WWTP) effluent and stormwater runoff tend to deliver less dissolved silicate than riverine sources of freshwater, potentially leading to the selection of non-diatom taxa over diatoms and/or increased prevalence of harmful algal bloom (HAB) forming diatoms with lower silica requirements (i.e., *Pseudonitzschia*) (Roelke et al. 1997; Quigg et al. 2013; Parsons et al. 2001; Davidson et al. 2014).

There is increasing evidence that climate change and anthropogenic activities that affect coastal watersheds have altered phytoplankton dynamics across the globe. Increasing temperatures associated with climate change have changed the timing of winter-spring blooms

(earlier), seasonal patterns in phytoplankton biomass (unimodal vs. bimodal), size structure of the phytoplankton community, and the overall magnitude of peak biomass (Guinder et al. 2010; Winder and Sommer 2012; Nohe et al. 2020). Increasing frequency of extreme precipitation conditions, both drought and flood, have also led to "boom and bust" cycles of phytoplankton following excessive freshwater inputs (Cloern and Dufford 2005; Paerl 2006) and the occurrence of HABs due to increased residence time and altered nutrient conditions under drought conditions (Phlips et al. 2011). The interactive effects of these physical conditions on driving changes in salinity and density-driven stratification have also been implicated in observed increases in HABs across numerous systems (Paerl and Paul 2012; Dorado et al. 2015; Wells et al. 2015; see Chapter III). Changing nutrient concentrations and ratios have also been shown to alter community composition both among and within major taxonomic groups of phytoplankton and influence the prevalence of HAB forming taxa and the formation of HABs (Quigg et al. 2013; Nohe et al. 2020; Wang et al. 2021).

Despite the widespread impacts of anthropogenic stressors on estuarine phytoplankton biomass and community composition, there is evidence that the magnitude and direction of these changes are specific to each system (Guinder et al. 2010; Winder and Sommer 2012; Nohe et al. 2020). It is therefore critical to understand how climate variability/change and nutrient availability act to influence phytoplankton across a wide range of estuarine conditions in order to better predict how continued alteration of environmental dynamics will affect phytoplankton in the future. Corpus Christi Bay (CCB) is a shallow, micro-tidal, wind-driven system located in Corpus Christi, Texas. The city of Corpus Christi has undergone rapid population growth over the past 2 decades (8.5% increase 2000 to 2010; 7% increase 2010 to 2019) (U.S. Census Bureau), with an ~13% increase in developed areas occurring from 2001-2016, leading to

increased stormwater inputs. Stormwater runoff has been shown to increase nutrient concentrations, leading to increased phytoplankton biomass following inputs (Turner et al. 2015). WWTPs in increasingly urban areas are also an influential source of inorganic nutrients, especially in low inflow systems like CCB (Yeager et al. 2006; Wetz et al. 2017; https://sparrow.wim.usgs.gov/sparrow-southwest-2012/). Bugica et al. (2020) found a "hot spot" of eutrophication in Oso Bay, a sub-bay of CCB, where WWTP effluent has been shown to be a driver of decreasing water quality (Wetz et al. 2016). Another factor negatively impacting the CCB system is the long-term decrease in freshwater inflows (Montagna et al. 2009), increases in salinity (Applebaum et al. 2005; Bugica et al. 2020), and decreased loading of riverine N (Dunn 1996) to CCB. Combined these trends indicate long term increases in estuarine residence time and decreased nutrient availability. The long-term increase in salinity has also been related to the increased frequency of occurrence of *Karenia brevis* red tides in this system (see Chapter III).

To date there have been no comprehensive studies on phytoplankton dynamics in this ecologically/economically important estuary. Studies addressing the spatial-temporal distribution of phytoplankton and potential environmental drivers are necessary to establish baseline conditions and to begin to project how further population growth and land use change, increased frequency of drought/flood conditions, and continued decrease in freshwater inflows will affect the ecosystem in the future (Texas State Data Center, http://txsdc.utsa.edu/Data/TPEPP/Projections/Index.aspx; Pachauri et al. 2014; Nielson-Gammon et al. 2020). Here, a 27-month field study was conducted across six sites representing different levels of anthropogenic influence. It was hypothesized that both phytoplankton biomass and community structure would display spatial variability in response to different levels of anthropogenic nutrient inputs. Specifically, regions of greatest nutrient input would support the

highest overall biomass (Flint 1984) and a greater proportion of community biovolume attributed to dinoflagellate and cryptophyte taxa (Cloern and Dufford 2005; Burkholder et al. 2008; Davidson et al. 2014). Seasonal fluctuations in temperature, rainfall, and wind were also hypothesized to be important factors influencing phytoplankton biomass, with biomass maxima expected in summer months (Flint 1984; Pennock et al. 1999). These factors, along with nutrient availability, were hypothesized to play a role in seasonal variation in phytoplankton community structure, with diatoms expected to be important in cooler months, and flagellated taxa increasing in abundance in the fall (Holland et al. 1975). Findings generally agreed with the hypotheses here, though there were exceptions. In addition to representing the first study of its kind in a local estuary (Corpus Christi Bay-Upper Laguna Madre), this study is novel because there are few studies of its type in similar low inflow subtropical estuaries worldwide.

Methods

Study Area

Corpus Christi Bay is a shallow (~ 3 m, ship channel ~ 15 m), microtidal (~ 0.3 m range), wind-driven (~ 18 kilometers h^{-1} yearly mean) system (Ritter and Montagna 1999; Islam et al. 2014; Turner et al. 2015) that comprises the largest portion of the Nueces Estuary. Corpus Christi Bay is located on the semi-arid South Texas coast and is separated from the Gulf of Mexico by Padre Island, with two narrow inlets for water exchange (Packery Channel and Aransas Pass). Very little riverine inflow from the Nueces River reaches the bay compared to historic conditions (Montagna et al. 2009). This leads to a relatively long residence time (> 5 mo. – 1 year) and a generally well-mixed water column. Corpus Christi Bay is also susceptible seasonal hypoxia (Ritter and Montagna 1999) and *Karenia brevis* red tides, with the latter showing a marked increase in frequency of occurrence since the mid-1990s (see Chapter III).

Sampling Sites

Six sampling sites were selected to represent an estuarine nutrient-salinity gradient (Fig. 1.1). All sampling sites were located along the shoreline to both ensure sampling events could proceed under inclement weather conditions and to assess the direct impacts of growing (in influence) anthropogenic stressors (i.e., wastewater treatment plant effluent, stormwater runoff). The Laguna Madre site was located in the Upper Laguna Madre, where there is little connectivity with freshwater sources, and freshwater inputs are primarily from overland runoff. The Canal site was located in a residential neighborhood with extensive man-made canals and little connectivity to surrounding waters. The closest connected body of water is the Laguna Madre, and freshwater inputs were in the form of overland runoff from yards and roadways. The Packery Channel is a man-man inlet between the Gulf of Mexico and the Upper Laguna Madre/Lower Corpus Christi Bay. Oso Inlet was at the confluence of Oso Bay and Corpus Christi Bay, with freshwater sources including Oso Creek and a nearby WWTP effluent pipe. Cole Park was located directly in front of a stormwater runoff drain on the western shoreline of Corpus Christi Bay. The stormwater drain receives inputs from ~6 km^2 of drainage area. The South Shore site was located along the southern shoreline of Corpus Christi Bay and was adjacent to a stormwater runoff drain (~ 90 m away) that receives inputs from ~5 km^2 of suburban residential land use. Temporal frequency of sampling was variable based on the likelihood of a *K. brevis* red tide and was as follows: monthly in December, January, and February; biweekly in October (2017), November, and March through August; weekly in September and October (2016 and 2018). This resulted in a total of 59 sampling events spanning 27 months.

Field Sampling

Surface water hydrographic data (temperature, conductivity (salinity), pH, dissolved

oxygen) were collected using a calibrated YSI ProPlus multiparameter sonde (YSI Inc., Yellow Springs, Ohio). Light attenuation was measured at each site with a Secchi disc, however, there were instances where the current was too swift for the disk to descend at a near 90° angle (Packery Channel, n = 33 and Oso Inlet, n = 7). Water samples were collected from the top 15 cm of the water surface and transported to the lab in acid-washed amber polycarbonate bottles for further processing. Water for micro- and nanophytoplankton enumeration (500 mL) was stored at ambient temperature and samples for nutrient chemistry, chlorophyll *a* analysis, and picophytoplankton cell counts were collected as field duplicates (1-L each) and stored on ice ~ 0°C) until return to the lab (< 3 hours).

Laboratory Processing

Prior to sample processing, the collection bottles were gently inverted to homogenize the water and suspended materials. Water for micro- and nanophytoplankton enumeration was gently poured into 50 mL conical vials and fixed with acidified Lugol's solution to a final concentration of 1% and stored at room temperature in the dark. Water for dissolved nutrient (ammonium, nitrate plus nitrite, orthophosphate, silicate, dissolved organic carbon and total dissolved nitrogen) quantification was filtered through pre-combusted (4 hours at 450°C) Ahlstrom GF/F filters into HDPE bottles. Water for total organic carbon and total nitrogen quantification was poured directly into HDPE bottles. For chlorophyll *a* quantification, a known volume of water was gently filtered (≤ 5 mm Hg) through 25 mm Whatmann GF/F filters. For picophytoplankton quantification, site water was fixed with 50% glutaraldehyde to a final concentration of 1%. Following sample processing described above, all samples were immediately stored at -20°C

until analysis.

Phytoplankton Enumeration

Micro- and nanophytoplankton were counted by following the Utermöhl method on an Olympus IX71 inverted microscope at 200x magnification. The volume settled for each sample was variable based on chlorophyll *a* concentration and the amount of suspended solids noted during live screens. All samples were settled overnight (> 12 hrs), allowing more than 1 hour of settling time per mL of sample settled. Picophytoplankton were counted using an Accuri C6 Plus flow cytometer with the CSampler Plus adapter (Beckton Dickinson, San Jose, CA). Instrument QC was performed daily following manufacturer protocol prior to sample preparation. Samples were thawed at 0°C in the dark and gently filtered across 20 µm Nytex® mesh to remove large cells and particulate matter. All samples were run on the fast setting, with a flow rate of 66 µL min^{-1} and a core size of 22 µm. The auto-sampler was set to agitate the sampling plate and rinse the sample input port before and after each sample was analyzed. Additionally, polystyrene beads of known size (3.3 µm) were run at the same settings to ensure that only appropriate size ranges of cells were counted. Biovolumes were estimated for micro-, nano-, and picophytoplankton using the associated geometric shapes at the lowest taxonomic resolution recorded during counting (Sun and Liu, 2003) (Table S1.1). Picophytoplankton shape and size was not directly measured and was estimated to be spherical at 1.5 µm and 2.5 µm diameters for picocyanobacteria and picoeukaryotes, respectively.

Nutrients

Inorganic nutrient samples were thawed to room temperature and then analyzed on a Seal QuAAtro autoanalyzer. Standard curves with five different concentrations were run daily at the beginning of each run. Fresh standards were made prior to each run by diluting a primary

standard with low nutrient surface seawater. Deionized water (DIW) was used as a blank, and DIW blanks were run at the beginning and end of each run, as well as after every 8–10 samples to correct for baseline shifts. Method detection limits were 0.02 µM for nitrate plus nitrite (NO_x) and ammonium (NH_4^+), and < 0.01 µM for orthophosphate (PO_4^{3-}) and silicate (SiO_4). Dissolved inorganic nitrogen (DIN) was calculated as the sum of NH_4^+ and NOx. Samples for dissolved organic carbon (DOC) and total dissolved nitrogen (TDN) were thawed to room temperature and analyzed using the High Temperature Catalytic Oxidation method on a Shimadzu TOC-Vs analyzer with nitrogen module. Standard curves were run twice daily using a DIW blank and five concentrations of either acid potassium phthalate solution or potassium nitrate for DOC and TDN, respectively. Three to five subsamples were taken from each standard and water sample and injected in sequence. Reagent grade glucosamine was used as a laboratory check standard and inserted throughout each run, as were Certified Reference Material Program (CRMP) deep-water standards of known DOC/TDN concentration. Mean daily CRMP DOC and TDN concentrations were 43.0 ± 2.7 µmol L^{-1} and 32.2 ± 2.3 µmol L^{-1}, respectively. Dissolved organic nitrogen (DON) was determined by subtracting dissolved inorganic nitrogen (NH_4^+ and NO_x) from TDN.

Accessory Data Collection

Daily precipitation totals and mean daily wind speeds were downloaded from the NOAA National Climate Data Center for the Corpus Christi Naval Air Station (station code USW00012926; accessed 4/6/2020). The precipitation data was used to assign each sampling event a value representing days since rainfall > 0.1 inches (DSR). Where rainfall and sampling events overlapped, a value of 0 was assigned.

Data Analysis

All raw data and associated R code are available at doi:10.7266/NCPYG0DH. Data analyses were performed in R v 3.6.2 and PRIMER v7. Prior to statistical analyses, NOx (n = 70) and PO_4^{3-} (n = 3) measurements that were below the detection limit were coded as the method detection limits of 0.02 µM and 0.005 µM, respectively. There was one instance where calculated DON was negative, and the value was coded as 0. DIN:DIP was calculated as DIN divided by PO_4^{3-}, DIN:Si was calculated as DIN divided by SiO_4. Where averages are presented (i.e., site or season averages), DIN:DIP and DIN:Si were calculated with average DIN and average PO_4^{3-} and SiO_4, respectively. The error for the ratios was then calculated using the formula

$$(DIN/var) \times \sqrt{(sd\ DIN/DIN)^2 + (sd\ var/var)^2}$$

where sd indicates standard deviation, DIN is mean DIN, and var is either the mean of PO_4^{3-} or SiO_4 for the DIN:DIP and DIN:Si ratios, respectively.

Two-way ANOVAs with site and season were used to explore spatial and seasonal patterns in individual environmental and biological variables (stats v 3.6.2; (R Core Team 2019)). For environmental variables, where sampling was conducted on sub-monthly time scales, data were averaged by sampling month at each site prior to conducting ANOVAs to achieve a more balanced dataset. For each variable examined, the interaction term for site and season was used as an explanatory factor to test for a significant interaction between factor levels. If there was no significant interaction, one-way ANOVAs were used to test for site and season differences individually, without regard to the other factor (stats v 3.6.2; (R Core Team 2019)). If a significant interaction was detected, one-way ANOVAs were used to test for site differences within each level of season, and vice versa. No significant interaction between site and season

was detected for salinity, dissolved oxygen, NH_4^+, NOx, DIN:DIP ratios. There was a significant interaction between site and season for PO_4^{3-}, SiO_4, DON, DIN:Si ratios. Each one-way ANOVA was tested for assumptions of normality (Shapiro-Wilk test) and homoscedasticity of variance (Brown-Forsythe Levene test). If necessary, terms to address heteroscedasticity were included in the ANOVA models (nlme v. 3.1-145; (Pinheiro et al. 2020). Multiple comparison procedures with Tukey contrasts were then used to compare all possible season and site pairs with a Westfall correction applied to the p-values (multcomp v 1.4-12; (Horthorn et al. 2008)). Corrected p-values were compared to $\alpha = 0.1$ to account for introduction of Type II error (Quinn and Keough 2002).

Phytoplankton abundance and biovolume were significantly linearly related ($p = < 0.001$; $R^2 = 0.29$; slope = 0.46), though because biovolume is a more direct measure of phytoplankton biomass and more accurately represents the contribution of different major taxonomic groups to phytoplankton carbon, further analyses focus on phytoplankton biovolume. Due to an exceptional outlier event in phytoplankton biovolume associated with the occurrence of a short-lived *K. brevis* red tide (one event 10/14/2016), median values of phytoplankton biovolume as well as the biovolume of major taxonomic groups were reported instead of means as they were more representative of overall site and season conditions. The Kruskal-Wallis rank-based non-parametric test is better suited for comparing conditions among factor levels when there are a few strong outliers (stats v. 3.6.2; (R Core Team 2019; Quinn and Keough 2002)) and was therefore used to compare sites and seasons for phytoplankton biovolume, and the biovolume of diatoms, dinoflagellates, picocyanobacteria, and picoeukaryotes. To determine if there was a significant interaction between site and season, the five datasets were rank-transformed and an ANOVA with the interaction term between site and season was used as a response variable, since

the Kruskal-Wallis test is only for one-way designs (stats v. 3.6.2; (R Core Team 2019; Quinn and Keough 2002)). There was no significant interaction found for phytoplankton biovolume, diatom biovolume, picocyanobacteria biovolume, or picoeukaryote biovolume. One-way Kruskal-Wallis tests were performed on site and season individually for these four response variables (stats v. 3.6.2; (R Core Team 2019)). A borderline interaction was found for dinoflagellate biovolume. One-way comparisons of sites within each level of season and comparisons of seasons within each level of site, however, yielded similar results as the one-way Kruskal-Wallis comparisons for sites and seasons individually. Therefore, the results of the one-way Kruskal-Wallis tests are presented in the results. Multiple comparison procedures with Tukey contrasts were then used to compare all possible season and site pairs with a Holm correction applied to the p-values. Corrected p-values were compared to $\alpha = 0.1$ to account for introduction of Type II error (Quinn and Keough 2002).

To assess seasonal and spatial environmental variability, principal component analyses (PCA) were conducted in PRIMER v7 (Clarke and Gorley 2015). One PCA was conducted including all sampling events across all sites to characterize temporal and spatial variability. Salinity, temperature, dissolved oxygen, pH, DON, NOx, NH_4^+, SiO_4, PO_4^{3-}, DIN:DIP, and DIN:Si were included in the PCAs, and all variables were normalized prior to analysis. To quantify the relationships among environmental factors and phytoplankton biovolume pairwise Kendall's Tau correlations were conducted on untransformed data (stats v. 3.6.2; (R Core Team 2019)). Pairwise Kendall's Tau correlations between environmental variables and diatom, dinoflagellate, picocyanobacteria, and picoeukaryote biovolume were conducted on untransformed data (stats v. 3.6.2; (R Core Team 2019)). These four taxonomic groups, on average, comprised approximately 90% of the phytoplankton community in the Corpus Christi

Bay system and were considered important contributors to the phytoplankton community across nearly all sampling events.

Results

Environmental Dynamics

Temperature was similar across sites and demonstrated seasonality, with the lowest temperatures observed during winter (mean = 14.3 ± 4.4°C) and the highest temperatures observed during summer (mean = 30.1 ± 1.1°C). All other environmental parameters demonstrated spatial variability, though for some nutrient parameters this was seasonally dependent. Salinity, NH_4^+, NOx, DIN:DIP ratios, and dissolved oxygen varied across sites and the spatial variability was independent of seasonal patterns, whereas the spatial patterns observed for DIN, PO_4^{3-}, SiO_4, DON, and DIN:Si ratios were not independent of observed seasonal variability. Where there was no interaction, ANOVA results along with the mean ± standard deviation comparing sites and seasons are presented below (Table 1.1). Highest salinity was observed in the summer, followed by spring, then fall and winter. Cole Park, South Shore, and Oso Inlet demonstrated lower salinity than the Laguna Madre and Canal sites, and Packery Channel was no different than any site other than the Laguna Madre. Higher NH_4^+ concentrations were observed during spring and summer than fall, while winter was no different than any other season. NH_4^+ was highest at the Canal site, followed by Packery Channel and Cole Park, then Oso Inlet, and lastly South Shore and the Laguna Madre. Lowest NOx concentrations were observed during the summer, highest concentrations in the winter, and intermediate concentrations during the spring and fall. The highest concentrations of NOx were observed at Cole Park, followed by the Canal, Oso Inlet, South Shore, Packery Channel, and the Laguna Madre. PO_4^{3-} concentrations demonstrated little seasonal variability, ranging from 0.94

µM to 1.44 µM. This was also seen in the site-specific seasonal comparisons, with no differences among seasonal concentrations except for the Canal site where concentrations were significantly higher in winter and spring than summer and fall. Concentrations at the Laguna Madre site were generally low, while concentrations at Cole Park and Oso Inlet were higher. In the fall, PO_4^{3-} at Cole Park was significantly higher than all other sites. During the spring, Oso Inlet PO_4^{3-} was significantly higher than at the Laguna Madre and Packery Channel site, with no other differences detected. During the winter, Oso Inlet PO_4^{3-} was higher than at the South Shore, Laguna Madre, and Packery Channel sites. Cole Park PO_4^{3-} was also significantly higher than at the Laguna Madre and Packery Channel, and no other differences were detected. Summer concentrations of PO_4^{3-} demonstrated no spatial variability. DIN:DIP ratios were significantly lower in fall than all other seasons, and no differences were detected among spring, summer, and winter. The Canal and Packery Channel sites had higher DIN:DIP than the Oso Inlet and South Shore sites, and Cole Park higher than Oso Inlet. The Laguna Madre was no different than any other site. Though there was an interaction between season and site for DON, SiO_4, PO_4^{3-}, and DIN:Si, the patterns observed in the season and site means were generally similar to the results of the one-way ANOVAs comparing seasons at each site and vice versa. DON concentrations were highest in the summer and fall, followed by spring, and then winter. The only site that demonstrated no seasonal variability in DON concentrations was Packery Channel. Concentrations of DON at the Laguna Madre, Canal, and Oso Inlet sites were higher than at Packery Channel, Cole Park, and South Shore. This pattern was most pronounced during the summer, whereas no spatial variability was observed during the spring.

Concentrations of SiO_4 were generally higher during spring, summer, and fall when compared to winter, though there were no differences among seasons detected at the Packery

Channel or Cole Park sites. The South Shore site also demonstrated a departure from this pattern, with the only difference detected between fall (higher) and spring. Spatially, SiO_4 tended to be lowest at Packery Channel, highest at the Cole Park site and intermediate at all other sites. This pattern was most pronounced during the fall. During the winter, Cole Park SiO_4 was significantly higher than other sites. During the summer, Packery Channel SiO_4 was significantly lower than all other sites, but no other differences were detected. Lastly, during the spring, SiO_4 concentrations at the Canal site were significantly higher than at South Shore and Packery Channel, with SiO_4 concentrations at Cole Park and Oso Inlet also higher than at Packery Channel.

Seasonal patterns in DIN:Si ratios were generally similar among sites, with the highest ratios typically observed during the winter and no other differences among seasons. This pattern was observed at the Laguna Madre, Canal, and Oso Inlet sites, whereas there was no seasonal variability detected at Packery Channel and Cole Park. The South Shore site deviated from this pattern with the only observed difference between spring (higher) and fall. PCA was used to explore spatial and temporal variability. The first principal component (PC1) was primarily composed of NOx, PO_4^{3-}, and salinity, with temperature and dissolved oxygen contributing moderately, and explained approximately 23.0% of the variability (Fig 1.2). This axis likely represents variability in rainfall. Many of the sampling events that demonstrated variability along this axis were from Cole Park and Oso Inlet, which are closer to freshwater sources. PC2 was primarily composed of temperature, dissolved oxygen, DON, and SiO_4, and explained approximately 19.8% of the variability. The strong contribution of temperature and dissolved oxygen to this axis suggests that it is representative of a seasonal metabolism signal. There is also evidence that this axis captures spatial variability. The Canal site demonstrated the lowest

average dissolved oxygen over the course of the study followed by the Laguna Madre site, though the latter was not significantly different than the Cole Park and Packery Channel sites (data not shown). Despite the strong contribution of rainfall variability in driving the creation of PC1, there was also a seasonal component represented on this axis (Fig 1.3). Variability in rainfall patterns was seasonal and most pronounced during the fall and winter, though some variability was also seen during early spring. Oso Inlet and South Shore also demonstrated increased variability during the summer-fall of 2018 when there were periods of prolonged precipitation associated with an El Niño event. The seasonal metabolism axis of variability demonstrated relatively consistent patterns among sites, though during the summer, PC scores tended to be lower at the Laguna Madre and Canal sites (Fig 1.3b), representative of higher temperatures and concentrations of DON and lower dissolved oxygen. In contrast, PC scores tended to be higher at the Packery Channel site, representative of lower temperatures and DON concentrations and higher dissolved oxygen. Departures from the "average" seasonal signal also occurred at the Cole Park site, though these were inconsistent and short-lived in comparison to the generally different conditions observed at the Laguna Madre and Canal sites during the summer and were likely driven by freshwater inflow variability.

Plots of inorganic nutrients versus salinity and temperature further resolved spatial variability in the response of nutrient conditions to changes in these variables (Fig 1.4). The inverse relationship between salinity and inorganic nutrients was most pronounced at Cole Park, with clear patterns of increased NOx, SiO_4, and PO_4^{3-} related to decreased salinity (Fig 1.4). Despite similarities in the trajectory of NH_4^+ and NOx in the PCA plot (Fig 1.2), the relationship between NH_4^+ and salinity was less pronounced, even at the Cole Park site, though there were instances of increased NH_4^+ associated with decreased salinity (Fig 1.4). The only clear

relationship between salinity and NH_4^+ was found at the Packery Channel site where salinity was positively related to NH_4^+ (Fig. 1.4). In line with observations from the PCA plot, NOx was inversely related to salinity at all sites other than Packery Channel. Relationships between SiO_4, PO_4^{3-} and salinity were less consistent across sites. There was an inverse relationship between SiO_4 and salinity at the Cole Park site and positive relationships between the two at the Laguna Madre and Canal sites. PO_4^{3-} on the other hand, appeared inversely related to salinity at all sites other than the Laguna Madre and Canal sites. Lastly, DON was positively related to salinity across all sites.

Despite ANOVA results indicating seasonality in NH_4^+, there were no clear relationships between NH_4^+ and temperature across sites though there was greater variability at warmer temperatures (Fig 1.4). Conversely, at the Laguna Madre, Canal, Oso Inlet, and Cole Park sites, inverse relationships between NOx and temperature are in agreement with the observed seasonality. SiO_4 was positively related to temperature at the Laguna Madre site. Relationships between PO_4^{3-} and temperature were inverse at the Oso Inlet and Canal site and positive at the Packery Channel site. Concentrations of DON were positively related to temperature at all sites other than the Packery Channel site. These similarities and differences among the relationships between nutrients, salinity, and temperature indicate that seasonality in temperature and rainfall, as well as stochastic variability in rainfall are important drivers of nutrient condition.

Phytoplankton Population Dynamics

Phytoplankton biovolume varied spatially and seasonally (Fig 1.5). Phytoplankton biovolume was significantly lower at Cole Park (1.53×10^6 μm^3 L^{-1}) than all other sites. Biovolume at the Laguna Madre site (2.25×10^6 μm^3 L^{-1}) was significantly lower than only the Canal site (3.74×10^6 μm^3 L^{-1}), with both sites similar to the South Shore (2.56×10^6 μm^3 L^{-1}),

Oso Inlet (3.01 x 10^6 μm^3 L^{-1}), and Packery Channel (2.83 x 10^6 μm^3 L^{-1}) sites. Phytoplankton biovolume also varied by season, with the highest biovolume in the spring (3.52 x 10^6 μm^3 L^{-1}) and summer (2.80 x 10^6 μm^3 L^{-1}), and lowest in the fall (2.28 x 10^6 μm^3 L^{-1}) and winter (2.02 x 10^6 μm^3 L^{-1}). On average, diatoms were the largest contributor to phytoplankton biovolume, accounting for approximately 34.0% of total phytoplankton biovolume (Figs 1.6 and 1.7; Table 1.2). Dinoflagellates and picocyanobacteria were the next largest contributors, and these groups accounted for approximately 27.7% and 20.3% of the phytoplankton community, respectively. Picoeukaryotes contributed approximately 8.1% to the Corpus Christi Bay phytoplankton community, and these four major taxonomic groups accounted for 90% of phytoplankton biovolume. There were, however, spatial and seasonal differences in the contribution of each of the major taxonomic groups. Packery Channel demonstrated the highest diatom biovolume at 1.27 x 10^6 μm^3 L^{-1}, with the only other difference observed between the South Shore (6.14 x 10^5 μm^3 L^{-1}) and Cole Park sites (3.00 x 10^5 μm^3 L^{-1}) (Fig 1.6; Table 1.2). Winter (9.82 x 10^5 μm^3 L^{-1}) and spring (7.90 x 10^5 μm^3 L^{-1}) diatom biovolume was significantly higher than summer (4.49 x 10^5 μm^3 L^{-1}) and fall (3.67 x 10^5 μm^3 L^{-1}).

Dinoflagellate biovolume was significantly higher at the Canal site (7.96 x 10^5 μm^3 L^{-1}) than at all other sites. The Laguna Madre (4.33 x 10^5 μm^3 L^{-1}), Oso Inlet (5.54 x 10^5 μm^3 L^{-1}), and South Shore (3.98 x 10^5 μm^3 L^{-1}) dinoflagellate biovolumes were also significantly higher than at the Cole Park (2.25 x 10^5 μm^3 L^{-1}) site, with no differences found between these sites and the Packery Channel site (2.89 x 10^5 μm^3 L^{-1}). The seasonal differences in dinoflagellate biovolume mirrored that seen for diatoms, with summer (5.76 x 10^5 μm^3 L^{-1}) and fall (5.48 x 10^5 μm^3 L^{-1}) significantly higher than spring (2.10 x 10^5 μm^3 L^{-1}) and winter (1.92 x 10^5 μm^3 L^{-1}).

Picocyanobacteria biovolume at the Oso Inlet site (1.22×10^6 μm^3 L^{-1}) was significantly higher than all sites but the Canal site (7.39×10^5 μm^3 L^{-1}), with the latter significantly higher than the Laguna Madre (4.55×10^5 μm^3 L^{-1}), Packery Channel (5.02×10^5 μm^3 L^{-1}), and Cole Park (3.93×10^5 μm^3 L^{-1}) sites. The South Shore (6.00×10^5 μm^3 L^{-1}) site was no different than any site other than Oso Inlet (higher). Spring (7.40×10^5 μm^3 L^{-1}) and summer (8.11×10^5 μm^3 L^{-1}) picocyanobacteria biovolume were significantly higher than both fall (4.79×10^5 μm^3 L^{-1}) and winter (1.65×10^5 μm^3 L^{-1}) picocyanobacteria biovolume, with winter also significantly lower than fall. At the Canal site (3.30×10^5 μm^3 L^{-1}), picoeukaryote biovolume was significantly higher than all sites other than the Oso Inlet site (2.29×10^5 μm^3 L^{-1}). Picoeukaryote biovolume at the Oso Inlet site was significantly higher than the Laguna Madre (1.16×10^5 μm^3 L^{-1}) and Packery Channel (1.12×10^5 μm^3 L^{-1}) sites, though was not different from the South Shore site (1.29×10^5 μm^3 L^{-1}). The Cole Park site demonstrated significantly lower picoeukaryote biovolume (7.10×10^4 μm^3 L^{-1}) than all other sites. The highest picoeukaryote biovolume was observed in the spring (2.96×10^5 μm^3 L^{-1}), followed by summer (1.86×10^5 μm^3 L^{-1}), fall (9.00×10^4 μm^3 L^{-1}), and lastly winter (5.20×10^4 μm^3 L^{-1}).

The remaining ~ 10% of the phytoplankton community was comprised of euglenoids (5.0%), cryptophytes (2.2%), cyanobacteria (1.3%), raphidophytes (1.1%), small unidentified flagellates (0.4%), silicoflagellates (0.2%), chlorophytes (0.1%), and unidentified organisms (0.1%). Despite the relatively low overall contributions of euglenoids, cyanobacteria, and raphidophytes, there were occasions where these groups contributed a larger percentage to the phytoplankton community (Fig. 1.7). Peaks in euglenoid biovolume (≥ 50% of total biovolume) occurred on 2/9/2017 (Oso Inlet), 12/14/2017 (Canal, Cole Park, South Shore), and 2/15/2018 (Cole Park). Cyanobacteria and raphidophyte peaks occurred less frequently, with two

cyanobacteria peaks occurring on 4/21/2017 (Packery Channel) and 5/5/2017 (Canal) and only a single peak in raphidophyte biovolume on 7/12/2018 (Canal).

Environmental Drivers of Phytoplankton Dynamics

Phytoplankton Biovolume

Pairwise correlations (Kendall's Tau) between phytoplankton biovolume and environmental parameters used in the PCAs, in addition to days since the last rainfall greater than 0.1 inches (DSR) and average daily wind speed, were used to assess individual relationships between phytoplankton biovolume and environmental conditions. At the system wide level, phytoplankton biovolume was negatively related to NOx, PO_4^{3-}, and SiO_4, and positively related to DSR, temperature, pH, and salinity (Table 1.3).

Phytoplankton Community Composition

To understand how different environmental variables related to the biovolume of the four most abundant major taxonomic groups, pairwise comparisons (Kendall's Tau) were performed between diatom, dinoflagellate, picocyanobacteria, or picoeukaryote biovolume, and the aforementioned environmental variables (Table 1.4). Diatom biovolume was inversely related to NOx, PO_4^{3-}, SiO_4, DON, and temperature, and positively related to dissolved oxygen, DIN:Si ratios, and wind speed. Dinoflagellate biovolume was positively related to temperature, DON, SiO_4, and salinity, and inversely related to NOx, wind speed, dissolved oxygen, DIN:Si ratios, and NH_4^+. Picocyanobacteria biovolume was inversely related to DIN:Si ratios, dissolved oxygen, and NOx, and positively related to SiO_4, salinity, temperature, DON, and DSR. Lastly, picoeukaryote biovolume was also inversely related to dissolved oxygen, DIN:Si ratios, NOx, and PO_4^{3-}, and positively related to SiO_4, salinity, temperature, DON, and DSR.

Discussion

Corpus Christi, Texas has experienced rapid population growth and increases in urbanization, which have led to decreased freshwater inflows due to damming of the Nueces River (Montagna et al. 2009), increased demand for wastewater treatment, and increased cover of impervious surfaces (~13% increase in developed land from 2001-2016). Many estuaries around the globe have, and are continuing to, experience similar changes in land use and reductions in freshwater inflows due to damming and water diversions for human consumption (Gillanders and Kingsford 2002; Paerl et al. 2014; Jordan et al. 2018; Cloern 2019). Urbanization has been associated with increased loads of N and P delivered to estuarine environments, changes in the ratios of and bioavailability of nutrients supplied, and increases in primary production and symptoms of eutrophication (i.e., hypoxia, loss of benthic organisms, loss of seagrasses) (Seitzinger et al. 2002; Paerl et al. 2014; Jordan et al. 2018). Increases in the coverage of impervious surfaces and hydrologic modifications (i.e., dams, water withdrawals) have also been shown to alter the timing and magnitude of freshwater inflows, further influencing nutrient and phytoplankton dynamics (Shuster et al. 2005; Paerl et al. 2018). Overall decreases in freshwater inflows from riverine sources have been shown to alter nutrient inputs and increase water residence times. In the Nueces Estuary, extensive damming has decreased freshwater inflows (Montagna et al. 2009) and has been related to decreased loads of inorganic N reaching the estuary (Dunn 1996). Decreased inputs of nutrients coupled with longer residence times within an estuary have the potential to create a system that is more reliant on internal cycling of nutrients to support primary production and more susceptible to high biomass phytoplankton blooms following pulsed inputs of nutrients (Phlips et al. 2011).

Despite the large-scale urbanization and long-term decrease in freshwater inflows to Corpus Christi Bay, however, a recent trend analysis revealed only localized eutrophication

symptoms (Bugica et al. 2020). Nonetheless, with additional population increases projected, warming due to climate change, and further decreases in freshwater inflows expected due to both factors, it is important to understand what environmental conditions are important for regulating phytoplankton biovolume and phytoplankton community composition in the system. The purpose of this study was to quantify phytoplankton biovolume, community composition, and the environmental factors driving seasonal and spatial variability phytoplankton dynamics. To date there have been few studies addressing phytoplankton dynamics in the CCB system, and as such there is little information to guide resource managers in predicting possible changes to the system under future climate change scenarios.

Environmental Dynamics

Nutrient dynamics in the CCB system were driven by localized inputs of allochthonous nutrients and internal cycling of nutrients. NOx and PO_4^{3-} were inversely related to salinity at most of the sites studied here, indicating a relationship with freshwater inflows, though PO_4^{3-} demonstrated no relationship with salinity at sites with no freshwater inflows (Laguna Madre, Canals). These findings are in line with a previous study in CCB (Turner et al. 2015) and other studies documenting NOx as a predominantly watershed derived nutrient (Caffrey et al. 2007; Jordan et al. 2018; Cira et al. 2021) and increased orthophosphate concentrations in urban stormwater runoff (Yang and Toor 2017) and runoff from streams impacted by human-influenced land uses (Mallin et al. 2009; Cloern 2019). Concentrations of NH_4^+ were generally unrelated to salinity. This lack of a relationship indicates that like other shallow lagoonal systems, sources of NH_4^+ were predominantly internal such as porewater, groundwater and/or water column recycling (McCarthy et al. 2008; Glibert et al. 2010; Reyna et al. 2017; Geyer et al. 2018; Cira et al. 2021). Temperature and salinity were positively correlated with DON at all

sites other than Packery Channel indicating an internal source for this nutrient. This pattern of increased DON during warm, high salinity periods, indicates that increased phytoplankton production and subsequent remineralization through cellular degradation, combined with lack of dilution from freshwater inflows, is important in the accumulation of DON. Sources of SiO_4 were more variable across sites than the other nutrients examined. At Cole Park, SiO_4 was inversely related to salinity, consistent with a watershed source. Other sites showed no relationship or a positive relationship (Laguna Madre, Canal). These findings indicate that while there may be a watershed source of SiO_4 that was important directly adjacent to a stormwater runoff drain, there are internal sources of regenerated SiO_4 at sites that do not receive freshwater inflows (Paudel et al. 2015; Wetz et al. 2016).

Phytoplankton Biovolume and Community Composition

Phytoplankton biovolume varied in a unimodal pattern with biovolume peaking in spring and summer, followed by a decline into fall and winter. The seasonal patterns observed were similar to those reported in other Texas estuaries (Reyna et al. 2017; Chin 2020; Cira et al. 2021) and around the globe (Pinckney et al. 1998; Cloern and Jassby 2010; Guinder et al. 2010; Baek et al. 2015; Nohe et al. 2020). Phytoplankton dynamics in the CCB system were not exclusively driven by nutrient availability, as relationships with temperature, salinity, rainfall, and DSR were also evident. Fall and winter biovolume tended to be limited by factors other than nutrients, with temperature, light, and physical loss processes influencing phytoplankton growth, whereas spring and summer biovolume tended to be limited by nutrient availability. I elaborate below.

During the fall, decreases in salinity driven by precipitation events resulted in declines in phytoplankton biovolume. Patterns of decreased biovolume following precipitation has been observed in other Texas estuaries (Dorado et al. 2015; Reyna et al. 2017; Chin 2020; Cira et al.

2021), typically followed by an increase in biovolume associated with increased nutrient availability. In a nutrient addition bioassay conducted during the fall of 2017, phytoplankton growth was stimulated by additions of N, indicating that phytoplankton during this season were indeed nutrient limited (see Chapter II). Microzooplankton grazing rates during the fall were found to approximate phytoplankton growth rates under ambient nutrient conditions (Tominack unpubl. data), but the net growth of phytoplankton following N additions (Chapter II) suggests that following inputs of precipitation-derived nutrients *in situ*, microzooplankton grazing is likely not able to control phytoplankton growth. Therefore, in line with findings from other estuarine systems, this lack of growth in situ must have been related to increased hydraulic flushing and washout of phytoplankton biovolume (Roelke et al. 2013; Dorado et al. 2015). The more pronounced declines in biovolume associated with prolonged El Niño-driven rainfall during the fall of 2018 support the role of flushing in limiting fall phytoplankton biovolume accumulation. Other factors such as seasonal declines in temperature and day length likely also acted to diminish a potential response of phytoplankton to inputs of watershed derived nutrients. During the winter, despite generally high concentrations of NOx and NH_4^+ and near balanced DIN:DIP ratios (15.94), phytoplankton biovolume remained low. Limitation of winter phytoplankton communities by low temperatures and shorter day length have been observed elsewhere (Cloern et al. 1999; Fisher et al. 1999; Lomas and Glibert 1999; Örnólfsdóttir et al. 2004; Cira et al. 2016). Likewise, during a winter nutrient addition bioassay in CCB, phytoplankton growth rates did not respond to added N over 48 hours (see Chapter II).

During the spring and summer, phytoplankton biovolume appears to be influenced by nutrient availability. As the availability of light and temperature increased in the spring, phytoplankton biovolume also increased concomitant with a decrease in NOx and PO_4^{3-}.

Increased temperatures and light availability have often been related to spring phytoplankton blooms across estuarine ecosystems (Sverdrup 1953; Pinckney et al. 1998; Winder and Sommer 2012; Nohe et al. 2020). Despite continued declines in ambient NOx, phytoplankton biovolume remained elevated through the summer. The high degree of nutrient regeneration typical of shallow low-inflow estuaries (Pinckney et al. 2001; Glibert et al. 2010; Geyer et al. 2018), was likely an important factor in supplying phytoplankton with N to maintain elevated biovolume, though accumulation was still limited by N availability. Peaks in biovolume during these seasons tended to occur following precipitation events, in contrast to that observed during the fall, indicating that nutrients were a strong controlling factor for phytoplankton accumulation. Like that observed in the fall, microzooplankton grazing rates were similar to phytoplankton growth rates (Tominack unpubl. data) and pulsed N additions elicited phytoplankton growth rates that outpaced grazing rates (see Chapter II), further supporting a primary role for nutrient limitation in regulating phytoplankton biovolume during these seasons. During the spring and summer, the ability of phytoplankton to overcome the effects of flushing was likely related to the frequency of precipitation events. Over the course of this study fall months experienced a total of 35 precipitation events producing greater than 0.1 inch of rain, whereas spring months experienced a total of 18 events and summer months experienced a total of 19 events. The more frequent occurrence of precipitation during the fall may have produced more continuous effects of washout compared to spring and summer. Additionally, the warmer temperatures during the spring and summer would have supported faster growth rates in response to nutrient inputs compared to the fall.

Biovolume of each of the four major taxonomic groups investigated here also varied in unimodal patterns and the timing of peak biovolume for each group reflected known

physiological tolerances and environmental condition preferences. The winter community tended to be dominated by diatoms, with all other groups demonstrating significantly lower biovolume during winter compared to other seasons. Diatoms are known to be favored when temperatures are lower, the water column is well mixed, and concentrations of nutrients, especially NOx, are relatively high (Cloern and Dufford 2005; Suggett et al. 2009; Baek et al. 2015). During the spring, the community was more diverse, with diatoms, picocyanobacteria, and picoeukaryotes all demonstrating higher biovolume than summer (except picocyanobacteria), fall, and winter. Maintenance of elevated diatom biovolume through the spring is consistent with the ability of diatoms to respond rapidly to conditions favorable for growth (i.e., release from light and temperature limitations). Additionally, wind speed was higher during the spring than other seasons and was positively correlated with diatom biovolume, consistent with observations that diatoms are favored in more turbulent environments (Cloern and Dufford 2005; Baek et al. 2015). Importance of picocyanobacteria and picoeukaryotes during the spring was related to their preference for warmer temperatures (Worden et al. 2004; Gaulke et al. 2010; Paerl et al. 2020) and ability to be strong competitors for nutrients under both limiting (Agawin et al. 2000) and replete conditions (Gaulke et al. 2010). The summer and fall communities were also generally diverse, though the prevalence of dinoflagellates increased while the prevalence of diatoms and picoeukaryotes declined. In the summer, increased availability of reduced N forms (Glibert et al. 2016; Shangguan et al. 2017), decreased frequency of precipitation events, increased salinity, and increased water column stability (Paerl and Justić 2013; Baek et al. 2015; Dorado et al. 2015), as well as increased temperatures (Paerl et al. 2014; Dorado et al. 2015) drove the shift from diatom to dinoflagellate and picocyanobacteria dominance. During the fall of 2016 there was also a short-lived *K. brevis* red tide. Red tides are a frequent occurrence in the CCB system

and have been shown to be inversely related to El Niño conditions and positively related to salinity (see Chapter III). In contrast, during late summer-early fall of 2017, Hurricane Harvey made landfall on the south Texas coast and during 2018 El Niño conditions resulted in prolonged rainfall, which may have prevented significant *K. brevis* presence in the system (see Chapter III). Given future projections of drier and warmer conditions in this region, this indicates that the pattern of *K. brevis* occurrence may become more frequent and the prevalence of dinoflagellate taxa in general may become more pronounced during the fall.

Spatially, phytoplankton biovolume reflected both nutrient conditions and proximity to freshwater inflows (Bonilla et al. 2005; Roelke et al. 2013; Dorado et al. 2015). The lowest phytoplankton biovolume was observed at Cole Park where, despite higher nutrients, loss processes related to hydraulic flushing were likely most pronounced. The next lowest biovolume was observed at the Laguna Madre where nutrient concentrations tended to be lower than at all other sites. At this site, there were moderate increases in phytoplankton biovolume as salinity increased following precipitation events, supporting a role for nutrient availability in regulating phytoplankton biovolume. Overall, the Canal site demonstrated the highest phytoplankton biovolume and occasional occurrence of very high biovolume blooms. Nutrient concentrations (especially NH_4^+) were also generally high at the Canal site. The highly restricted flow typical of canal systems (Maxted et al. 1997) likely contributed to the accumulation of nutrients, phytoplankton, and limited hydraulic flushing observed at this site. This finding is in line with results from other studies demonstrating generally high phytoplankton biomass in canals compared to open portions of bay systems (Maxted et al. 1997; Ma et al. 2006). Additionally, the occurrence of high biomass blooms of dinoflagellates and raphidophytes following pulsed

nutrient inputs as seen here in the Canal site have also been documented in dead-end canal systems in coastal Delaware (Bourdelais et al. 2002; Ma et al. 2006).

Spatial variability in the prevalence of the four major taxonomic groups investigated here was not as pronounced as seasonal variability. Diatom biovolume was higher at Packery Channel compared to all other sites, with little variability found among the remaining sites. Tidal exchange with the Gulf of Mexico was likely influential in the prevalence of diatoms observed at this site. Diatoms are known to be important contributors to nearshore coastal phytoplankton communities throughout the northwestern Gulf of Mexico, where rapid growth rates help to balance growth and loss processes in this highly dynamic environment (Lambert et al. 1999; Chakraborty and Lohrenz 2015; Anglès et al. 2019). Dinoflagellate biovolume was higher at the Canal site than all other sites and lower at the Cole Park site than all sites other than Packery Channel. At the Canal site, the generally calm water conditions coupled with high concentrations of reduced N forms likely supported the higher biovolume of dinoflagellates observed here, whereas the high rates of hydraulic flushing at Cole Park and constant water movement via tidal exchange at Packery Channel were unfavorable for the accumulation of relatively slow growing dinoflagellates (Glibert et al. 2016; Shangguan et al. 2017; Paerl and Justić 2013; Baek et al. 2015; Dorado et al. 2015). Picocyanobacteria and picoeukaryotes both tended to be more prevalent at the Canal and Oso Inlet sites compared to others. Picocyanobacteria and picoeukaryotes are both known to be favored by reduced N forms (Glibert et al. 2010; Glibert et al. 2016; Shangguan et al. 2017), though both groups have also been shown to respond to pulsed inputs of oxidized N (Agawin et al. 2000; see Chapter II). At Oso Inlet, despite closer proximity to freshwater inflows from Oso Creek, export of picocyanobacteria and picoeukaryotes from upper reaches of Oso Bay may have contributed to the high prevalence of these groups, as has

been seen in other systems (Reyna et al. 2017; Paerl et al. 2020). At the Canal site, the generally calm conditions and limited flushing during precipitation events may have allowed both picocyanobacteria and picoeukaryotes to flourish (Gaulke et al. 2010; Zhang et al. 2013; Dorado et al. 2015; Paerl et al. 2020).

Future Implications

Under future climate change scenarios, the Texas Coastal Bend region is predicted to become warmer and drier overall, with continued population growth and expanding urban areas (Pachauri et al. 2014; Nielsen-Gammon et al. 2020; U.S. Census Bureau). There is potential for these changes in climatology to affect phytoplankton biovolume accumulation and community composition. As the region becomes drier and freshwater withdrawals to meet human demands increase, further decreases in freshwater inflows are expected to result in decreases in nutrient inputs and increased salinity/residence time throughout the system. The increased prevalence of dinoflagellates and picocyanobacteria during periods of low precipitation (summer-early fall) and increased concentrations of reduced N forms indicate that these groups may become more persistently dominant in the future (Ferreira et al. 2005; Glibert et al. 2005; Altman and Paerl 2012; de Souza et al. 2014). Documented linkages between the frequency of *K. brevis* red tides and salinity also indicate that there is likely to be a shift to more frequent occurrence of red tides under future climate scenarios. It can also be expected that localized high biovolume blooms will continue to occur and possibly expand following pulsed inputs of nutrients, given the observed high biomass blooms at the Canal site and the expansion of these man-made landforms in this region. Furthermore, increased winter-spring temperatures will likely shift the spring bloom forward in time (Guinder et al. 2010; Winder and Sommer 2012; Nohe et al. 2020), potentially resulting in earlier depletion of NOx and succession from diatoms to picophytoplankton and

dinoflagellates, which will have important implications for system productivity and food webs. Observed differences in average cell size of diatoms (smaller) and dinoflagellates (larger) over the course of this study also indicate that a shift to increased prevalence of dinoflagellates has the potential to alter carbon cycling and availability to higher trophic levels.

Continued field monitoring programs throughout the CCB system are warranted given minimal current knowledge and potential for change outlined here. Additionally, further work investigating the response of phytoplankton to pulsed nutrient inputs under varying climatic conditions is needed to better resolve future impacts of a changing climate. Longer duration nutrient addition bioassays (> 48 hours) over a wider range of initial conditions, regions of the system, and nutrient amendments should be conducted to help tease apart the interactive effects of temperature, nutrients, and initial phytoplankton community in driving observed climate change effects. During the 48-hour experiments conducted concurrent with this study (see Chapter II), dinoflagellate growth rates did not respond to added N, though during this field study, precipitation-derived N inputs were seen to stimulate a high biovolume bloom in the restricted Canal site (~ 72 hours between rainfall and sampling). As suggested by Roelke et al. (1999) and the results of the bioassays reported in Chapter II, pulsed nutrient inputs may help to buffer a system from extreme changes in phytoplankton biovolume and community composition in response to nutrient enrichment. Chin (2020), however, demonstrated increased dinoflagellate biovolume following El Niño-driven precipitation and nutrient inputs at sites located in central CCB. Combined with the dynamics observed at the Canal site here and projected changing climatology of the south Texas region these results indicate that this buffer may not persist in the CCB system where hydraulic flushing and changes in residence time are most pronounced along the immediate shoreline that is heavily influenced by stormwater runoff drains. The high

capacity of this system for internal nutrient cycling, tight benthic-pelagic coupling, and lack of dominant riverine inflows make understanding and managing nutrient conditions in this system a challenge. A better understanding of internal sources of nutrients, the role of environmental conditions in driving nutrient cycling pathways, and the role phytoplankton productivity plays in driving these dynamics will provide natural resource managers with the information necessary to project future conditions. Lastly, freshwater management assessments do not explicitly take phytoplankton community composition or HAB formation potential into account. In a system such as CCB where decreased flows have the potential to lead to shifts in total phytoplankton biovolume and community composition, as well as the occurrence of *K. brevis* red tides (see Chapter III), assessing the role freshwater management may play in phytoplankton dynamics will be paramount.

Conclusion

Phytoplankton in the CCB system, similar to many other estuarine systems, are primarily limited by the availability of nutrients, N in particular. Factors such as freshwater inflows, precipitation, hydrological modifications, and temperature were, however, also important in driving whole community and major taxonomic group dynamics. The general low riverine inflows and the limited spatial extent of influence from sources such as stormwater runoff and wastewater may be acting to buffer the CCB system from displaying widespread effects of eutrophication, compared to river dominated systems where watershed nutrients follow a more direct, concentrated path to the estuary. Given projections for further alterations in nutrient dynamics, freshwater inflows, temperature, and other climatological characteristics, however, it is critical to continue working towards a more complete understanding of the drivers of phytoplankton dynamics in the CCB system.

References

Agawin, N. S. R., C. M. Duarte, and S. Agustí. 2000. Nutrient and temperature control of the contribution of picoplankton to phytoplankton biomass and production. *Limnology and Oceanography* 45. American Society of Limnology and Oceanography Inc.: 591–600. https://doi.org/10.4319/lo.2000.45.3.0591.

Altman, J. C., & Paerl, H. W. (2012). Composition of inorganic and organic nutrient sources influences phytoplankton community structure in the New River Estuary, North Carolina. *Aquatic Ecology*, *46*(3), 269–282. https://doi.org/10.1007/s10452-012-9398-8

Applebaum, S., Montagna, P. A., & Ritter, C. (2005). Status and trends of dissolved oxygen in Corpus Christi Bay, Texas, U.S.A. *Environmental Monitoring and Assessment*, *107*(1–3), 297–311. https://doi.org/10.1007/s10661-005-3111-5

Azam, F., T. Fenchel, J. Field, J. Gray, L. Meyer-Reil, and F. Thingstad. 1983. The Ecological Role of Water-Column Microbes in the Sea. *Marine Ecology Progress Series* 10: 257–263. https://doi.org/10.3354/meps010257.

Baek, S. H., D. Kim, M. Son, S. M. Yun, and Y. O. Kim. 2015. Seasonal distribution of phytoplankton assemblages and nutrient-enriched bioassays as indicators of nutrient limitation of phytoplankton growth in Gwangyang Bay, Korea. *Estuarine, Coastal and Shelf Science* 163. Academic Press: 265–278. https://doi.org/10.1016/j.ecss.2014.12.035.

Bonilla, S., D. Conde, L. Aubriot, and M. D. C. Pérez. 2005. Influence of hydrology on phytoplankton species composition and life strategies in a subtropical coastal lagoon periodically connected with the Atlantic Ocean. *Estuaries* 28: 884–895. https://doi.org/10.1007/BF02696017.

Bourdelais, A. J., C. R. Tomas, J. Naar, J. Kubanek, and D. G. Baden. 2002. New fish-killing alga in coastal Delaware produces neurotoxins. *Environmental Health Perspectives* 110: 465–470.

Bugica, K., B. Sterba-Boatwright, and M. S. Wetz. 2020. Water quality trends in Texas estuaries. *Marine Pollution Bulletin* 152. Elsevier Ltd. https://doi.org/10.1016/j.marpolbul.2020.110903.

Burkholder, J. A. M., P. M. Glibert, and H. M. Skelton. 2008. Mixotrophy, a major mode of nutrition for harmful algal species in eutrophic waters. *Harmful Algae* 8: 77–93. https://doi.org/10.1016/j.hal.2008.08.010.

Caffrey, J. M., T. P. Chapin, H. W. Jannasch, J. C. Haskins. 2007. High nutrient pulses, tidal mixing and biological response in a small California estuary: Variability in nutrient Concentrations from decadal to hourly time scales. *Estuarine, Coastal and Shelf Science* 71: 368-380. doi:10.1016/j.ecss.2006.08.015.

Caron, D. A., and D. A. Hutchins. 2013. The effects of changing climate on microzooplankton grazing and community structure: Drivers, predictions and knowledge gaps. *Journal of Plankton Research* 35: 235–252. https://doi.org/10.1093/plankt/fbs091.

Chakraborty, S., and S. E. Lohrenz. 2015. Phytoplankton community structure in the river-influenced continental margin of the northern Gulf of Mexico. *Marine Ecology Progress Series* 521: 31–47. https://doi.org/10.3354/meps11107.

Chin, T. L. 2020. Comparison of phytoplankton biomass and community composition in three Texas estuaries differing in freshwater inflow regime. Doctoral Dissertation Texas A&M University – Corpus Christi.

Cira, E. K., H. W. Paerl, and M. S. Wetz. 2016. Effects of nitrogen availability and form on phytoplankton growth in a eutrophied estuary (Neuse River Estuary, NC, USA). Edited by Christopher J. Gobler. *PLoS ONE* 11. Public Library of Science: e0160663. https://doi.org/10.1371/journal.pone.0160663.

Cira, E. K., T. A. Palmer, M. S. Wetz. 2021. Phytoplankton dynamics in a low-inflow estuary (Baffin Bay, TX) during drought and high-rainfall conditions associated with an El Niño event. *Estuaries and Coasts*. doi:10.1007/s12237-021-00904-7.

Clarke, K. R., & Gorley, R. N. (2015). Getting started with PRIMER v7. *PRIMER-E: Plymouth, Plymouth Marine Laboratory*, 20.

Cloern, J. E. 1999. The relative importance of light and nutrient limitation of phytoplankton growth: A simple index of coastal ecosystem sensitivity to nutrient enrichment. *Aquatic Ecology* 33: 3–19.

Cloern, J. E. 2019. Patterns, pace, and processes of water-quality variability in a long-studied estuary. *Limnology and Oceanography* 64: S192-S208. doi:10.1002/lno.10958.

Cloern, J. E., & Nichols, F. H. (1985). Time scales and mechanisms of estuarine variability, a synthesis from studies of San Francisco Bay. *Hydrobiologia*, *129*(1), 229–237. https://doi.org/10.1007/BF00048697

Cloern, J. E., and A. D. Jassby. 2008. Complex seasonal patterns of primary producers at the land-sea interface. *Ecology Letters* 11: 1294–1303. https://doi.org/10.1111/j.1461-0248.2008.01244.x.

Cloern, J. E., and A. D. Jassby. 2010. Patterns and scales of phytoplankton variability in estuarine-coastal ecosystems. *Estuaries and Coasts* 33: 230–241. https://doi.org/10.1007/s12237-009-9195-3.

Cloern, J. E., and R. Dufford. 2005. Phytoplankton community ecology: Principles applied in San Francisco Bay. *Marine Ecology Progress Series* 285: 11–28. https://doi.org/10.3354/meps285011.

Cloern, J. E., Foster, S. Q., & Kleckner, A. E. (2014). Phytoplankton primary production in the world's estuarine-coastal ecosystems. *Biogeosciences*, *11*(9), 2477–2501. https://doi.org/10.5194/bg-11-2477-2014

Davidson, K., R. J. Gowen, P. J. Harrison, L. E. Fleming, P. Hoagland, and G. Moschonas. 2014. Anthropogenic nutrients and harmful algae in coastal waters. *Journal of Environmental Management* 146. Academic Press: 206–216. https://doi.org/10.1016/j.jenvman.2014.07.002.

de Souza, K. B., Jephson, T., Hasper, T. B., & Carlsson, P. (2014). Species-specific dinoflagellate vertical distribution in temperature-stratified waters. *Marine Biology*, *161*(8), 1725–1734. https://doi.org/10.1007/s00227-014-2446-2

Dorado, S., T. Booe, J. Steichen, A. S. McInnes, R. Windham, A. Shepard, A. E. B. Lucchese, et al. 2015. Towards an understanding of the interactions between freshwater inflows and phytoplankton communities in a subtropical estuary in the Gulf of Mexico. *PLoS ONE* 10. Public Library of Science. https://doi.org/10.1371/journal.pone.0130931.

Dunn, D. E. 1996. Trends in nutrient inflows to the Gulf of Mexico from streams draining the conterminous United States, 1972-93. *U.S. GEOLOGICAL SURVEY Water-Resources Investigations Report 96–4113*: 68.

Ferreira, J. G., Wolff, W. J., Simas, T. C., & Bricker, S. B. (2005). Does biodiversity of estuarine phytoplankton depend on hydrology? *Ecological Modelling*, *187*(4), 513–523. https://doi.org/10.1016/j.ecolmodel.2005.03.013

Finkel, Z. v., J. Beardall, K. J. Flynn, A. Quigg, T. A. v. Rees, and J. A. Raven. 2010. Phytoplankton in a changing world: Cell size and elemental stoichiometry. *Journal of Plankton Research* 32: 119–137. https://doi.org/10.1093/plankt/fbp098.

Fisher, T. R., A. B. Gustafson, K. Sellner, R. Lacouture, L. W. Haas, R. L. Wetzel, R. Magnien, D. Everitt, B. Michaels, and R. Karrh. 1999. Spatial and temporal variation of resource limitation in Chesapeake Bay. *Marine Biology* 133: 763–778. https://doi.org/10.1007/s002270050518.

Flint, R. W. 1984. Phytoplankton production in the Corpus Christi Bay Estuary. *Contributions in Marine Science*.

Gaulke, A. K., M. S. Wetz, and H. W. Paerl. 2010. Picophytoplankton: A major contributor to planktonic biomass and primary production in a eutrophic, river-dominated estuary. *Estuarine, Coastal and Shelf Science* 90: 45–54. https://doi.org/10.1016/j.ecss.2010.08.006.

Geyer, N. L., M. Huettel, and M. S. Wetz. 2018. Phytoplankton Spatial Variability in the River-Dominated Estuary, Apalachicola Bay, Florida. *Estuaries and Coasts* 41. Springer New York LLC: 2024–2038. https://doi.org/10.1007/s12237-018-0402-y.

Gillanders, B., and M. Kingsford. 2002. Impact of Changes in Flow of Freshwater on Estuarine and Open Coastal Habitats and the Associated Organisms. *Oceanography and marine biology and annual review* 40: 233–309. https://doi.org/10.1201/9780203180594.ch5.

Glibert, P. M., Anderson, D. M., Gentien, P., Granéli, E., & Sellner, K. G. (2005). The Global, Complex Phenomena of Harmful Algal Blooms. *Oceanography*, *18*(2), 136–147. https://doi.org/10.1016/B978-0-12-385876-4.00020-7

Glibert, P. M., F. P. Wilkerson, R. C. Dugdale, J. A. Raven, C. L. Dupont, P. R. Leavitt, A. E. Parker, J. M. Burkholder, and T. M. Kana. 2016. Pluses and minuses of ammonium and nitrate uptake and assimilation by phytoplankton and implications for productivity and community composition, with emphasis on nitrogen-enriched conditions. *Limnology and Oceanography* 61. John Wiley & Sons, Ltd: 165–197. https://doi.org/10.1002/LNO.10203@10.1002/(ISSN)1939-5590.STABLE-ISOTOPES.

Glibert, P. M., J. N. Boyer, C. A. Heil, C. J. Madden, B. Sturgis, C. S. Wazniak. 2010. Blooms in lagoons: different from those of river-dominated estuaries. In *Coastal Lagoons: Critical Habitats of Environmental Change*, ed M. J. Kennish and H. W. Paerl, 91-113. Boca Raton: CRC Press.

Guinder, V. A., C. A. Popovich, J. C. Molinero, and G. M. E. Perillo. 2010. Long-term changes in phytoplankton phenology and community structure in the Bahía Blanca Estuary, Argentina. *Marine Biology* 157: 2703–2716. https://doi.org/10.1007/s00227-010-1530-5.

Hays, G. C., A. J. Richardson, and C. Robinson. 2005. Climate change and marine plankton. *Trends in Ecology and Evolution* 20. Elsevier Ltd: 337–344. https://doi.org/10.1016/j.tree.2005.03.004.

Holland, J., N. J. Maciolek, R. D. Kalke, L. Mullins, and C. H. Oppenheimer. *A Benthos and Plankton Study of the Corpus Christi, Copano and Aransas Bay Systems III. Report on Data Collected During the Period July 1974-May 1975 and Summary of the Three-year Project*.

Hothorn, T., Bretz, F., & Westfall, P. (2008). Simultaneous Inference in General Parametric Models. *Biometrical Journal*, *50*(3), 346–363.

Islam, M. S., J. S. Bonner, B. L. Edge, and C. A. Page. 2014. Hydrodynamic characterization of Corpus Christi Bay through modeling and observation. *Environmental Monitoring and Assessment* 186. Kluwer Academic Publishers: 7863–7876. https://doi.org/10.1007/s10661-014-3973-5.

Jordan, T. E., D. E. Weller, and C. E. Pelc. 2018. Effects of Local Watershed Land Use on Water Quality in Mid-Atlantic Coastal Bays and Subestuaries of the Chesapeake Bay. *Estuaries and Coasts* 41. Springer New York LLC: 38–53. https://doi.org/10.1007/s12237-017-0303-5.

Lambert, C. D., T. S. Bianchia, and P. H. Santschi. 1998. Cross-shelf changes in phytoplankton community composition in the Gulf of Mexico (Texas shelf/slope): The use of plant pigments as biomarkers. *Continental Shelf Research* 19: 1–21. https://doi.org/10.1016/S0278-4343(98)00075-2.

Lomas M. W., P. M. Glibert. 1999. Interactions between NH4+ and NO3- uptake and assimilation: comparisons of diatoms and dinoflagellates at several growth temperatures. *Marine Biology* 133: 541-551. doi:10.1007/s002270050494.

Ma, S., E. B. Whereat, and G. W. Luther III. 2006. Shift of algal community structure in dead end lagoons of the Delaware Inland Bays during seasonal anoxia. *Aquatic microbial ecology* 44: 279–290.

Mallin, M. A., and H. W. Paerl. 1994. Planktonic trophic transfer in an estuary: Seasonal, diel, and community structure effects. *Ecology* 75: 2168–2184. https://doi.org/10.2307/1940875.

Mallin, M. A., V. L. Johnson, and S. H. Ensign. 2009. Comparative impacts of stormwater runoff on water quality of an urban, a suburban, and a rural stream. *Environmental Monitoring and Assessment* 159: 475–491. https://doi.org/10.1007/s10661-008-0644-4.

Maxted, J. R., S. B. Weisberg, J. C. Chaillou, R. A. Eskin, and F. W. Kutz. 1997. The ecological condition of dead-end canals of the Delaware and Maryland coastal bays. *Estuaries* 20: 319–327. https://doi.org/10.2307/1352347.

McCarthy, M. D., and D. A. Bronk. 2008. Analytical Methods for the Study of Nitrogen. In *Nitrogen in the Marine Environment*, 1219–1275. Elsevier Inc. https://doi.org/10.1016/B978-0-12-372522-6.00028-1.

Montagna, P. A., E. M. Hill, and B. Moulton. 2009. Role of science-based and adaptive management in allocating environmental flows to the Nueces Estuary, Texas, USA. *WIT Transactions on Ecology and the Environment* 122. WITPress: 559–570. https://doi.org/10.2495/ECO090511.

Nielsen-Gammon, J., J. Banner, B. Cook, D. Tremaine, C. Wong, R. Mace, H. Gao, et al. 2020. Unprecedented drought challenges for Texas water resources in a changing climate: what do researchers and stakeholders need to know? *Earth's Future* 8. John Wiley & Sons, Ltd. https://doi.org/10.1029/2020EF001552.

Nohe, A., A. Goffin, L. Tyberghein, R. Lagring, K. de Cauwer, W. Vyverman, and K. Sabbe. 2020. Marked changes in diatom and dinoflagellate biomass, composition and seasonality in the Belgian Part of the North Sea between the 1970s and 2000s. *Science of the Total Environment* 716. Elsevier B.V. https://doi.org/10.1016/j.scitotenv.2019.136316.

Örnólfsdóttir, E. B., S. E. Lumsden, and J. L. Pinckney. 2004. Nutrient pulsing as a regulator of phytoplankton abundance and community composition in Galveston Bay, Texas. *Journal*

of Experimental Marine Biology and Ecology 303: 197–220. https://doi.org/10.1016/j.jembe.2003.11.016.

Pachauri, R. K., Allen, M. R., Barros, V. R., Broome, J., Cramer, W., Christ, R., Church, J. A., Clarke, L., Dahe, Q., Dasgupta, P., Dubash, N. K., Edenhofer, O., Elgizouli, I., Field, C. B., Forster, P., Friedlingstein, P., Fuglestvedt, J., Gomez-Echeverri, L., Hallegatte, S., … van Ypserle, J.-P. (2014). *Climate Change 2014: Synthesis Report. Contribution of Working Groups I, II and III to the Fifth Assessment Report of the Intergovernmental Panel on Climate Change* (R. K. Pachauri & L. Meyer, Eds.). IPCC.

Paerl, H. W. 2006. Assessing and managing nutrient-enhanced eutrophication in estuarine and coastal waters: Interactive effects of human and climatic perturbations. *Ecological Engineering* 26: 40–54. https://doi.org/10.1016/j.ecoleng.2005.09.006.

Paerl, H. W., and D. Justić. 2013. Estuarine phytoplankton. In *Estuarine ecology*, Second, 85–110. Wiley Online Library.

Paerl, H. W., and V. J. Paul. 2012. Climate change: Links to global expansion of harmful cyanobacteria. *Water Research* 46. Elsevier Ltd: 1349–1363. https://doi.org/10.1016/j.watres.2011.08.002.

Paerl, H. W., N. S. Hall, B. L. Peierls, and K. L. Rossignol. 2014. Evolving Paradigms and Challenges in Estuarine and Coastal Eutrophication Dynamics in a Culturally and Climatically Stressed World. *Estuaries and Coasts* 37. https://doi.org/10.1007/s12237-014-9773-x.

Paerl, H. W., T. G. Otten, and R. Kudela. 2018. Mitigating the Expansion of Harmful Algal Blooms Across the Freshwater-to-Marine Continuum. *Environmental Science and*

Technology 52. American Chemical Society: 5519–5529. https://doi.org/10.1021/acs.est.7b05950.

Paerl, H. W., K. L. Rossignol, S. N. Hall, B. L. Peierls, and M. S. Wetz. 2010. Phytoplankton community indicators of short- and long-term ecological change in the anthropogenically and climatically impacted neuse river estuary, North Carolina, USA. *Estuaries and Coasts* 33: 485–497. https://doi.org/10.1007/s12237-009-9137-0.

Paerl, R. W., R. E. Venezia, J. J. Sanchez, H. W. Paerl. 2020. Picophytoplankton dynamics in a large temperature estuary and impacts of extreme storm events. *Scientific Reports* 10:22026. doi:10.1038/s41598-020-79157-6.

Parsons, M. L., and Q. Dortch. 2002. Sedimentological evidence of an increase in Pseudo-nitzschia (Bacillariophyceae) abundance in response to coastal eutrophication. *Limnology and Oceanography* 47: 551–558. https://doi.org/10.4319/lo.2002.47.2.0551.

Paudel, B., P. A. Montagna, and L. Adams. 2015. Variations in the release of silicate and orthophosphate along a salinity gradient: Do sediment composition and physical forcing have roles? *Estuarine, Coastal and Shelf Science* 157. Elsevier Ltd: 42–50. https://doi.org/10.1016/j.ecss.2015.02.011.

Peierls, B. L., N. S. Hall, and H. W. Paerl. 2012. Non-monotonic responses of phytoplankton biomass accumulation to hydrologic variability: A comparison of two coastal plain north carolina estuaries. *Estuaries and Coasts* 35. https://doi.org/10.1007/s12237-012-9547-2.

Peierls, B. L., R. R. Christian, and H. W. Paerl. 2003. Water Quality and Phytoplankton as Indicators of Hurricane Impacts on a Large Estuarine Ecosystem. *Estuaries* 26. https://doi.org/10.1007/BF02803635.

Pennock, J. R., J. N. Boyer, J. A. Herrera-Silveira, R. L. Iverson, T. E. Whitledge, B. Mortazavi, and F. A. Comin. 1999. Nutrient Behavior and Phytoplankton Production in Gulf of Mexico Estuaries. In *Biogeochemistry of Gulf of Mexico Estuaries*, ed. T. S. Bianchi, J. R. Pennock, and R. R. Twilley, 109–162. John Wiley and Sons, Inc.

Phlips, E. J., S. Badylak, M. Christman, J. Wolny, J. Brame, J. Garland, L. Hall, et al. 2011. Scales of temporal and spatial variability in the distribution of harmful algae species in the Indian River Lagoon, Florida, USA. *Harmful Algae* 10. Elsevier B.V.: 277–290. https://doi.org/10.1016/j.hal.2010.11.001.

Phlips, E. J., S. Badylak, N. G. Nelson, and K. E. Havens. 2020. Hurricanes, El Niño and harmful algal blooms in two sub-tropical Florida estuaries: Direct and indirect impacts. *Scientific Reports* 10: 1–12. https://doi.org/10.1038/s41598-020-58771-4.

Pinckney, J. L., H. W. Paerl, M. B. Harrington, and K. E. Howe. 1998. Annual cycles of phytoplankton community-structure and bloom dynamics in the Neuse River Estuary, North Carolina. *Marine Biology* 131: 371–381. https://doi.org/10.1007/s002270050330.

Pinckney, J. L., H. W. Paerl, P. Tester, T. L. Richardson. 2001. The role of nutrient loading and eutrophication in estuarine ecology. *Environmental Health Perspectives* 109: 699-706. doi:10.1289/ehp.01109s5699.

Pinheiro, J., D. Bates, S. DebRoy, D. Sarkar, and R Core Team. 2020. {nlme}: Linear and Nonlinear Mixed Effects Models.

Quigg, A., M. Al-Ansi, N. N. al Din, C. L. Wei, C. C. Nunnally, I. S. Al-Ansari, G. T. Rowe, et al. 2013. Phytoplankton along the coastal shelf of an oligotrophic hypersaline environment in a semi-enclosed marginal sea: Qatar (Arabian Gulf). *Continental Shelf Research* 60. Elsevier: 1–16. https://doi.org/10.1016/j.csr.2013.04.015.

Quinn, G. P., and M. J. Keough. 2002. *Experimental design and data analysis for biologists*. Cambridge university press.

R Core Team. 2019. R: A Language and Environment for Statistical Computing. Vienna, Austria.

Reyna, N. E., A. K. Hardison, Z. Liu. 2017. Influence of major storm events on the quantity and composition of particulate organic matter and the phytoplankton composition in a subtropical estuary, Texas. *Frontiers in Marine Science* 4: 43. doi:10.3389/mars.2017.00043.

Ritter, C., and P. A. Montagna. 1999. Seasonal hypoxia and models of benthic response in a Texas Bay. *Estuaries* 22: 7–20. https://doi.org/10.2307/1352922.

Roelke, D. L., H. P. Li, N. J. Hayden, C. J. Miller, S. E. Davis, A. Quigg, and Y. Buyukates. 2013. Co-occurring and opposing freshwater inflow effects on phytoplankton biomass, productivity and community composition of Galveston Bay, USA. *Marine Ecology Progress Series* 477: 61–76. https://doi.org/10.3354/meps10182.

Roelke, D. L., L. A. Cifuentes, and P. M. Eldridge. 1997. Nutrient and phytoplankton dynamics in a sewage-impacted gulf coast estuary: A field test of the PEG-model and Equilibrium Resource Competition theory. *Estuaries* 20: 725–742. https://doi.org/10.2307/1352247.

Roelke, D. L., P. M. Eldridge, and L. A. Cifuentes. 1999. A model of phytoplankton competition for limiting and nonlimiting nutrients: Implications for development of estuarine and nearshore management schemes. *Estuaries* 22: 92–104. https://doi.org/10.2307/1352930.

Seitzinger, S. P., R. W. Sanders, and R. Styles. 2002. Bioavailability of DON from natural and anthropogenic sources to estuarine plankton. *Limnology and Oceanography* 47: 353–366. https://doi.org/10.4319/lo.2002.47.2.0353.

Shangguan, Y., P. M. Glibert, J. A. Alexander, C. J. Madden, and S. Murasko. 2017. Nutrients and phytoplankton in semienclosed lagoon systems in Florida Bay and their responses to changes in flow from Everglades restoration. *Limnology and Oceanography* 62: S327–S347. https://doi.org/10.1002/lno.10599.

Shuster, W. D., J. Bonta, H. Thurston, E. Warnemuende, and D. R. Smith. 2005. Impacts of impervious surface on watershed hydrology: A review. *Urban Water Journal* 2. Taylor \& Francis: 263–275.

Suggett, D. J., C. M. Moore, A. E. Hickman, and R. J. Geider. 2009. Interpretation of fast repetition rate (FRR) fluorescence: Signatures of phytoplankton community structure versus physiological state. *Marine Ecology Progress Series* 376: 1–19. https://doi.org/10.3354/meps07830.

Sun, J., & Liu, D. (2003). Geometric models for calculating cell biovolume and surface area for phytoplankton. *Journal of Plankton Research, 25*(11), 1331–1346. https://doi.org/10.1093/plankt/fbg096

Sverdrup, H. U. 1953. On conditions for the vernal blooms of phytoplankton. *Journal du Conseil* 18: 287-295.

Turner, E. L., B. Paudel, and P. A. Montagna. 2015. Baseline nutrient dynamics in shallow well mixed coastal lagoon with seasonal harmful algal blooms and hypoxia formation. *Marine Pollution Bulletin* 96. Elsevier Ltd: 456–462. https://doi.org/10.1016/j.marpolbul.2015.05.005.

Wang, Y., H. Xu, and M. Li. 2021. Long-term changes in phytoplankton communities in China's Yangtze Estuary driven by altered riverine fluxes and rising sea surface temperature.

Geomorphology 376. Elsevier B.V.: 107566. https://doi.org/10.1016/j.geomorph.2020.107566.

Wells, M. L., V. L. Trainer, T. J. Smayda, B. S. O. Karlson, C. G. Trick, R. M. Kudela, A. Ishikawa, et al. 2015. Harmful algal blooms and climate change: Learning from the past and present to forecast the future. *Harmful Algae* 49. Elsevier B.V.: 68–93. https://doi.org/10.1016/j.hal.2015.07.009.

Wetz, M. S., E. K. Cira, B. Sterba-Boatwright, P. A. Montagna, T. A. Palmer, and K. C. Hayes. 2017. Exceptionally high organic nitrogen concentrations in a semi-arid South Texas estuary susceptible to brown tide blooms. *Estuarine, Coastal and Shelf Science* 188. Elsevier Ltd: 27–37. https://doi.org/10.1016/j.ecss.2017.02.001.

Wetz, M. S., K. C. Hayes, K. V. B. Fisher, L. Price, and B. Sterba-Boatwright. 2016. Water quality dynamics in an urbanizing subtropical estuary(Oso Bay, Texas). *Marine Pollution Bulletin* 104. Elsevier Ltd: 44–53. https://doi.org/10.1016/j.marpolbul.2016.02.013.

Winder, M., and U. Sommer. 2012. Phytoplankton response to a changing climate. *Hydrobiologia* 698: 5–16. https://doi.org/10.1007/s10750-012-1149-2.

Worden, A. Z., J. K. Nolan, and B. Palenik. 2004. Assessing the dynamics and ecology of marine picophytoplankton: The importance of the eukaryotic component. *Limnology and Oceanography* 49: 168–179. https://doi.org/10.4319/lo.2004.49.1.0168.

Yang, Y. Y., and G. S. Toor. 2017. Sources and mechanisms of nitrate and orthophosphate transport in urban stormwater runoff from residential catchments. *Water Research* 112. Elsevier Ltd: 176–184. https://doi.org/10.1016/j.watres.2017.01.039.

Yeager, K. M., P. H. Santschi, K. J. Schindler, M. J. Andres, and E. A. Weaver. 2006. The relative importance of terrestrial versus marine sediment sources to the Nueces-Corpus

Christi Estuary, Texas: An isotopic approach. *Estuaries and Coasts* 29: 443–454. https://doi.org/10.1007/BF02784992.

Yin, K., J. Zhang, P. Y. Qian, W. Jian, L. Huang, J. Chen, and M. C. S. Wu. 2004. Effect of wind events on phytoplankton blooms in the Pearl River estuary during summer. *Continental Shelf Research* 24: 1909–1923. https://doi.org/10.1016/j.csr.2004.06.015.

Zhang, X., Z. Shi, Q Liu, F. Ye, L Tian, X. Huang. 2013. Spatial and temporal variations of picoplankton in three contrasting periods in the Peral River Estuary, South China. *Continental Shelf Research* 56:1-12. doi:10.1016/j.csr.2013.01.015.

Zingone, A., E. J. Phlips, and P. J. Harrison. 2010. Multiscale variability of twenty-two coastal phytoplankton time series: A global scale comparison. *Estuaries and Coasts* 33: 224–229. https://doi.org/10.1007/s12237-009-9261-x.

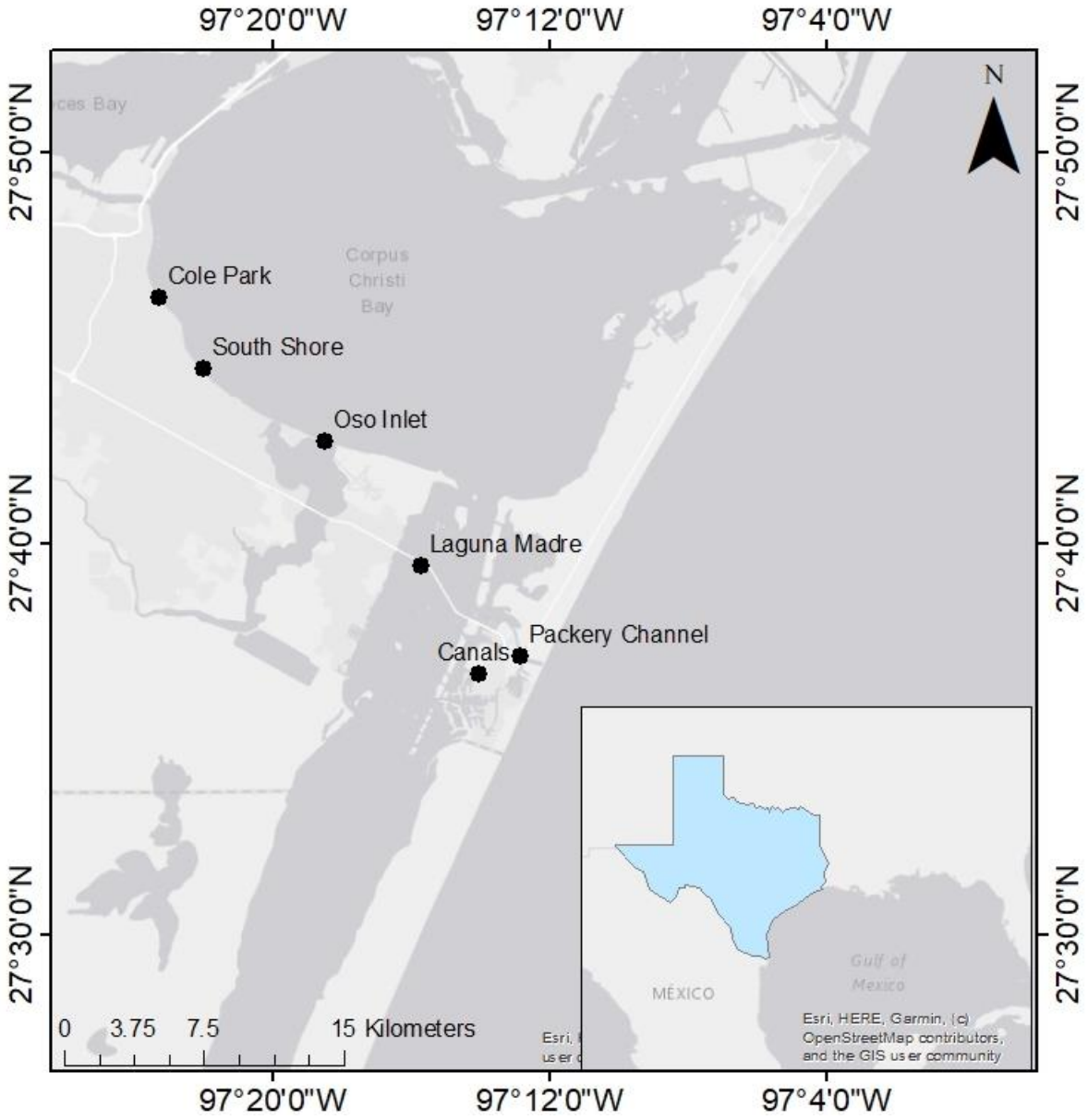

Fig. 1.1 Location of sampling sites throughout Corpus Christi Bay. Corpus Christi is denoted with a star in the inset map.

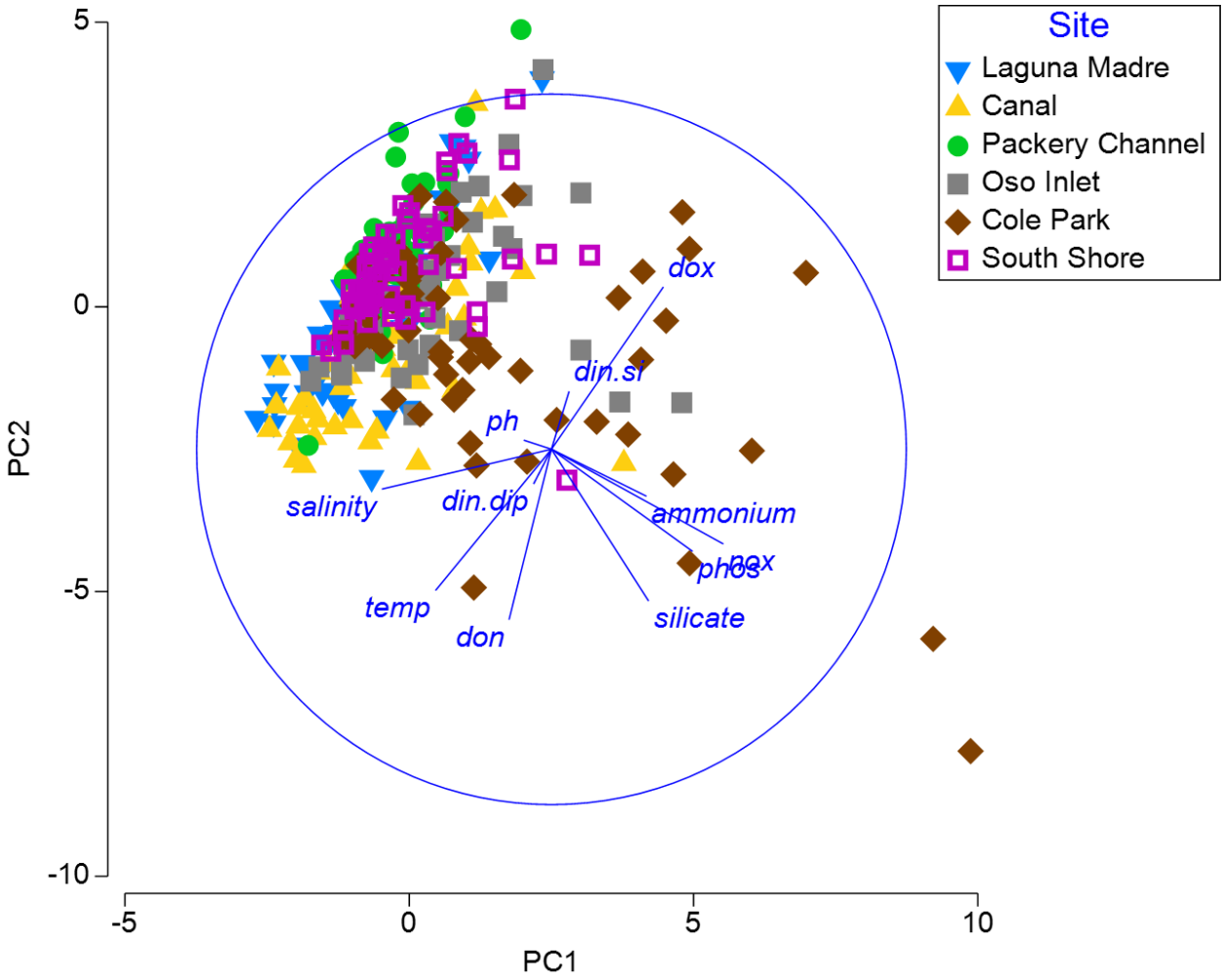

Fig 1.2 PCA plot with sampling events coded by sampling site. Variable abbreviations are as follows, temperature (temp), dissolved oxygen (dox), dissolved organic nitrogen (don), and nitrate + nitrite (nox), phosphate (phos). All other variables are as displayed.

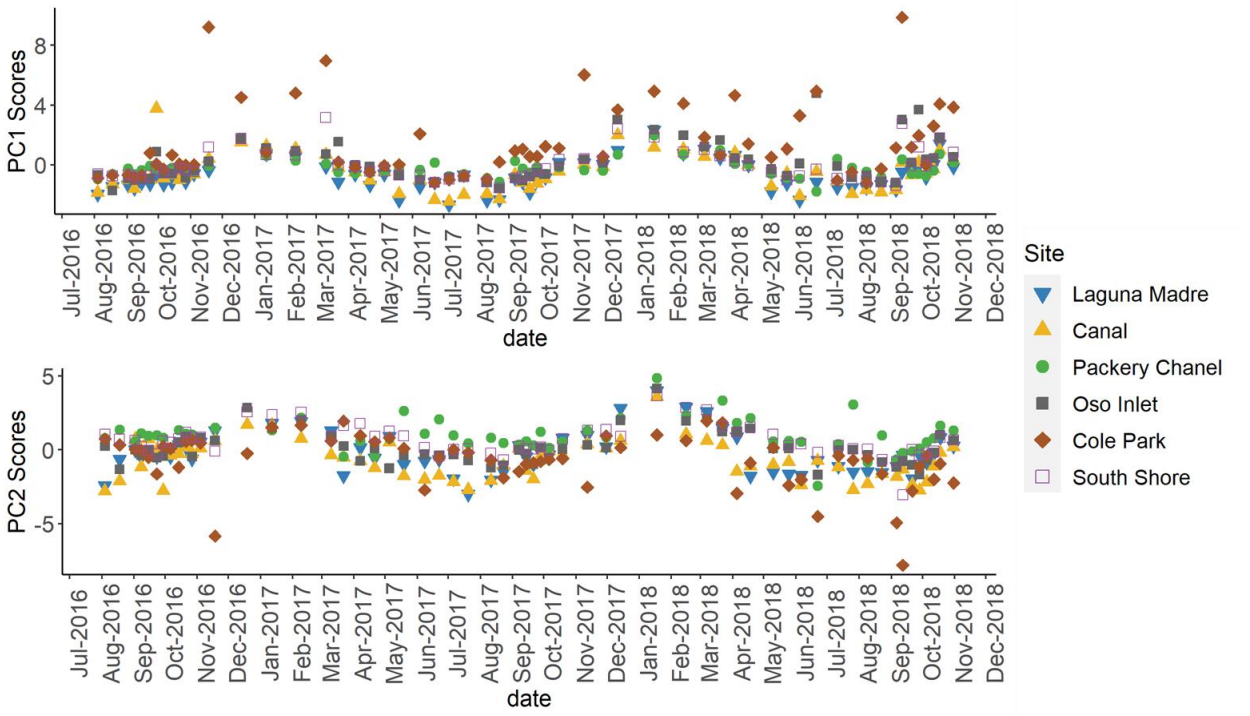

Fig 1.3 Principal component scores plotted over time and coded by site to better resolve the spatial variability associated with stochasticity and seasonality.

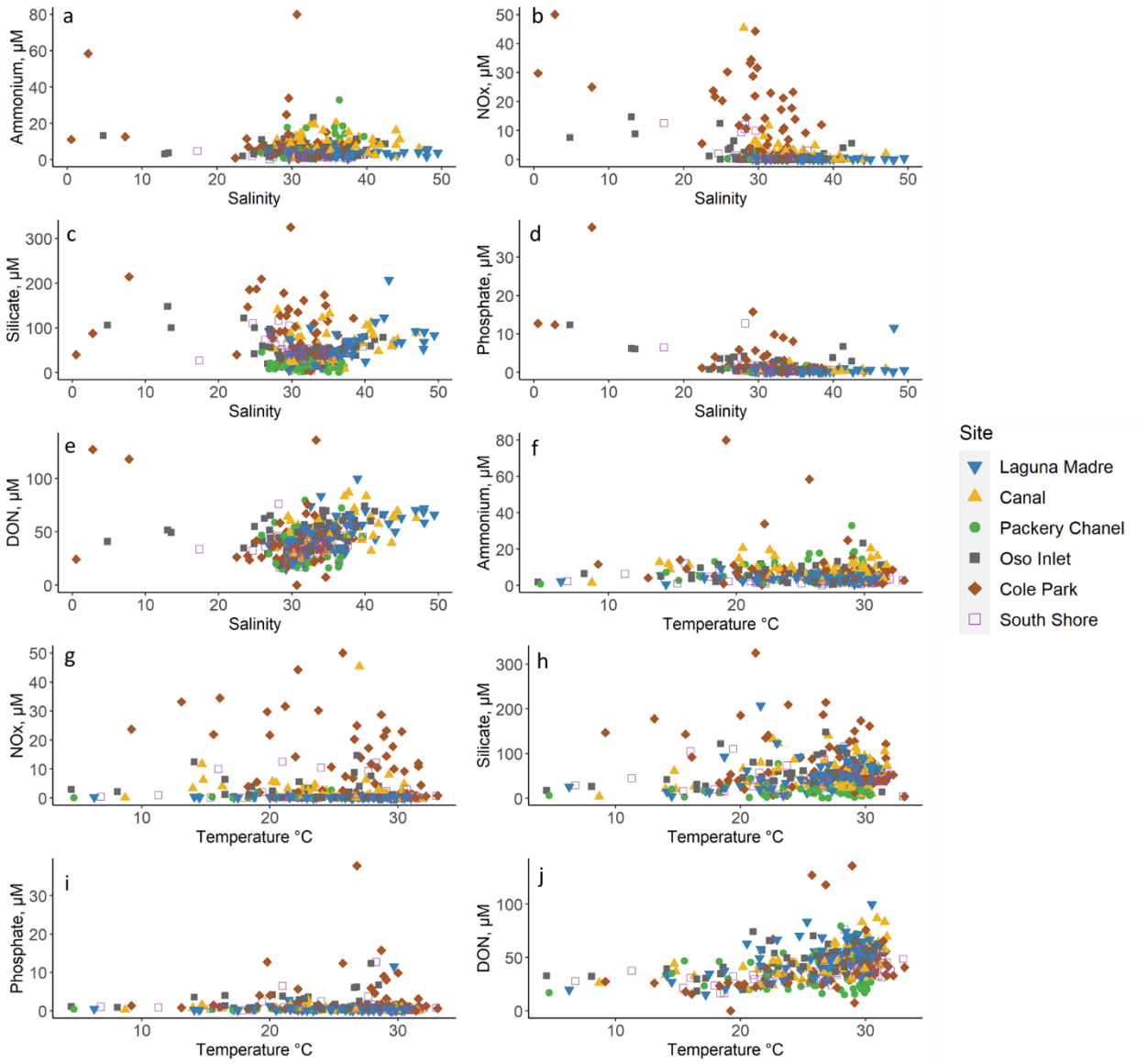

Fig 1.4 Plots of ammonium, NOx, silicate, phosphate, and DON plotted against salinity (a - e) and temperature (f - j) coded by site.

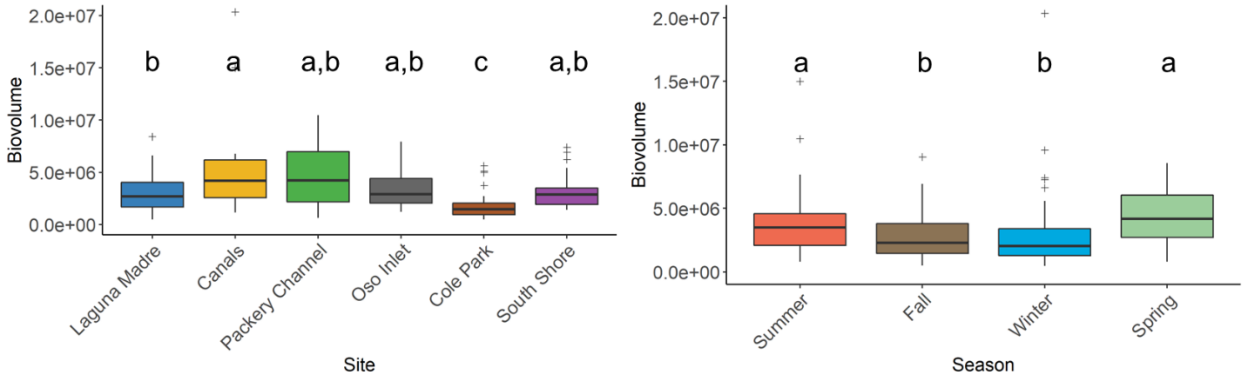

Fig. 1.5 Boxplots of phytoplankton biovolume (µm^3 mL^{-1}) across sites (a) and seasons (b). Thick line represents median values and outliers are represented by (+). There is a single outlier not shown on these graphs that occurred at Cole Park during the fall of 2016 (10/14/2016) associated with a *K. brevis* red tide. The total biovolume of that event was 1.94 x 10^8 µm^3 mL^{-1}.

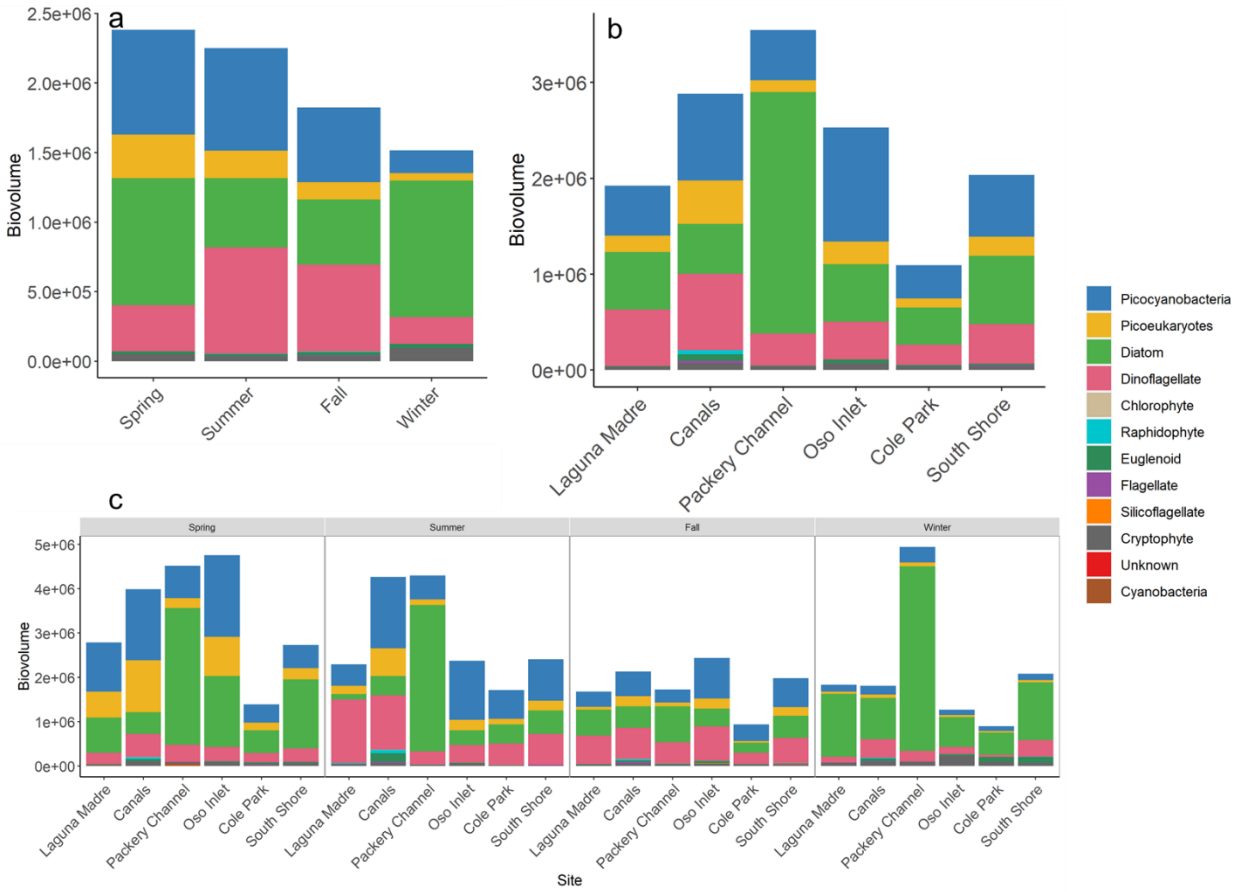

Fig. 1.6 Stacked bar graphs of median phytoplankton biovolume (µm^3 mL^{-1}) coded by major taxonomic group. Panels a and b represent season and site-specific medians. Panel c is site medians across seasons.

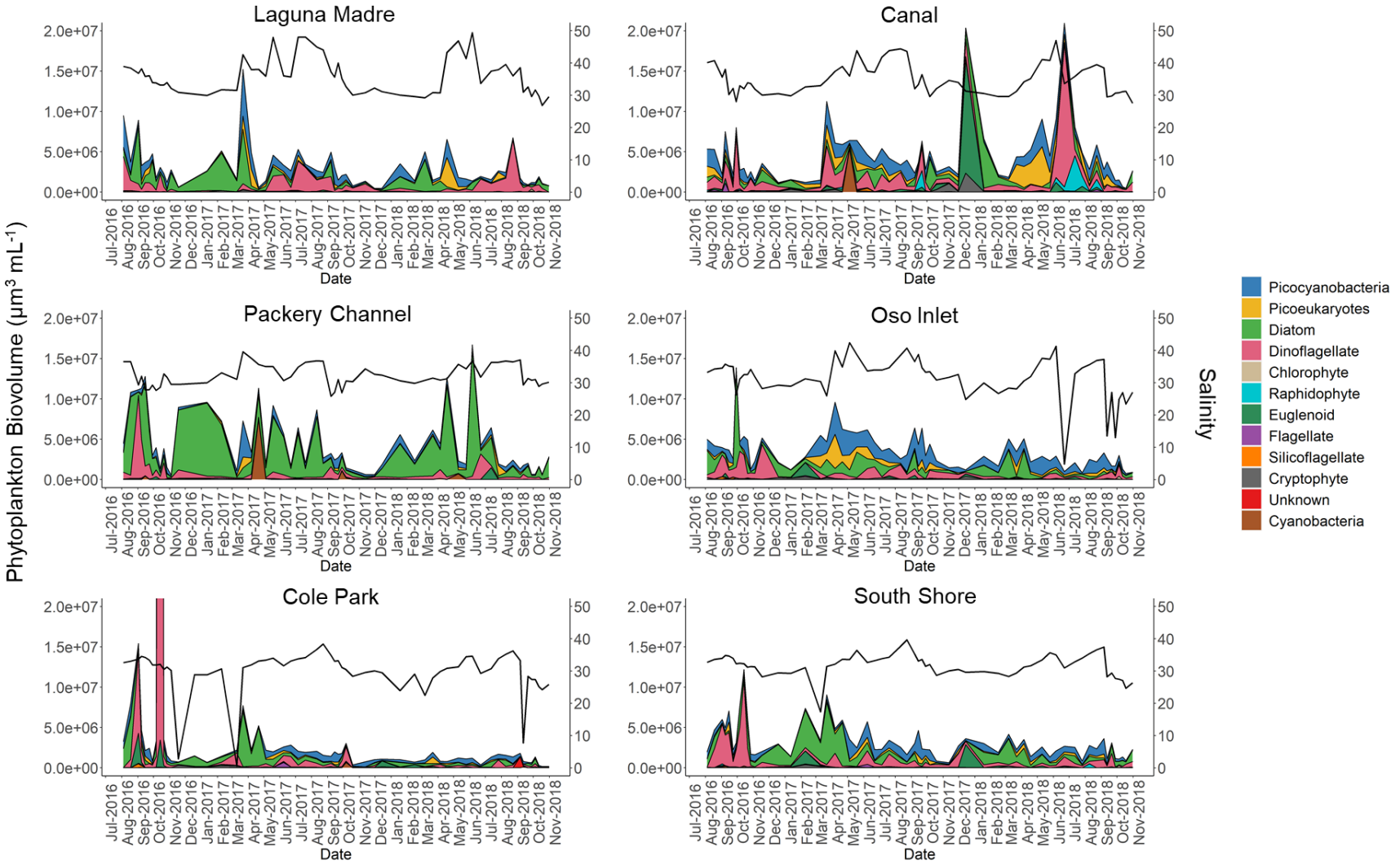

Fig. 1.7 Temporal variability in phytoplankton biovolume (μm^3 mL^{-1}) and major group contribution at all sites studied. Black line represents salinity. At Cole Park, the sampling event with phytoplankton biovolume greater than the scale of the plot was on 10/14/2016 associated with a *K. brevis* red tide. The total biovolume was 1.94 x 10^8 μm^3 mL^{-1}.

Table 1.1 Mean and (standard deviation) of salinity and selected nutrient parameters across sites and seasons. Salinity, DIN:DIP, and DIN:Si are unitless. All others are in µM. Parameters denoted with an asterisk (*) demonstrated a significant interaction between site and season. Superscript letters indicate the results of a one-way ANOVA, with a > b > c > d > e.

	Sites						Seasons			
	Laguna Madre	Canal	Packery Channel	Oso Inlet	Cole Park	South Shore	Spring	Summer	Fall	Winter
Salinity	35.71 (5.21)^{a}	34.87 (4.42)^{a,b}	32.72 (2.81)^{b,c}	31.60 (4.72)^{c,d}	29.68 (5.11)^{d}	31.61 (2.99)^{c,d}	33.65 (5.47)^{b}	36.31 (4.28)^{a}	30.81 (3.58)^{c}	29.80 (1.85)^{c}
NH_4^+	3.94 (1.82)^{c}	9.18 (4.07)^{a}	7.43 (4.66)^{a,b}	6.37 (3.29)^{b}	11.15 (15.14)^{a,b}	3.83 (2.39)^{c}	7.02 (3.47)^{a}	7.08 (4.47)^{a}	5.29 (4.93)^{b}	9.29 (13.33)^{a,b}
NOx	0.27 (0.20)^{e}	2.59 (2.82)^{b}	0.38 (0.30)^{d,e}	2.02 (2.87)^{b,c}	12.69 (10.66)^{a}	1.34 (2.45)^{c,d}	2.47 (4.79)^{a,b}	1.75 (4.43)^{b}	3.44 (6.18)^{a,b}	5.67 (9.24)^{a}
DON*	46.54 (15.33)	45.63 (15.05)	33.55 (11.49)	44.76 (12.07)	36.67 (17.79)	34.89 (8.73)	36.03 (12.72)	48.81 (14.81)	44.5 (11.89)	28.58 (9.85)
PO_4^{3-}*	0.64 (1.13)	0.68 (0.41)	0.52 (0.29)	1.72 (1.92)	2.55 (3.46)	0.83 (0.99)	1.09 (1.25)	1.11 (2.37)	1.44 (2.24)	0.94 (1.01)
SiO_4*	49.61 (29.30)	52.68 (28.71)	16.45 (11.52)	46.72 (21.60)	86.00 (55.65)	40.22 (22.01)	52.31 (44.89)	49.56 (30.09)	52.08 (31.16)	39.56 (43.12)
DIN:DIP	6.55 (11.89)^{a,b,c}	17.31 (13.20)^{a}	14.96 (12.15)^{a}	4.88 (6.05)^{c}	9.33 (14.61)^{a,b}	6.22 (8.95)^{b,c}	8.73 (11.39)^{a}	7.99 (18.41)^{a}	6.07 (11.86)^{b}	15.94 (24.49)^{a}
DIN:Si*	0.09 (0.07)	0.22 (0.16)	0.47 (0.43)	0.18 (0.13)	0.28 (0.29)	0.13 (0.13)	0.18 (0.19)	0.18 (0.19)	0.17 (0.23)	0.38 (0.59)

Table 1.2 Median and (range) of biovolume ($\mu m^3 L^{-1} \times 10^5$) of the four most abundant major taxonomic groups across sites and seasons. Results of one-way Kruskal-Wallis ANOVAs comparing differences among sites and seasons denoted by superscript letters, with the order a > b > c > d.

Sites	Diatoms	Dinoflagellates	Picocyanobacteria	Picoeukaryotes
Laguna Madre	4.60 ^{b,c} (0.26 – 71.63)	4.33 ^{b} (0.00 – 64.71)	4.55 ^{c} (0.16 – 58.06)	1.06 ^{c} (0.04 – 36.25)
Canal	3.71 ^{b,c} (0.15 – 56.88)	7.96 ^{a} (0.31 – 177.33)	7.39 $^{a.b}$ (0.32 – 34.25)	3.30 ^{a} (0.13 – 49.69)
Packery Channel	12.66 ^{a} (0.88 – 156.47)	2.89 ^{b,c} (0.19 – 103.21)	5.02 ^{c} (0.36 – 44.80)	1.12 ^{c} (0.04 – 13.43)
Oso Inlet	4.27 ^{b,c} (0.46 – 118.89)	5.54 ^{b} (0.20 – 42.98)	12.24 ^{a} (0.17 – 39.75)	2.29 ^{a,b} (0.08 – 42.43)
Cole Park	3.00 ^{c} (0.00 – 68.68)	2.25 ^{c} (0.06 – 1856.92)	3.93 ^{c} (0.18 – 35.31)	0.71 ^{d} (0.04 – 8.05)
South Shore	6.14 ^{b} (0.28 – 77.14)	3.98 ^{b} (0.02 – 106.30)	6.00 ^{b,c} (0.12 – 31.47)	1.29 ^{b,c} (0.00 – 10.51)
Seasons	Diatoms	Dinoflagellates	Picocyanobacteria	Picoeukaryotes
Summer	4.49 ^{b} (0.15 – 156.47)	5.76 ^{a} (0.02 – 177.33)	8.11 ^{a} (1.26 – 39.47)	1.86 ^{b} (0.17 – 14.60)
Fall	3.67 ^{b} (0.00 – 118.89)	5.48 ^{a} (0.05 – 1856.92)	4.79 ^{b} (0.16 – 38.97)	0.90 ^{c} (0.00 – 12.14)
Winter	9.82 ^{a} (0.15 – 90.10)	1.92 ^{b} (0.00 – 21.64)	1.65 ^{c} (0.13 – 15.93)	0.52 ^{d} (0.08 – 5.01)
Spring	7.90 ^{a} (0.43 – 113.37)	2.10 ^{b} (0.02 – 48.36)	7.40 ^{a} (1.43 – 58.06)	2.96 ^{a} (0.42 – 49.69)

Table 1.3 Environmental variables found to be significantly ($p < 0.05$) related to phytoplankton biovolume based on pairwise Kendall's Tau correlations. Days since rainfall > 0.1 in. is abbreviated as DSR.

Variables	Correlation Coefficient	p-value
NOx	-0.168	< 0.001
PO_4^{3-}	-0.118	0.001
SiO_4	-0.098	0.006
DSR	0.096	0.017
Temperature	0.125	< 0.001
pH	0.196	<0.001
Salinity	0.243	< 0.001

Table 1.4 Environmental variables found to be significantly ($p < 0.05$) related to diatom, dinoflagellate, picocyanobacteria, and picoeukaryote biovolume based on pairwise Kendall's Tau correlations. Days since rainfall > 0.1 in. is abbreviated as DSR and dissolved oxygen is abbreviated DOx. Italicized rows indicate relatively weak correlations.

Diatoms			Dinoflagellates		
Variables	Correlation Coefficient	p-value	Variables	Correlation Coefficient	p-value
SiO_4	-0.365	< 0.001	DIN:Si	-0.239	< 0.001
DON	-0.208	< 0.001	Wind Speed	-0.123	0.001
NOx	-0.153	< 0.001	NH_4^+	-0.123	0.001
PO_4^{3-}	-0.136	< 0.001	NOx	-0.115	0.001
Temperature	*-0.084*	*0.019*	*SiO_4*	*0.089*	*0.012*
DIN:Si	0.168	< 0.001	Salinity	0.169	< 0.001
Wind Speed	0.216	< 0.001	DON	0.218	< 0.001
			Temperature	0.255	< 0.001
Picocyanobacteria			Picoeukaryotes		
Variables	Correlation Coefficient	p-value	Variables	Correlation Coefficient	p-value
DIN:Si	-0.164	< 0.001	*DIN:Si*	*-0.099*	*0.006*
NOx	-0.131	< 0.001	*NOx*	*-0.083*	*0.021*
SiO_4	*0.081*	*0.023*	*PO_4^{3-}*	*-0.080*	*0.026*
DSR	*0.092*	*0.022*	*SiO_4*	*0.075*	*0.037*
DON	0.171	< 0.001	DSR	0.109	0.007
Temperature	0.250	< 0.001	DON	0.120	0.001
Salinity	0.361	< 0.001	Temperature	0.147	< 0.001
			Salinity	0.348	< 0.001

CHAPTER II: PHYTOPLANKTON RESPONSE TO PULSED NITROGEN ADDITIONS FROM NATURAL AND ANTHROPOGENIC SOURCES IN A RAPIDLY URBANIZING, LOW INFLOW ESTUARY (CORPUS CHRISTI BAY, TX, USA)

Abstract

Nutrient enrichment and cultural eutrophication are increasingly affecting estuarine and coastal systems worldwide, and often result in losses of ecologically and economically important ecosystem services. The Corpus Christi Bay watershed has undergone rapid urbanization resulting in reduced riverine inflows and changes in the dominant sources of nutrients (riverine vs. stormwater or wastewater), though only localized evidence of increasing eutrophication symptoms has been found. To better resolve phytoplankton-nutrient dynamics, seasonal nutrient addition bioassays were conducted to quantify the response of phytoplankton biovolume and community composition following amendment with natural (i.e., porewater and fish tissue) and anthropogenic (i.e., wastewater treatment plant effluent and stormwater runoff) nutrient sources. Results indicate that phytoplankton in this system are limited by nitrogen availability during spring, summer, and fall, and by temperature during the winter. Long-term anthropogenic nutrient enrichment is therefore likely to result in increased symptoms of eutrophication. Wastewater treatment plant effluent, porewater, and stormwater runoff consistently stimulated phytoplankton growth rates, though of the major taxonomic groups investigated here only diatom growth rates were consistently stimulated. These findings indicate that anthropogenic nutrient pollution from pulsed sources (stormwater runoff, porewater) likely have different effects on phytoplankton biovolume and community composition than chronic sources (wastewater treatment plant effluent). Continued population growth and urbanization combined with projections of drier and warmer conditions, however, necessitate further resolution of nutrient-

phytoplankton dynamics to guide ecosystem and nutrient management strategies moving forward.

Introduction

Cultural eutrophication is a problem facing many estuaries across the globe and is considered one of the greatest threats to estuarine ecosystem health (Glibert et al. 2006; Lotze et al. 2006; Bricker et al. 2008). Increased urbanization due to growing coastal populations has altered nutrient loads and the forms of nutrients delivered to the coastal zone (Reed et al. 2016; Wetz et al. 2016; Glibert 2017). Increased accumulation of organic matter as phytoplankton biomass due to increased anthropogenic nutrient inputs is often the first symptom of cultural eutrophication and can lead to loss of seagrasses, bottom water hypoxia, loss of benthic community diversity, and altered food webs (Cloern 1999; Paerl 2006; Spatharis et al. 2007; Bricker et al. 2008; Killberg-Thoreson et al. 2013).

Phytoplankton growth is regulated from the bottom-up by the availability of light, macronutrients, and trace elements, and from the top-down by zooplankton grazing and cell lysis due to algicidal bacteria and viruses (Alpine and Cloern 1992; Brussaard 2004; Örnólfsdóttir et al. 2004). Macronutrient availability is often a dominant factor controlling phytoplankton growth. The major nutrients required by phytoplankton are nitrogen (N) and phosphorus (P), though diatoms also require silica (Si) (Reynolds 2006; Paerl and Justić 2013; Baek et al. 2015). In coastal and estuarine environments, N is most frequently in limiting supply (Glibert et al. 2005; Cira et al. 2016; Paerl et al. 2018), though ephemeral P limitation has been observed in some systems (Anderson et al. 2002; Sylvan et al. 2007; Baek et al. 2015). This general pattern of N limitation is supported by evidence of strong correlations between N inputs to coastal

waters and phytoplankton growth across numerous systems (Mallin et al. 1993; Cloern 2001; Bricker et al. 2008; Cira et al. 2016; Paerl et al. 2018).

In addition to increases in total N load, alterations in the supply of different N forms due to anthropogenic activities can affect phytoplankton growth and accumulation of biomass (Glibert et al. 2005; Reed et al. 2016; Glibert 2017). Dissolved inorganic nitrogen (DIN) includes ammonium (NH_4^+), nitrate (NO_3^-), and nitrite (NO_2^-), and is the most readily available N pool for phytoplankton uptake and assimilation. Within the DIN pool, NH_4^+ is preferentially taken up by phytoplankton relative to NO_3^- or NO_2^- (reviewed in Glibert et al. 2016). Dissolved organic nitrogen (DON) has often been considered less bioavailable, though there is evidence that most major phytoplankton taxonomic groups can utilize at least some portion of the DON pool to support growth (Seitzinger et al. 2002; Altman and Paerl 2012; Killberg-Thoreson et al. 2013; Cira et al. 2016). Despite an increased understanding of the importance of DON for phytoplankton production, the large portion of uncharacterized DON compounds makes it difficult to determine the extent to which different sources of DON contribute to cultural eutrophication (Seitzinger et al. 2002; Killberg-Thoreson et al. 2013).

Changes in the availability of the various N forms can also affect phytoplankton community structure (Anderson 2002; Burkholder et al 2008; Killberg-Thoreson et al. 2013; Glibert 2017). Physiological adaptations of major phytoplankton groups, including genetic potential for production of NH_4^+ versus NO_3^- transporters (Glibert 2017) and enhanced mixotrophy under DIN limitation (Burkholder et al. 2008), often result in different responses to the quantity and form of N delivered to a system. This has the potential to manifest as a long-term shift in the dominant taxa of a system subject to chronic nutrient pollution, alteration in the timing of spring/fall blooms, increased occurrence of nuisance and/or toxic algae blooms

(HABs), and even increased toxicity of some HAB forming taxa (Anderson et al. 2002; Killberg-Thoreson et al. 2013; Glibert 2017; Nohe et al. 2020). Changes in community composition, even without a concomitant increase in total phytoplankton biomass, can also negatively impact estuarine ecosystems (Glibert et al. 2005; Glibert 2017). Dinoflagellates and cyanobacteria account for a majority of known HAB forming taxa, though HAB formers can be found in nearly all major taxonomic groups of phytoplankton (Paerl 1988; Moestrup et al. 2009; Glibert and Burkholder 2011). Diatoms, on the other hand, are considered a highly desirable group of phytoplankton despite the presence of some toxic HAB taxa (Cloern and Dufford 2005). Understanding the role of N concentration and form in the success of one major taxonomic group over another is crucial to determine if, how, and when to implement management strategies.

Diatoms tend to be favored under moderate to high N conditions, especially when N is in the form of NO_3^- (Cloern and Dufford 2005; Suggett et al. 2009; Baek et al. 2015). In contrast, dinoflagellates, cryptophytes, and chlorophytes tend to be favored by reduced forms of N (NH_4^+, DON), with all three groups favored over diatoms in stratified conditions (Cloern and Dufford 2005; Bricker et al. 2008; Paerl and Justić 2013; Baek et al. 2015; Nohe et al. 2020). Additionally, some dinoflagellates have mixotrophic capabilities, including phagotrophy of smaller-celled organisms (Burkholder et al. 2008; Paerl and Justić 2013). Cyanobacteria are a diverse group and as such different nutrient conditions can favor different cyanobacterial groups. Picocyanobacteria tend to be favored under lower total N concentrations due to their high surface area to volume ratio (Paerl 1998; Paerl and Paul 2012; Paerl and Justić 2013), though there is evidence that they can contribute substantially to phytoplankton biovolume even in eutrophic systems (Gaulke et al. 2010; Paerl et al. 2020). Lastly, picoeukaryotes are a potentially diverse group comprised of chlorophytes, cryptophytes, haptophytes, and small diatoms (Paerl et al.

2020). Like the picocyanobacteria, this group is favored under warm temperatures and increased concentrations of total dissolved N and can utilize both NH_4^+ and NO_3^-, though are thought to prefer reduced N (Worden et al. 2004; Gaulke et al. 2010; Paerl et al. 2020).

The Corpus Christi Bay watershed is dominated by agriculture (~47%) and has experienced sustained population growth over the past 20 years (8.5% increase 2000 to 2010; 7% increase 2010 to 2019) (U.S. Census Bureau), resulting in growing urbanization and wastewater inputs (Wetz et al. 2016; Bugica et al. 2020). A previous study showed that Corpus Christi Bay phytoplankton are strongly influenced by N availability, with a site near the mouth of Oso Bay demonstrating the highest average NH_4^+ concentrations as well as highest rates of primary productivity (Flint 1984). Given the recent and projected population growth estimates for the South Texas coast, and associated changes in land use and nutrient loadings, it is critical to understand how N availability from dominant watershed or estuarine sources will affect phytoplankton growth and community composition. There is also evidence of increasing frequency of harmful *Karenia brevis* "red tides" in Corpus Christi Bay (see Chapter III), furthering the need to better understand nutrient-phytoplankton dynamics. To assess relationships among N availability, N form, and phytoplankton growth, I addressed three main hypotheses, 1) alleviation of N limitation would result in increased growth rates relative to a control, 2) the pulsed nutrient delivery would favor faster growing taxa over slower growing taxa, and 3) the form of N provided would favor different taxonomic groups based on preferences for oxidized or reduced N. The results from this study offer a quantitative assessment of the influence of nutrient pulses from various sources that are likely important to the system, add to the limited understanding of phytoplankton-nutrient dynamics in Corpus Christi Bay, and

more broadly increase understanding of phytoplankton ecology in sub-tropical, low to moderate freshwater inflow estuaries.

Methods

Study Site

Corpus Christi Bay is a shallow (~ 3 m, ship channel ~ 15 m), microtidal (~ 0.3 m range), wind-driven system (Ritter and Montagna 1999; Islam et al. 2014; Turner et al. 2015) and comprises the largest portion of the Nueces Estuary. Corpus Christi Bay is located on the semi-arid South Texas coast and is separated from the Gulf of Mexico by Padre Island, with two narrow inlets for water exchange (Packery Channel and Aransas Pass). Corpus Christi Bay hydrodynamics are further influenced by the extensively altered freshwater inflows from the Nueces River with very little riverine inflow reaching the bay compared to historic conditions (Montagna et al. 2009). This combination of characteristics leads to a relatively long residence time (> 5 mo. – 1 year) and a generally well mixed water column (Ritter and Montagna, 1999; Islam et al. 2014). Rapid urbanization in the Corpus Christi Bay watershed has resulted in increased impervious surfaces and need for wastewater treatment (Wetz et al. 2016). Oso Bay, a sub-bay that flows into Corpus Christi Bay, is fed by Oso Creek which is heavily influenced by wastewater treatment plant effluent (Wetz et al. 2016).

Data Collection

Nutrient Source Collection

To assess the influence of nutrients on phytoplankton growth and community composition in Corpus Christi Bay, natural and anthropogenic sources of nitrogen were used as treatments in bioassays. Natural sources included sediment porewater and fish tissue extract, and anthropogenic sources included wastewater treatment plant effluent and urban stormwater

runoff. Sources consisting of solely ammonium or nitrate as well as a control that received no nutrients were also included as treatments for comparison. Bioassays were conducted quarterly over one year to assess seasonal variability in the phytoplankton response to these sources.

Sediment porewater was collected in Corpus Christi Bay near Oso Inlet (Fig. 2.1). Sediment cores were collected and the top 2.5 cm of each core was sectioned into an acid washed (10% HCl) bucket. Sediment was settled via sonication and porewater was decanted. This process was repeated until one liter of porewater was collected. The porewater was then sterile filtered (0.22 µm) under gentle vacuum filtration and frozen until needed. To simulate the potential role of nutrients derived from decaying fish during toxic algal blooms in the system, fish tissue extract was created by: 1) collecting local dead baitfish (220 g mullet, and 135 g croaker), 2) macerating fish tissue with an immersion blender and 500 mL Instant Ocean artificial seawater (salinity 35), 3) filtering large pieces of material out of the macerated fish tissue with cheese cloth, and 4) filtering (2.7 µm) under gentle vacuum filtration and frozen until needed. Wastewater treatment plant (WWTP) effluent was collected directly from the outfall of the Oso Wastewater Treatment Plant (Fig. 2.1), sterile filtered (0.22 µm) under gentle vacuum filtration, and frozen until needed. Stormwater runoff was collected during active rainfall from a stormwater outfall that drains directly into Corpus Christi Bay (Fig. 2.1), sterile filtered (0.22 µm) under gentle vacuum filtration, and frozen until needed. Ammonium and nitrate working solutions were made with ammonium chloride (NH_4Cl) and potassium nitrate (KNO_3) at a concentration of 100 mM.

Corpus Christi Bay Water Collection

Water for nutrient addition bioassays was collected along the south shore of Corpus Christi Bay at a site that was also part of a continuous monitoring effort (Fig. 2.1). Surface water

hydrographic data (temperature, conductivity (salinity), pH, dissolved oxygen) were collected using a calibrated YSI ProPlus multiparameter sonde (YSI Inc., Yellow Springs, Ohio). Water for initial site water analyses and nutrient addition bioassays was collected from the top 15 cm of the water surface in acid washed (10% HCl) carboys (20 L) and stored in dark bags at ambient temperature until return to Texas A&M University – Corpus Christi campus.

Experimental Design

Nutrient addition bioassays were conducted quarterly with experiments beginning on July 20 and October 25, 2017, and January 18 and May 29, 2018, hereafter summer, fall, winter, and spring. During summer, fall, and winter experiments, the treatments were control (no nutrient addition), sediment porewater, WWTP effluent, fish tissue extract, stormwater runoff, ammonium, and nitrate. Treatments were applied in triplicate and normalized to a final TDN concentration of 20 µmol L^{-1}. The stormwater runoff treatment was, however, only applied in duplicate during the winter experiment and was excluded from the spring experiment (six total treatments) due to insufficient supply of amendment stock. Experiments were conducted using 1-L cubitainers, which allow 85% of PAR to pass through (Paerl 1987), and incubated *in situ* in Oso Bay for 48 hours (Fig. 2.1). Due to differences in the concentration of total dissolved nitrogen in each of the natural amendment stocks, 850 mL of site water was added to each cubitainer with the appropriate volume of nutrient source, then brought to a final volume of 1000 mL with artificial seawater to match ambient salinity at the time of collection. All treatments were conducted using whole water, i.e., grazers were not filtered out of site water prior to experimental setup.

Initial measurements of phytoplankton abundance and biovolume, chlorophyll *a*, and dissolved nutrients were made from site water prior to experimental set up. Nutrient bioassays

were subsampled at T0, T24, and T48 following nutrient amendment additions for dissolved organic carbon, total dissolved nitrogen, dissolved inorganic nitrogen (ammonium + nitrate + nitrite), orthophosphate, and silicate. At each experimental time point, subsamples were also collected for chlorophyll *a* and pico-, nano-, and micro-phytoplankton enumeration.

Laboratory Processing

Prior to sample processing, the collection bottles were gently inverted to homogenize the water and suspended materials. Water for micro- and nanophytoplankton enumeration was gently poured into 50 mL conical vials and fixed with acidified Lugol's solution to a final concentration of 1% and stored at room temperature in the dark. All other samples were immediately stored at -20°C until analysis. Water for dissolved nutrients (ammonium, nitrate plus nitrite, orthophosphate, silicate, dissolved organic carbon, and total dissolved nitrogen) was filtered through pre-combusted (4 hours at 450°C) Ahlstrom GF/F filters into acid-washed high-density polyethylene bottles. For chlorophyll *a,* a known volume of water was gently filtered (≤ 5 mm Hg) through 25 mm GF/F filters. For picophytoplankton quantification site water was fixed with glutaraldehyde to a final concentration of 1%.

Phytoplankton Enumeration

Micro- and nanophytoplankton were counted following the Utermöhl method on an Olympus IX71 inverted microscope at 200x magnification. The volume settled for each sample was variable based on chlorophyll *a* concentration and amount of suspended sediment noted during live screens. All samples were settled overnight (> 12 hrs), allowing more than 1 hour of settling time per mL of sample settled. Picophytoplankton were counted using an Accuri C6 Plus flow cytometer using the CSampler Plus adapter (Beckton Dickinson, San Jose, CA). Instrument QC was performed daily following manufacturer protocol prior to sample preparation. Samples

were thawed at 0°C in the dark and gently filtered across 20 µm Nytex® mesh to remove large cells and particulate matter. The auto-sampler was set to agitate the sampling plate and rinse the sample input port before each sample was analyzed. Additionally, polystyrene beads of known size (3.3 µm) were run to ensure that only appropriate size ranges of cells were counted. Biovolumes were estimated for micro-, nano-, and picophytoplankton using the associated geometric shapes at the lowest taxonomic resolution recorded during counting (Sun and Liu 2003). Picophytoplankton shape and size were not directly measured and were estimated to be spherical at 1.5 µm and 2.5 µm diameters for picocyanobacteria and picoeukaryotes, respectively.

Chlorophyll *a* and Nutrient Quantification

Chlorophyll *a* was extracted in 90% HPLC-grade acetone at -20°C for 18-24 hours. Chlorophyll *a* was then determined fluorometrically without acidification using a Turner Trilogy fluorometer. Inorganic nutrient samples were thawed to room temperature and then analyzed on a Seal QuAAtro autoanalyzer. Standard curves with five different concentrations were run daily at the beginning of each run. Fresh standards were made prior to each run by diluting a primary standard with low nutrient surface seawater. Deionized water (DIW) was used as a blank, and DIW blanks were run at the beginning and end of each run, as well as after every 8–10 samples to correct for baseline shifts. Method detection limits were 0.02 µM for nitrate plus nitrite (NO_x) and ammonium (NH_4^+), and < 0.01 µM for orthophosphate (PO_4^{-3}) and silicate (SiO_4). Samples for dissolved organic carbon and total dissolved nitrogen were thawed to room temperature and analyzed using the High Temperature Catalytic Oxidation method on a Shimadzu TOC-Vs analyzer with nitrogen module. Standard curves were run twice daily using a DIW blank and five concentrations of either acid potassium phthalate solution or potassium nitrate for DOC and

TDN, respectively. Three to five subsamples were taken from each standard and water sample and injected in sequence. Reagent grade glucosamine was used as a laboratory check standard and inserted throughout each run, as were Certified Reference Material Program (CRMP) deep-water standards of known DOC/TDN concentration. Average daily CRMP DOC and TDN concentrations were 43.0 ± 2.7 μM and 32.2 ± 2.3 μM^1, respectively. Dissolved organic nitrogen was determined by subtracting dissolved inorganic nitrogen (NH_4^+ and NO_x) from total dissolved nitrogen.

Data Analysis

All raw data and associated R code are available at doi:10.7266/NCPYG0DH. Data analyses were performed in R v 3.6.2 and PRIMER v7. To account for dilution during experimental set-up (850 mL of site water/1000 mL total experimental volume) initial site water measurements were multiplied by 0.85 prior to comparison to experimental time point measurements.

Growth Rate Calculations

Apparent growth rates (μ d^{-1}) were calculated using formula 1 where P_t and P_0 are the final and initial measurements and t is the duration of the experiment in days.

$$\mu = \ln (P_t/P_0)/t \qquad \text{Formula 1}$$

Chlorophyll *a* (μg L^{-1}) and phytoplankton biovolume (μm^3 mL^{-1}) were used as different metrics (P) for the calculation of growth rates.

Statistical Analyses

A three-way ANOVA (stats v 3.6.2; (R Core Team 2019)) with the interaction terms for season and treatment, season and metric, and treatment and metric as explanatory factors for phytoplankton growth rates was used to test for any significant interactions among factor levels.

Significant interactions were found between season and treatment, season and metric, and treatment and metric. As such a one-way ANOVA was used to test for differences in growth rates calculated using different metrics and one-way ANOVAs were used to test for treatment and season effects individually.

To compare the growth rates calculated using chlorophyll *a* and biovolume, a one-way ANOVA with metric as a fixed factor (stats v 3.6.2; (R Core Team 2019)) was conducted. The ANOVA model was tested for assumptions of normality (Shapiro-Wilk test) and homoscedasticity (Brown-Forsythe Levene test), and the model passed. To better interpret the relationship between growth rates calculated with the two different metrics, a simple linear regression (stats v 3.6.2; (R Core Team 2019)) with chlorophyll *a* growth rates as the response variable and biovolume growth rates as the explanatory variable was conducted. The regression model was tested for assumptions of normality (Shapiro-Wilk test), homoscedasticity (Breusch-Pagan test), and linearity, and the model passed.

To assess season and treatment effects on phytoplankton growth rates one-way ANOVAs (stats v 3.6.2; (R Core Team 2019)) were used to compare T0-T48 growth rates among seasons within each level of treatment and among treatments within each level of season, respectively. The ANOVA models were tested for assumptions of normality (Shapiro-Wilk test) and homoscedasticity (Brown-Forsythe Levene test), and all models passed. Multiple comparison procedures with Tukey contrasts (multcomp v 1.4-12; (Horthorn et al. 2008)) were then used to test for differences among treatment pairs with a Westfall correction applied to the p-values (multcomp v 1.4-12; (Quinn and Keough 2002; Hothorn et al. 2008)). Corrected p-values were compared to $\alpha = 0.1$ to account for introduction of Type II error (Quinn and Keough 2002). The same procedure was followed to assess treatment effects (within season) on growth rates of the

major taxonomic groups of phytoplankton present.

To resolve any changes in phytoplankton community composition at the genus level non-parametric multivariate analyses comparing seasons, treatments (T48), and the initial community (T0) were conducted in PRIMER v7 (Clarke and Gorley 2015). Community biovolume data were averaged across all season-treatment-time point replicates, log transformed, and used to create resemblance matrices using the Bray-Curtis similarity index. Resemblance matrices including all combinations of season, treatment, and time point factor levels were then used to create hierarchical clustering dendrograms. The group-average algorithm was used for the clustering procedure and the Simprof routine was simultaneously used to determine the significance level of the clusters created.

Results

Temperature and salinity were seasonally variable with highest temperatures in spring and summer and lowest temperatures in winter (Table 2.1). Throughout each experiment, *in situ* temperature remained similar to the initial site conditions (< 2°C change) with the exception of winter, where temperature increased more than 10°C (T48 = 18.2°C) before the conclusion of the experiment.

Initial concentrations and composition of the DIN pool varied seasonally. In the summer, NH_4^+ accounted for 100% of the measurable DIN pool with an ambient concentration of 4.48 ± 2.09 µM while NOx was below the limit of detection (Table 2.2). Ambient DIN preceding the fall experiment was 0.52 ± 0.10 µM, with an NH_4^+ concentration of 0.39 ± 0.10 µM and an NOx concentration of 0.14 ± 0.01 µM. In the winter ambient DIN was 2.38 ± 0.28 µM and NH4+ was more abundant than NOx, with concentrations of 1.98 ± 0.25 µM and 0.41 ± 0.03 µM, respectively. In the spring, the initial DIN concentration was the lowest observed at 0.27 ± 0.18

µM, and in contrast to the other seasons the concentration of NOx (0.19 ± 0.10 µM) was greater than the concentration of NH4+ (0.08 ± 0.08 µM).

Orthophosphate concentrations and DIN:DIP ratios were also seasonally variable, and despite orthophosphate consistently ≤ 0.90 µM, DIN:DIP was never above the Redfield ratio of 16, which is suggestive of N limitation. Ambient orthophosphate in the summer was 0.41 ± 0.03 µM and the DIN:DIP ratio was the highest observed at 10.88. In the fall, orthophosphate concentration and the ratio of DIN:DIP were lower than the summer at 0.19 ± 0.03 µM and 2.68. Winter orthophosphate was the highest observed at 0.90 ± 0.35 µM and the DIN:DIP ratio was similar to that observed in the fall at 2.66. Orthophosphate concentrations in the spring were similar to the summer at 0.49 ± 0.06 µM and the DIN:DIP ratio was the lowest observed at 0.55. Secchi depth varied seasonally as well, with greater depth of light penetration recorded in the fall (0.8 m) and spring (0.6 m) compared to winter (0.4 m) and summer (0.5 m). Si concentrations were ≥ 18.50 µmol L^{-1}, and DIN:Si ratios were ≤ 0.11, showing no indication of Si limitation across seasons.

In general, the total dissolved N (TDN) concentrations measured following nutrient additions at T0 were in the vicinity of the targeted concentration (20 µM added N), though there were exceptions (Table 2.2). T0 subsamples were obtained and processed no more than 20 minutes following nutrient additions. The total added N, as calculated by mean T0 TDN minus mean initial TDN for each treatment individually, was consistently > 15 µM in the ammonium, runoff, and WWTP effluent treatments. Total added N in the nitrate treatment was < 15 µM in the summer and fall experiments, though in both cases the added NOx was > 15 µM. The porewater treatment total added N was also < 15 µM during the spring experiment. Lastly, the total added N in the fish treatment was only > 15 µM during the winter experiment.

Enrichment of the different N forms and other nutrients also varied by treatment. The ammonium treatment was enriched solely in NH_4^+, the nitrate treatment was enriched solely in NOx, the fish treatment provided moderate amounts of NH_4^+ and DON, the porewater treatment was enriched in NH_4^+, DON, and Si, the runoff treatment was also predominantly enriched NH_4^+ but also provided NOx, DON, Si, and orthophosphate, and lastly the WWTP effluent treatment was predominantly enriched in NOx but also provided NH_4^+, DON, Si and orthophosphate. In each experiment except for winter, nutrient drawdown was the most rapid in the first 24 hours (Figs 2.2-2.5) with most treatments reaching or dropping below initial nutrient conditions by T24. The concentrations of NH_4^+ and NOx in the ammonium and nitrate treatments, however, rarely reached as low as the initial conditions even after 48 hours. In October, a similar pattern was seen for the WWTP effluent treatment with NOx concentrations remaining high throughout the experiment. During the fall there is evidence of some internal nutrient cycling, especially of orthophosphate, despite the relatively short duration of the experiment.

Lastly, phytoplankton biovolume and community composition also varied seasonally. Total phytoplankton biovolume was highest in the summer at 2.47×10^9 μm^3 L^{-1}, followed by winter at 2.17×10^9 μm^3 L^{-1}, spring at 1.53×10^9 μm^3 L^{-1}, and fall at 1.19×10^9 μm^3 L^{-1} (Table 2.3). Picocyanobacteria contributed between 32% and 57% of community biovolume across seasons with the greatest contribution during the fall and the lowest in the summer, though actual picocyanobacteria biovolume was greater in the summer (8.09×10^8 μm^3 L^{-1}) than the fall (6.82×10^8 μm^3 L^{-1}). Picoeukaryote community contribution was lower than picocyanobacteria ranging from 5% to 10%, with the highest contribution during the summer and the lowest during the winter. The highest observed picoeukaryote biovolume, 2.48×10^8 μm^3 L^{-1}, also occurred during the summer, whereas the lowest observed picoeukaryote biovolume, 7.80×10^7 μm^3 L^{-1},

occurred during the spring. Diatoms accounted for 16% to 43% of phytoplankton biovolume across seasons, with the highest contribution in the winter and the lowest in the spring. Diatom biovolume was also the highest in the winter at 9.37 x 10^8 μm^3 L^{-1} and lowest in the spring at 1.73 x 10^8 μm^3 L^{-1}. Dinoflagellate contribution to community biovolume ranged from 5% to 38%, with the fall and winter demonstrating the lowest contribution of dinoflagellates at 5% and 10%, respectively. Dinoflagellate biovolume and community contribution were the highest in the summer at 9.33 x 10^8 μm^3 L^{-1} and 38%. Spring dinoflagellate biovolume was 5.00 x 10^8 μm^3 L^{-1} and contribution was near that of summer at 33%. All other groups accounted for < 2% of the community.

Whole Community Growth Rate Response

Growth rates ranged from -0.39 d^{-1} to 0.78 d^{-1} for chlorophyll *a*-based, from -0.91 d^{-1} to 0.33 d^{-1} for abundance-based, and from -0.20 d^{-1} to 0.62 d^{-1} for biovolume-based calculations. Linear regression indicated that there was a significant linear relationship between the growth rates estimated with chlorophyll *a* and biovolume (p = < 0.001; R^2 = 0.38; slope = 0.84) and between the growth rates estimated with abundance and biovolume (p = < 0.001; R^2 = 0.52; slope = 0.97). Because biovolume is a more direct measure of phytoplankton growth compared to the pigment chlorophyll and total number of cells (i.e., due to changes in pigment $cell^{-1}$ and/or cell size), experimental results and discussion are presented for biovolume-based measures of growth rates and community composition.

Treatment Comparisons

Results from within season ANOVAs indicated that phytoplankton growth rates were stimulated in summer, fall, and spring (i.e., significantly different than control at $p \leq 0.1$) in one or more N-addition treatments (Fig. 2.6). In the summer, all treatments except for fish extract

elicited growth rates significantly higher than the control. Phytoplankton growth rates in the WWTP effluent treatment were the highest observed and significantly different than all other treatments. The runoff treatment growth rates were significantly greater than the porewater treatment and there were no significant differences compared to the ammonium and nitrate treatments. Likewise, the growth rates measured in the porewater treatment were not significantly different than the ammonium and nitrate treatments. The fish extract growth rates were similar to those in the control and significantly lower than all other treatments, and there was no difference between the ammonium and nitrate treatment growth rates.

During the fall experiment, again all treatments other than the fish extract elicited growth rates greater than the control. The WWTP effluent treatment growth rates were significantly greater than the nitrate and fish treatments and no different than the runoff, porewater, and ammonium treatments. The porewater treatment was also significantly greater than the nitrate and fish extract treatments, and there was no difference between the ammonium and nitrate growth rates. In contrast, no treatments during the winter experiment elicited growth rates greater than the control, indicating that factors other than N availability were inhibiting phytoplankton. Lastly, during the spring experiment only the porewater and WWTP effluent treatments stimulated phytoplankton growth rates relative the control. Growth rates in these two treatments were also significantly greater than the ammonium, nitrate, and fish extract treatments. The lack of increased growth rates observed in the ammonium and nitrate treatments, however, was likely due to insufficient supply of another macronutrient because total N added for each of these treatments was 24.44 µM and 19.84 µM, respectively.

Major Taxonomic Group Growth Rate Response

In the analysis of group-specific responses, we focus only on picocyanobacteria, picoeukaryotes, diatoms and dinoflagellates, as other groups always accounted for <2% of community biovolume.

Summer

Picocyanobacteria, picoeukaryote, and diatom growth rates were stimulated in response to at least one N addition relative to the control, whereas dinoflagellate growth rates were not (Fig. 2.7). Picocyanobacteria growth rates were elevated relative to the control in the WWTP effluent, runoff, nitrate, and ammonium treatments, and there was no difference among the growth rates among these treatments. Additionally, the WWTP effluent, ammonium, and nitrate growth rates were significantly higher than the porewater treatment. Picoeukaryote growth rates were elevated relative to the control in all treatments other than the fish extract. The WWTP effluent treatment growth rates were greater than the porewater, runoff, ammonium, and nitrate treatments. Diatom growth rates were also greater than the control in all treatments except for the fish extract. The WWTP effluent growth rates were greater than those of the ammonium and porewater treatments.

Fall

Picocyanobacteria and diatoms were the only major groups where there was evidence of growth rate stimulation following N addition (Fig. 2.8). Picocyanobacteria growth rates were elevated in the WWTP effluent, porewater, nitrate, and ammonium treatments relative to the control, and there was no difference among these treatments. Diatom growth rates were elevated in the WWTP effluent, porewater, runoff, and ammonium treatments, and again there was no difference among these treatments.

Winter

None of the major phytoplankton groups considered here responded to the addition of N during the winter experiment (Fig. 2.9).

Spring

Picoeukaryote, diatom, and dinoflagellate growth rates were elevated relative to the control in at least one N addition treatment (Fig. 2.10). Picoeukaryote growth rates were elevated relative to the control in the ammonium, porewater, and WWTP effluent treatments, with the latter two also significantly greater than the former. Diatom growth rates were only stimulated relative to the control in the WWTP effluent treatment. Dinoflagellate growth rates were only elevated relative to the control in the porewater treatment.

Lastly, community composition analyses revealed that the genus-level response to treatments was more strongly related to season than to the N addition source. Group average hierarchical clustering with SIMPROF testing (Fig. 2.11) showed greatest similarity among treatments within seasons. Initial communities in the summer and fall, and the summer nitrate T48 community were different from all other communities. Winter and fall phytoplankton communities at the time of sampling were different than one another, though there were no differences detected among phytoplankton communities at T48 across all treatments. Further analyses at the within-season level of resolution confirmed that summer was the only season with statistically different communities at any combination of treatments and time points (data not shown).

Discussion

Corpus Christi Bay has been described as an oligo-mesotrophic estuary (Flint 1984), though there has been rapid population growth and urbanization over the past 20 years (Bugica et

al. 2020). Increased wastewater treatment loadings, land use changes such as increased impervious surface coverage that can lead to elevated nutrient loadings (Seitzinger et al. 2002; Dillon and Chanton 2005; Yang and Toor 2016), and reduced freshwater inflows associated with this growth have the potential to alter phytoplankton dynamics in myriad ways (Anderson 2002; Glibert et al. 2005; Nohe et al. 2020). Here, nutrient addition bioassays were conducted seasonally using natural (porewater and fish tissue) and anthropogenic (urban stormwater runoff, WWTP effluent) sources to mimic those that are currently influencing Corpus Christi Bay. The goal was to assess phytoplankton response to N loading and elucidate the role of seasonality in these responses. The results from these experiments address three main hypotheses, 1) alleviation of N limitation would result in increased growth rates relative to a control, 2) the pulsed nutrient delivery would favor faster growing taxa over slower growing taxa, and 3) the form of N provided would favor different taxonomic groups based on preferences for oxidized or reduced N. In general, these hypotheses were well supported by the experimental data, though there are exceptions.

Whole Community Growth Rates

Phytoplankton growth in response to pulsed nutrient inputs indicated that Corpus Christi Bay is predominantly N limited, consistent with the paradigm that estuarine and coastal phytoplankton growth is largely limited by the availability of N (Örnólfsdóttir et al. 2004; Glibert et al. 2005; Paerl et al. 2018). Average DIN:DIP ratios from a 2-year field study concurrent with the experiments conducted here support the findings of N limitation, with an average bay-wide DIN:DIP ratio of 7.5 and an average DIN:DIP ratio of 4.8 at the site of experimental water collection (Chapter I). Here, during summer and fall experiments phytoplankton growth rates were elevated relative to the control (no nutrients) in all treatments

other than the fish extract. Strong N limitation during the summer and fall has been observed elsewhere (Fisher et al. 1999; Piehler et al. 2004; Baek et al. 2015; Cira et al. 2016). Seasonality of N concentrations and extent of phytoplankton N limitation has previously been related to variation in rainfall, riverine inputs, and water column stability (Rudek et al. 1991; Fisher et al. 1999; Piehler et al. 2004; Baek et al. 2015). In Corpus Christi Bay, new N is provided to the system during episodic precipitation events, primarily through urban stormwater runoff rather than enhanced riverine inflows due to the heavily managed nature of the Nueces River (Montagna et al. 2009; Turner et al. 2015). In the summer experiment, there was also evidence of secondary P limitation, with phytoplankton growth rates in the WWTP effluent treatment significantly higher than all others. Following nutrient additions, the DIN:DIP ratios in all treatments except for WWTP effluent and runoff indicated P limitation, supporting the growth rate results. Comparison of added orthophosphate further supports this conclusion, with the added 2.7 µM of orthophosphate from the WWTP effluent treatment eliciting growth rates significantly higher than the runoff and porewater treatments, which only added 1.1 µM and 0.6 µM, respectively.

During the fall experiment, however, there was no clear evidence of secondary P limitation. Phytoplankton growth rates in the nitrate treatment were significantly lower than the WWTP effluent and porewater treatments, though there were no differences between the latter and the ammonium treatment. The DIN:DIP ratio measured in the fall (2.68) showed evidence of much stronger N limitation than that measured in the summer (10.88), and only the ammonium and nitrate treatment DIN:DIP ratios (123.5, 30.4) indicated the potential for P limitation following N addition. There are alternative sources of P, such as intracellular stores from luxury uptake during P-replete conditions, uptake and assimilation of low-molecular weight organic P,

and microbially mediated DIP regeneration, that have the potential to alleviate P limitation under otherwise limiting conditions (Piehler et al. 2004; Canfield et al. 2005; Martin et al. 2014). Piehler et al. (2004) also hypothesized that luxury uptake of inorganic P prior to a nutrient addition experiment could have provided sufficient P for several rounds of cell division despite P limiting conditions at the onset of the experiment. Increases in the availability of inorganic P in the nitrate, fish, and WWTP effluent treatments over the course of the fall experiment, in contrast to rapid drawdown of inorganic P in all treatments during the summer, provides further evidence for the role of alternative P sources and/or rapid P remineralization during the fall experiment.

Similar to the summer bioassay, the spring bioassay results were indicative of co-limitation by another macronutrient in addition to N. The lack of increased growth rates in the ammonium and nitrate treatments relative to the control during the spring indicates that following N addition, P and/or Si may have limited phytoplankton growth. Ambient DIN:DIP ratios at the time of this experiment (0.55) compared to that in summer (10.88) and fall (2.68) showed the strongest stoichiometric N limitation and surplus of P during the spring. It was hypothesized above that alternate sources of P were more readily available in the fall than the summer due to the P-replete conditions preceding the experiment (Piehler et al. 2004; Canfield et al. 2005; Martin et al. 2014). If we assume that the relative surplus of P prior to the spring experiment resulted in similar alternative P source utilization, then it is less likely that induced P limitation alone can explain the lack of increased growth rates in the ammonium and nitrate treatments. Indeed, there was evidence during the spring of an increase in orthophosphate between 24 and 48 hours in the fish, nitrate, and control treatments, similar to that observed in the fall, supporting this hypothesis. Furthermore, picoeukaryote and dinoflagellate growth rates were elevated in the porewater treatment, with the former also elevated in the ammonium

treatment though diatom growth rates were not elevated in either treatment. This may indicate that Si was limiting to diatoms following addition of N.

The ammonium and nitrate treatments during spring demonstrated higher DIN:Si ratios (1.10 and 0.82, respectively) than during the summer (0.77, 0.51) and fall (0.58, 0.41), supporting the potential for induced Si limitation following N additions in the spring but not the summer or fall. The timing of the spring experiment (late May) here may also provide support for the hypothesized Si limitation. During the field study accompanying these experiments, average diatom biovolume at the water collection site was higher in the winter (1.82×10^9 μm^3 L^{-1}) and spring (2.26×10^9 μm^3 L^{-1}) than in the summer (7.76×10^8 μm^3 L^{-1}) and fall (1.82×10^8 μm^3 L^{-1}). Additionally, the average percent contribution of diatoms was highest in the spring (61%) and winter (54%), followed by the summer (28%) and fall (20%) (Chapter I). The biovolume and contribution of diatoms prior to the spring experiment, however, more closely resembled summer averages than spring averages, potentially indicating that the diatom spring bloom had already depleted Si and begun to senesce by late May in 2018. Si limited community growth rates are not always found during nutrient addition bioassays (Rudek et al. 1991; Fisher et al. 1999; Piehler et al. 2004), though there are examples of Si limited diatom growth in microcosm experiments (Neale et al. 2014), as well as of the role Si limitation plays in the timing and extent of diatom blooms and the success of non-diatom taxa (Conley et al. 1993; Fisher et al. 1999; Mallin et al. 2005). Patterns of silicate availability and diatom biovolume observed during the field study concurrent with these experiments (Chapter I) are similar to those reviewed by Conley et al. (1993), with increasing contribution of diatom biovolume associated with decreased silicate concentrations. In contrast to other regions, riverine inflows are an unlikely source of Si to Corpus Christi Bay given the extensive damming and decreased freshwater flows reaching the

system (Montagna et al. 2009), potentially indicating that internal cycling of Si is an important process driving phytoplankton community growth, and diatom growth in particular.

During the winter experiment, none of the N addition treatments stimulated phytoplankton growth rates. These results indicate limitation by something other than the availability of N in winter. There was relatively little drawdown of N, P, and Si observed in all treatments during the winter compared to other seasons. Decreased growth rates have been observed for phytoplankton in taxa-specific and community-based bioassays under low winter-like temperatures (Lomas and Glibert 1999; Örnólfsdóttir et al. 2004). Light has also been described as a limiting factor for phytoplankton under nutrient replete conditions (Cloern et al. 1999; Fisher et al. 1999; Cira et al. 2016). It is possible that during the winter experiment here, both temperature and light were playing a role in limiting phytoplankton growth. The water temperature recorded during experimental setup (6.8°C) was lower than the average winter temperatures at the water collection site (14.3 ± 4.3°C) reported during the accompanying field study (Chapter I). Additionally, the Secchi depth recorded during experimental setup was relatively shallow at 0.4 m compared to the average winter Secchi depth at the water collection site (0.6 ± 0.3 m) reported during the accompanying field study (Chapter I), supporting a role for light limited phytoplankton growth.

The lack of observed phytoplankton growth responses to the fish tissue extract across all seasons merits independent discussion. Decomposition of organic matter in natural environments, especially in low nutrient and/or long residence time systems, is a critical aspect of biogeochemical cycling of elements necessary for fueling primary productivity (Altman and Paerl 2012; Killberg-Thoreson et al. 2014; Paerl et al. 2014). In estuarine environments that experience frequent harmful algal blooms and concomitant fish kills it is necessary to assess the

role that fish derived nutrients may play in fueling phytoplankton growth under bloom and non-bloom conditions. It has been demonstrated through experimental (Killberg-Thoreson et al. 2014) and isotopic (Walsh et al. 2009) investigations that nutrients derived from fish can support phytoplankton growth in general, and of *K. brevis* in particular. In this study however, there was no evidence that fish tissue extract stimulated phytoplankton growth. The method employed here differs from that of Killberg-Thoreson et al. (2014) in that they allowed physical and biological degradation of the fish tissue to occur (~ 3 days) before utilizing the fish derived nutrients in bioassays, whereas we did not. The lack of "pre-degradation" here may have limited the availability of the provided nutrients to phytoplankton. The lack of an obvious growth response to fish tissue extract may also have been due to a lower than expected total N addition from this source. The winter experiment was the only instance of the fish tissue extract approximating a 20 µM addition (added N = 16.57 µM). In the summer, the quantity of added N (7.47 µM) was lower than in the winter, but still higher than the control (1.24 µM) and consisted of a small quantity of NH_4^+ and DON. In the fall and spring, however, the quantity of added was calculated as negative at -4.89 µM and -4.32 µM, respectively. In both cases, this sharp drop in added N is attributable to decreases in the concentration of DON. The rapid depletion of DON may be due to rapid uptake by bacteria or mixotrophic phytoplankton immediately following the addition of this source. Regardless of the mechanism, some caution must be exercised in drawing conclusions from the fish tissue extract treatments in regards to potential effects on phytoplankton growth.

Major Taxonomic Group Growth Rates

Diatoms responded to at least one N addition in summer, fall, and spring, consistent with observations that diatoms are favored by moderate to high N concentrations and are highly

competitive following pulsed nutrient inputs (Piehler et al. 2004; Pinckney et al. 1999). The well documented preference of diatoms for NO_3^- was also seen here, but only during the summer experiment. In the summer, diatom growth rates in the NOx enriched WWTP effluent treatment were significantly higher than the ammonium and porewater treatments (NH_4^+ enriched), but not significantly higher than the nitrate or runoff treatments (NOx enriched). In the fall there was little variation in diatom growth rates among the N addition treatments, with no significant differences detected among the ammonium, nitrate, porewater, runoff, and WWTP effluent treatments. In the spring there was again no clear evidence to support a role for N form preference in the response of diatoms to N addition, though there was evidence that Si limitation was induced by the addition of N. This aligns well with the discussion of Si limitation of whole community growth rates above. Taken together, these results indicate that bottom-up regulation of diatom growth is strongly tied to N availability, though N form and secondary Si limitation may be seasonally important.

In contrast, N addition responses of picocyanobacteria and picoeukaryotes indicate the importance of other bottom-up and/or top-down factors in regulating growth. Both picophytoplankton groups were stimulated by at least one N addition in the summer, with picocyanobacteria additionally responding to at least one N addition in the fall, and picoeukaryotes additionally responding to at least one N addition in the spring. Despite similar preferences for relatively warm temperatures (Worden et al. 2004; Gaulke et al. 2010; Paerl et al. 2020) and reduced N forms (Shangguan et al. 2017; Paerl et al. 2020), there is also evidence that picocyanobacteria and picoeukaryotes respond differently to changes in environmental conditions (Zhang et al. 2013; Paerl et al. 2020). For example, in the Pearl River Estuary a negative relationship was found between freshwater loading (increased turbidity, increased DIN,

increased P, and decreased salinity) and picocyanobacteria biomass, whereas the relationship between freshwater loading and picoeukaryote biomass was positive (Zhang et al. 2013). Similar findings come from the Neuse River Estuary, North Carolina, where picocyanobacteria negatively related to TDN and positively related to salinity (Paerl et al. 2020), whereas picoeukaryotes were positively related to TDN and negatively related to salinity. Taken together, these findings provide evidence that further studies considering phytoplankton-nutrient dynamics should consider picocyanobacteria and picoeukaryotes individually.

These experiments also revealed no clear relationships between the growth rates of picophytoplankton groups and N form, with both groups responding similarly to treatments primarily enriched in NOx and treatments enriched in NH_4^+. During the summer experiment, picocyanobacteria growth rates were greater than the control in the NH_4^+ enriched ammonium treatment as well as the NOx enriched nitrate, runoff, and WWTP effluent treatments, with no differences detected among these treatments. Similarly, picoeukaryote growth rates were elevated relative to the control in the NH_4^+ enriched ammonium and porewater treatments, and in the NOx enriched nitrate, runoff, and WWTP effluent treatments, indicating no preference for N form. In the fall, picocyanobacteria were again stimulated by nearly all treatments, regardless of N form. Growth rates in the ammonium, nitrate, porewater, and WWTP effluent treatments were greater than the control, with no differences among those treatments. Lastly, the spring experiment provided further evidence for this conclusion with picoeukaryote growth rates elevated relative to the control in the NH_4^+ enriched ammonium and porewater treatments as well as the NOx enriched WWTP effluent treatment.

Picoeukaryotes did, however, display secondary P limitation in the summer and spring, whereas there was no evidence of secondary P limitation affecting picocyanobacteria growth

rates, consistent with the known ability of picocyanobacteria to thrive in P limited environments (Shangguan et al. 2017). Picoeukaryote growth rates in the summer were higher in the WWTP effluent treatment than all others, and growth rates in the spring were higher in the porewater and WWTP effluent treatments than all others. These picoeukaryote-specific differences in growth rate response to N addition are quite similar to the whole community growth rate response discussed above and are in line with the hypothesized co/induced P limitation hypothesized above. The ability of picocyanobacteria to substitute non-P containing lipids for P-containing lipids, and relatively low cellular requirements for P may explain the lack of observed P limitation for the picocyanobacteria compared to the picoeukaryotes (Shangguan et al. 2017). A final consideration for the lack of seasonally coherent responses of the picophytoplankton groups to additions of N is the potential for heavy grazing. Picophytoplankton as a group are known to be susceptible to heavy grazing pressure, though some taxa are known to be preferentially grazed over others (Gaulke et al. 2010; Paerl et al. 2020). Additionally, Agawin et al. (2000) presented evidence that the turnover rate of picophytoplankton increased linearly with the growth rate of picophytoplankton following additions of NO_3^-, likely indicating tight coupling of growth and loss rates in this group. Picophytoplankton abundance and taxonomic composition can influence food web trophodynamics and biogeochemical cycling within a system (Finkel et al. 2010; Gaulke et al. 2010; Paerl et al. 2020), and as such further work to disentangle the factors supporting picocyanobacteria and picoeukaryotes in the Corpus Christi Bay system is warranted.

Lastly, dinoflagellate growth rates only increased relative to the control in the porewater treatment during the spring experiment. Limited growth response by dinoflagellates in response to N addition, however, has been observed elsewhere (Piehler et al. 2004; Cira et al. 2016; Shangguan et al. 2017). The lack of elevated dinoflagellate growth rates following N addition

may be attributable to the relatively slow growth rates of this group and the short duration of these experiments. Indeed, this is supported by results of other nutrient addition bioassays (Piehler et al. 2004; Shangguan et al. 2017) and modeling efforts (Roelke et al. 1999; Macias et al. 2010) that demonstrate the competitive advantage of fast-growing diatoms over dinoflagellates when nutrient inputs are pulsed. The Si limitation of diatoms in spring may have contributed to the success of dinoflagellates then compared to other seasons but is unlikely the sole factor influencing these results. If diatom limitation was the only factor driving dinoflagellate responses to N, then it would follow that dinoflagellate growth rates in the ammonium and nitrate treatments should have also been significantly higher than the control during the spring experiment, though this was not the case. Therefore, there are likely other unexplored factors influencing the response of dinoflagellates to N additions.

Despite differences in the growth rate response of the major phytoplankton taxonomic groups to N addition from different sources, results from the hierarchical clustering analysis provide only minimal evidence for changing phytoplankton community structure in response to pulsed N inputs. In general, the highest degree of similarity among phytoplankton communities was observed within season, with the only treatment-specific differences observed among the summer experiment. With the exception of spring, the initial communities deviated from this pattern, indicating that pulsed inputs, regardless of N source, similarly influence phytoplankton community composition on relatively short (48 hour) time scales. The pulsed nature of N inputs and consistently strong N limitation observed prior to experiments, may have played a role in the lack phytoplankton community variability related to N addition treatment. As evidenced by rapid drawdown of "new" nutrients, it is also possible that phytoplankton rapidly deplete pulsed nutrient inputs in Corpus Christi Bay and subsequently become dependent on "recycled"

nutrients. This may limit the duration of elevated growth rates for all phytoplankton taxa similarly, whereas chronic anthropogenic nutrient inputs, such as WWTP effluent, on time scales longer than 48 hours may be more likely to differentially select for some taxa over others (Roelke et al. 1999). In the accompanying field study (see Chapter I), short pulses of nutrient inputs following precipitation events resulted in only short-lived peaks in phytoplankton biovolume with little change in composition between the "before precipitation" community and the "after precipitation" community, supporting the hypothesis that rapid drawdown of "new" nutrients prevents shifts in community composition. At a site located in man-made canals with limited connectivity, however, the influence of precipitation-derived nutrients occasionally elicited shifts in community composition. Similar dynamics were observed in regions of the Indian River Lagoon, with regions that have relatively long residence times exhibiting greater potential for bloom formation following precipitation-driven nutrient inputs compared to regions with shorter residence times (Phlips et al. 2011). This indicates that not only is the duration of nutrient inputs a concern, but the general connectivity of waterways and the susceptibility of phytoplankton to hydraulic displacement (or lack thereof) will be an important determinant of the observed biomass and community composition response.

Influence of N Sources

Rapid drawdown of runoff-derived N in the summer, fall, and spring indicate that Corpus Christi Bay may be buffered against the anthropogenic impacts associated with increased impervious surfaces and nutrient loading by the pulsed nature of this source. This is supported by the relatively low phytoplankton biovolume observed at the site of an urban stormwater runoff drain that discharges directly into Corpus Christi Bay (see Chapter I). Indeed, if runoff-derived N was plentiful for longer periods following rainfall events it would be expected that there would

be evidence of increased phytoplankton biovolume due to prolonged release from N limitation. This source of N should not be discounted in the creation of management plans, however. Projected increases in human population indicate that impervious surfaces and associated nutrient loads will continue to increase in this region, and results from a study by Seitzinger et al. (2002) indicate that the relative proportion of bioavailable DON is higher in suburban/urban derived runoff compared to forest and agricultural runoff. Pollutant and nutrient loads in stormwater runoff are affected by event-based rainfall totals, seasonal rainfall totals, duration of the dry period preceding rainfall, and drainage area (Maniquiz et al. 2010). Projected changes in the timing and magnitude of extreme precipitation and seasonal and annual rainfall totals under future climate change scenarios then have the potential to increase the magnitude, duration, and composition of runoff-derived N pulses.

Porewater is similarly a pulsed source of N, with increased N release during wind-driven resuspension of surficial sediments. Additionally, N concentration and form fluxing into the water column from porewater are likely seasonally dependent. In Corpus Christi Bay increased rates of both denitrification and dissimilatory nitrate reduction to ammonium (DNRA) have been observed under hypoxic conditions relative to normoxic conditions, indicating greater potential release of NH_4^+ under hypoxic conditions (McCarthy et al. 2008). In these experiments porewater was predominantly enriched in NH_4^+, supporting the role of sediments in supplying reduced N to Corpus Christi Bay phytoplankton. The general lack of dinoflagellate response to this nutrient source was somewhat surprising given enrichment in reduced N, though this may be closely related to the success of diatoms as discussed above (Roelke et al. 1999; Piehler et al. 2004; Macias et al. 2010; Shangguan et al. 2017). The ability of dinoflagellates to migrate to near-bottom waters when nutrients are otherwise limiting, however, indicates that under typical

conditions in Corpus Christi Bay, porewater N may be more influential in the growth of dinoflagellates than that observed here. Lastly, considerations for future changes in watershed land-use and climate change scenarios indicate the potential for increased quantity of N supplied to the system by porewater. Under projected warmer and drier climate conditions, water column stratification will likely increase. Increased stratification may then increase the extent of hypoxic bottom water, thereby altering sediment N cycling, with a shift towards increasing rates of DNRA and NH_4^+ release from sediments. The more consistently available NH_4^+, and lower availability of Si noted above, may ultimately favor dinoflagellates or other flagellated taxa over diatoms, potentially leading to increased occurrences of HABs.

Unsurprisingly, the WWTP effluent used here elicited strong phytoplankton growth rate responses. Indeed, there is continuity in the effects of wastewater observed in Oso Bay, a sub-estuary of Corpus Christi Bay. Early work by Flint (1984) demonstrated increased primary productivity in Corpus Christi Bay near Oso Inlet, strongly related to NH_4^+ availability. Later work by Wetz et al. (2016) also demonstrated strong linkages between wastewater and declining water quality in Oso Bay, including the prevalence of hypoxic conditions despite strong, near-constant wind-driven mixing. Lastly, Bugica et al. (2020) found Oso Bay to be a "hot spot" for symptoms of eutrophication in the Corpus Christi Bay system. Interestingly, there was no observable increase in ambient N concentrations in Oso Bay despite the observed increase in chlorophyll *a*. This may indicate that though tight coupling of N inputs and phytoplankton uptake maintain relatively stable water column N concentrations, these concentrations likely do not reflect the level of anthropogenic nutrification and subsequent eutrophication occurring in this sub-estuary of Corpus Christi Bay. It is therefore critical that studies aimed at determining

when, where, and how to implement nutrient management strategies strongly consider the time integrated effects of pulsed versus continuous N inputs.

Additionally, when comparing the patterns in major taxonomic group growth rates across seasons, the WWTP effluent consistently elicited growth rates greater than the control for diatoms, picocyanobacteria, and picoeukaryotes. The WWTP effluent used here provided the highest concentrations of orthophosphate, Si, and NOx compared to the natural and anthropogenic sources, as well as small quantities of NH_4^+. This multi-nutrient enrichment may explain the observed success of multiple taxonomic groups. WWTP effluent has been implicated in declining water quality and accumulation of phytoplankton biomass in other estuaries (Mallin et al. 2005; Paerl et al. 2014), including Oso Bay here (Wetz et al. 2016). Additionally, the negative impacts of WWTP loadings are thought to be exacerbated in low flow systems with high residence times (Mallin et al. 2005). In comparison to the WWTP effluent, other natural and anthropogenic nutrient sources elicited more variable growth rate responses among the major phytoplankton groups.

Conclusion

The response of phytoplankton growth rates to N availability here indicates that long-term anthropogenic nutrient loading to Corpus Christi Bay could result in an increase in the prevalence of the symptoms of eutrophication. Microzooplankton grazing rate experiments conducted concurrently with those described here (Tominack unpubl. data) indicated that microzooplankton grazing is an important control on phytoplankton biovolume accumulation under ambient nutrient levels, with grazing rates approximating phytoplankton growth rates in spring, summer, and fall. However, release from N limitation elicited phytoplankton growth rates that surpassed microzooplankton grazing rates. Though there are no documented long-term

increases in N concentrations or chlorophyll *a* throughout Corpus Christi Bay, they are becoming apparent in one of its largest tributaries, Oso Bay, that receives significant WWTP inputs (Wetz et al. 2016; Bugica et al. 2020). Results from the experiments here highlight important aspects of nutrient pollution dynamics and management given the current conditions/status of Corpus Christi Bay. Short duration pulses of nutrients consistently favored increased diatom growth rates, except under Si limiting conditions, whereas the growth rate responses of other phytoplankton groups were less consistent. These results are consistent with the hypothesis of Roelke et al. (1999) suggesting the possibility of favoring edible fast-growing taxa over less edible slow-growing taxa by pulsing nutrient supplies to a system. These results also highlight the importance of understanding how chronic N inputs, such as WWTP effluent, may alter phytoplankton biomass accumulation and nutrient cycling pathways. Additionally, though the WWTP effluent used here was enriched in N, P and Si, similar to riverine inflows, enrichment of the latter two nutrients is not always observed (Roelke et al. 1997; Mallin et al. 2005). Assessing the nutrient enrichment of the many different wastewater outfalls affecting Oso Creek, Oso Bay, Nueces Bay, and Corpus Christi Bay will be paramount to understanding how this anthropogenic nutrient source will affect nutrient-phytoplankton dynamics in the future, especially as drier, hotter conditions may reduce or increase inputs from other watershed and estuarine nutrient sources.

References

Agawin, N. S. R., C. M. Duarte, and S. Agustí. 2000. Nutrient and temperature control of the contribution of picoplankton to phytoplankton biomass and production. *Limnology and Oceanography* 45. American Society of Limnology and Oceanography Inc.: 591–600. https://doi.org/10.4319/lo.2000.45.3.0591.

Alpine, A. E., and J. E. Cloern. 1992. Trophic interactions and direct physical effects control phytoplankton biomass and production in an estuary. *Limnology and Oceanography* 37: 946–955. https://doi.org/10.4319/lo.1992.37.5.0946.

Altman, J. C., and H. W. Paerl. 2012. Composition of inorganic and organic nutrient sources influences phytoplankton community structure in the New River Estuary, North Carolina. *Aquatic Ecology* 46: 269–282. https://doi.org/10.1007/s10452-012-9398-8.

Anderson, D. M., P. M. Glibert, and J. M. Burkholder. 2002. Harmful algal blooms and eutrophication: Nutrient Sources, Composition, and Consequences. *Estuaries* 25: 704–726.

Baek, S. H., D. Kim, M. Son, S. M. Yun, and Y. O. Kim. 2015. Seasonal distribution of phytoplankton assemblages and nutrient-enriched bioassays as indicators of nutrient limitation of phytoplankton growth in Gwangyang Bay, Korea. *Estuarine, Coastal and Shelf Science* 163. Academic Press: 265–278. https://doi.org/10.1016/j.ecss.2014.12.035.

Bricker, S. B., B. Longstaff, W. Dennison, A. Jones, K. Boicourt, C. Wicks, and J. Woerner. 2008. Effects of nutrient enrichment in the nation's estuaries: A decade of change. *Harmful Algae* 8: 21–32. https://doi.org/10.1016/j.hal.2008.08.028.

Brussaard, C. P. D. 2004. Viral Control of Phytoplankton Population--a Review. *Journal of Eukaryotic Microbiology* 51: 125–138. https://doi.org/10.1111/j.1550-7408.2005.000vol-cont.x.

Bugica, K., B. Sterba-Boatwright, and M. S. Wetz. 2020. Water quality trends in Texas estuaries. *Marine Pollution Bulletin* 152. Elsevier Ltd. https://doi.org/10.1016/j.marpolbul.2020.110903.

Burkholder, J. A. M., P. M. Glibert, and H. M. Skelton. 2008. Mixotrophy, a major mode of nutrition for harmful algal species in eutrophic waters. *Harmful Algae* 8: 77–93. https://doi.org/10.1016/j.hal.2008.08.010.

Canfield, Donald, E. Kristensen, B. Thamdrup. 2005. *Aquatic Geomicrobiology*. doi: 10.1016/S0065-2881(05)48017-7.

Cira, E. K., H. W. Paerl, and M. S. Wetz. 2016. Effects of nitrogen availability and form on phytoplankton growth in a eutrophied estuary (Neuse River Estuary, NC, USA). Edited by Christopher J. Gobler. *PLoS ONE* 11. Public Library of Science: e0160663. https://doi.org/10.1371/journal.pone.0160663.

Clarke, K. R., and R. N. Gorley. 2015. Getting started with PRIMER v7. *PRIMER-E: Plymouth, Plymouth Marine Laboratory*: 20.

Cloern, J. E. 1999. The relative importance of light and nutrient limitation of phytoplankton growth: A simple index of coastal ecosystem sensitivity to nutrient enrichment. *Aquatic Ecology* 33: 3–19.

Cloern, J. E. 2001. Our evolving conceptual model of the coastal eutrophication problem. *Marine Ecology Progress Series* 210: 223–253. https://doi.org/10.3354/meps210223.

Cloern, J. E., and R. Dufford. 2005. Phytoplankton community ecology: Principles applied in San Francisco Bay. *Marine Ecology Progress Series* 285: 11–28. https://doi.org/10.3354/meps285011.

Conley, Danil J., C. L. Schelski, E. F. Stoermer. 1993. Modification of the biogeochemical cycle of silica with eutrophication. *Marine Ecology Progress Series* 101:179-192.

Dillon, K. S., and J. P. Chanton. 2005. Nutrient transformations between rainfall and stormwater runoff in an urbanized coastal environment: Sarasota Bay, Florida. *Limnology and Oceanography* 50: 62–69. https://doi.org/10.4319/lo.2005.50.1.0062.

Finkel, Z. v., J. Beardall, K. J. Flynn, A. Quigg, T. A. v. Rees, and J. A. Raven. 2010. Phytoplankton in a changing world: Cell size and elemental stoichiometry. *Journal of Plankton Research* 32: 119–137. https://doi.org/10.1093/plankt/fbp098.

Fisher, T. R., A. B. Gustafson, K. Sellner, R. Lacouture, L. W. Haas, R. L. Wetzel, R. Magnien, D. Everitt, B. Michaels, and R. Karrh. 1999. Spatial and temporal variation of resource limitation in Chesapeake Bay. *Marine Biology* 133: 763–778. https://doi.org/10.1007/s002270050518.

Flint, R. W. 1984. Phytoplankton production in the Corpus Christi Bay Estuary. *Contributions in Marine Science*.

Gaulke, A. K., M. S. Wetz, and H. W. Paerl. 2010. Picophytoplankton: A major contributor to planktonic biomass and primary production in a eutrophic, river-dominated estuary. *Estuarine, Coastal and Shelf Science* 90: 45–54. https://doi.org/10.1016/j.ecss.2010.08.006.

Glibert, P. M. 2017. Eutrophication, harmful algae and biodiversity — Challenging paradigms in a world of complex nutrient changes. *Marine Pollution Bulletin* 124. Elsevier Ltd: 591–606. https://doi.org/10.1016/j.marpolbul.2017.04.027.

Glibert, P. M., and J. A. M. Burkholder. 2011. Harmful algal blooms and eutrophication: "strategies" for nutrient uptake and growth outside the Redfield comfort zone. *Chinese Journal of Oceanology and Limnology* 29: 724–738. https://doi.org/10.1007/s00343-011-0502-z.

Glibert, P. M., F. P. Wilkerson, R. C. Dugdale, J. A. Raven, C. L. Dupont, P. R. Leavitt, A. E. Parker, J. M. Burkholder, and T. M. Kana. 2016. Pluses and minuses of ammonium and nitrate uptake and assimilation by phytoplankton and implications for productivity and community composition, with emphasis on nitrogen-enriched conditions. *Limnology and Oceanography* 61. John Wiley & Sons, Ltd: 165–197. https://doi.org/10.1002/LNO.10203@10.1002/(ISSN)1939-5590.STABLE-ISOTOPES.

Glibert, P. M., J. Harrison, C. Heil, and S. Seitzinger. 2006. Escalating worldwide use of urea - A global change contributing to coastal eutrophication. *Biogeochemistry*. Springer. https://doi.org/10.1007/s10533-005-3070-5.

Glibert, P. M., S. Seitzinger, C. A. Heil, J. M. Burkholder, M. W. Parrow, L. A. Codispoti, and V. Kelly. 2005. The role of eutrophication in the global proliferation of harmful algal blooms. *Oceanography* 18: 198–209. https://doi.org/10.5670/oceanog.2005.54.

Hothorn, T., F. Bretz, and P. Westfall. 2008. Simultaneous Inference in General Parametric Models. *Biometrical Journal* 50: 346–363.

Islam, M. S., J. S. Bonner, B. L. Edge, and C. A. Page. 2014. Hydrodynamic characterization of Corpus Christi Bay through modeling and observation. *Environmental Monitoring and Assessment* 186. Kluwer Academic Publishers: 7863–7876. https://doi.org/10.1007/s10661-014-3973-5.

Killberg-Thoreson, L., R. E. Sipler, and D. A. Bronk. 2013. Anthropogenic Nutrient Sources Supplied to a Chesapeake Bay Tributary Support Algal Growth: A Bioassay and High-Resolution Mass Spectrometry Approach. *Estuaries and Coasts* 36: 966–980. https://doi.org/10.1007/s12237-013-9604-5.

Killberg-Thoreson, L., R. E. Sipler, C. A. Heil, M. J. Garrett, Q. N. Roberts, and D. A. Bronk. 2014. Nutrients released from decaying fish support microbial growth in the eastern Gulf of Mexico. *Harmful Algae* 38. Elsevier: 40–49. https://doi.org/10.1016/j.hal.2014.04.006.

Lomas, Michael W., P. M. Glibert. 1999. Temperature regulation of nitrate uptake: A novel hypothesis about nitrate uptake and reduction in cool-water diatoms. *Limnology and Oceanography* 44:556-572.

Lotze, H. K., H. S. Lenihan, B. J. Bourque, R. H. Bradbury, R. G. Cooke, M. C. Kay, S. M. Kidwell, M. X. Kirby, C. H. Peterson, and J. B. C. Jackson. 2006. Depletion, Degradation, and Recovery Potential of Estuaries and Coastal Seas. *Science* 312: 1806–1809. https://doi.org/10.1126/science.1128035.

Macias, D., E. Ramírez-Romero, C. M. García. 2010. Effect of nutrient input frequency on the structure and dynamics of the marine pelagic community: A modeling approach. *Journal of Marine Research* 68: 119-151.

Mallin, M. A., H. W. Paerl, J. Rudek, and P. W. Bates. 1993. Regulation of estuarine primary production by watershed rainfall and river flow. *Marine Ecology Progress Series* 93: 199–203.

Mallin, M. A., M. R. McIver, H. A. Wells, D. C. Parsons, and V. L. Johnson. 2005. Reversal of eutrophication following sewage treatment upgrades in the New River Estuary, North Carolina. *Estuaries* 28: 750–760. https://doi.org/10.1007/BF02732912.

Maniquiz, Marla M., S. Lee, L.-H. Kim. 2010. Multiple linear regression models of urban runoff pollutant load and event mean concentration considering rainfall values. *Journal of Environmental Science* 22: 946-952. doi: 10.1016/S1001-0742(09)60203-5.

Martin, Patrick, S. T. Dyhrman, M. W. Lomas, N. J. Poulton, B. A. S. Van Mooy. 2014. Accumulation and enhanced cycling of polyphosphate by Sargasso Sea plankton in response to low phosphorus. *PNAS* 111:8089-8094. doi: 10.1073/pnas.13217191111.

McCarthy, M. J., K. S. McNeal, J. W. Morse, and W. S. Gardner. 2008. Bottom-water hypoxia effects on sediment-water interface nitrogen transformations in a seasonally hypoxic, shallow bay (Corpus Christi Bay, TX, USA). *Estuaries and Coasts* 31: 521–531. https://doi.org/10.1007/s12237-008-9041-z.

Moestrup, Ø., R. Akselmann-Cardella, C. Churro, S. Fraga, M. Hoppenrath, M. Iwataki, J. Larsen, N. Lundholm, A. Zingone. 2009. IOC-UNESCO Taxonomic Reference List of Harmful Micro Algae. Accessed at http://www.marinespecies.org/hab on 2021-01-08. doi: 10.14284/362.

Montagna, P. A., E. M. Hill, and B. Moulton. 2009. Role of science-based and adaptive management in allocating environmental flows to the Nueces Estuary, Texas, USA. *WIT Transactions on Ecology and the Environment* 122. WITPress: 559–570. https://doi.org/10.2495/ECO090511.

Neale, P. J., C. Sobrino, M. Segovia, J. M. Mercado, P. Leon, M. D. Cortés, P. Tuite, et al. 2014. Effect of CO2, nutrients and light on coastal plankton. I. abiotic conditions and biological responses. *Aquatic Biology* 22. Inter-Research: 25–41. https://doi.org/10.3354/ab00587.

Nohe, A., A. Goffin, L. Tyberghein, R. Lagring, K. de Cauwer, W. Vyverman, and K. Sabbe. 2020. Marked changes in diatom and dinoflagellate biomass, composition and seasonality in the Belgian Part of the North Sea between the 1970s and 2000s. *Science of the Total Environment* 716. Elsevier B.V. https://doi.org/10.1016/j.scitotenv.2019.136316.

Örnólfsdóttir, E. B., S. E. Lumsden, and J. L. Pinckney. 2004. Nutrient pulsing as a regulator of phytoplankton abundance and community composition in Galveston Bay, Texas. *Journal of Experimental Marine Biology and Ecology* 303: 197–220. https://doi.org/10.1016/j.jembe.2003.11.016.

Paerl, H. W. 1988. Nuisance phytoplankton blooms in coastal, estuarine, and inland waters1. *Limnology and Oceanography* 33: 823–843. https://doi.org/10.4319/lo.1988.33.4part2.0823.

Paerl, H. W. 2006. Assessing and managing nutrient-enhanced eutrophication in estuarine and coastal waters: Interactive effects of human and climatic perturbations. *Ecological Engineering* 26: 40–54. https://doi.org/10.1016/j.ecoleng.2005.09.006.

Paerl, H. W., and D. Justić. 2013. Estuarine phytoplankton. In *Estuarine ecology*, Second, 85–110. Wiley Online Library.

Paerl, H. W., and N. D. Bowles. 1987. Dilution bioassays: Their application to assessments of nutrient limitation in. *Hydrobiologia* 146. Springer: 265–273.

Paerl, H. W., and V. J. Paul. 2012. Climate change: Links to global expansion of harmful cyanobacteria. *Water Research* 46. Elsevier Ltd: 1349–1363. https://doi.org/10.1016/j.watres.2011.08.002.

Paerl, H. W., T. G. Otten, and R. Kudela. 2018. Mitigating the Expansion of Harmful Algal Blooms Across the Freshwater-to-Marine Continuum. *Environmental Science and Technology* 52. American Chemical Society: 5519–5529. https://doi.org/10.1021/acs.est.7b05950.

Paerl, Hans W., N. S. Hall, B. L. Peierls, K. K. Rossignol. 2014. Evolving paradigms and challenges in estuarine and coastal eutrophication dynamics in a culturally and

climatically stressed world. *Estuaries and Coasts* 37:243-258. doi: 10.1007/s12237-014-9773-x.

Paerl, Ryan W., R. E. Venezia, J. J. Sanchez, H. W. Paerl. 2020. Picophytoplankton dynamics in a large temperate estuary and impacts of extreme storm events. *Scientific Reports* 10:22026. doi: 10.1038/s41598-020-79157-6.

Phlips, E. J., S. Badylak, M. Christman, J. Wolny, J. Brame, J. Garland, L. Hall, et al. 2011. Scales of temporal and spatial variability in the distribution of harmful algae species in the Indian River Lagoon, Florida, USA. *Harmful Algae* 10. Elsevier B.V.: 277–290. https://doi.org/10.1016/j.hal.2010.11.001.

Piehler, M. F., L. J. Twomey, N. S. Hall, and H. W. Paerl. 2004. Impacts of inorganic nutrient enrichment on phytoplankton community structure and function in Pamlico Sound, NC, USA. *Estuarine, Coastal and Shelf Science* 61: 197–209. https://doi.org/10.1016/j.ecss.2004.05.001.

Pinckney, J. L., H. W. Paerl, and M. B. Harrington. 1999. Responses of the phytoplankton community growth rate to nutrient pulses in variable estuarine environments. *Journal of Phycology* 35: 1455–1463. https://doi.org/10.1046/j.1529-8817.1999.3561455.x.

Quinn, G. P., and M. J. Keough. 2002. *Experimental design and data analysis for biologists*. Cambridge university press.

R Core Team. 2019. R: A Language and Environment for Statistical Computing. Vienna, Austria.

Reed, M. L., J. L. Pinckney, C. J. Keppler, L. M. Brock, S. B. Hogan, D. I. Greenfield. 2016. The influence of nitrogen and phosphorous on phytoplankton growth and assemblange

composition in four coastal, southeastern USA systems. *Estuaries, Coastal and Shelf Science* 177: 71-82. doi: 10.1016/j.ecss.2016.05.002.

Reynolds, C. S. 2006. *The Ecology of Phytoplankton*. https://doi.org/10.1017/CBO9780511542145.

Ritter, C., and P. A. Montagna. 1999. Seasonal hypoxia and models of benthic response in a Texas Bay. *Estuaries* 22: 7–20. https://doi.org/10.2307/1352922.

Roelke, D. L., L. A. Cifuentes, P. M. Eldridge. 1997. Nutrient and phytoplankton dynamics in a sewage-impacted Gulf Coast estuary: A Field test of the PEG-Model and Equilibrium Resource Competition Theory. *Estuaries* 20: 725-742.

Roelke, D. L., P. M. Eldridge, and L. A. Cifuentes. 1999. A model of phytoplankton competition for limiting and nonlimiting nutrients: Implications for development of estuarine and nearshore management schemes. *Estuaries* 22: 92–104. https://doi.org/10.2307/1352930.

Rudek, Joseph, H. W. Paerl, M. A. Mallin, P. W. Bates. 1991. Seasonal and hydrological control of phytoplankton nutrient limitation in the lower Neuse River Estuary, North Carolina. *Marine Ecology Progress Series* 75:133-142.

Seitzinger, S. P., R. W. Sanders, and R. Styles. 2002. Bioavailability of DON from natural and anthropogenic sources to estuarine plankton. *Limnology and Oceanography* 47: 353–366. https://doi.org/10.4319/lo.2002.47.2.0353.

Shangguan, Y., P. M. Glibert, J. Alexander, C. J. Madden, and S. Murasko. 2017. Phytoplankton assemblage response to changing nutrients in Florida Bay: Results of mesocosm studies. *Journal of Experimental Marine Biology and Ecology* 494: 38–53. https://doi.org/10.1016/j.jembe.2017.05.006.

Spatharis, S., G. Tsirtsis, D. B. Danielidis, T. do Chi, and D. Mouillot. 2007. Effects of pulsed nutrient inputs on phytoplankton assemblage structure and blooms in an enclosed coastal area. *Estuarine, Coastal and Shelf Science* 73: 807–815. https://doi.org/10.1016/j.ecss.2007.03.016.

Suggett, D. J., C. M. Moore, A. E. Hickman, and R. J. Geider. 2009. Interpretation of fast repetition rate (FRR) fluorescence: Signatures of phytoplankton community structure versus physiological state. *Marine Ecology Progress Series* 376: 1–19. https://doi.org/10.3354/meps07830.

Sun, J., and D. Liu. 2003. Geometric models for calculating cell biovolume and surface area for phytoplankton. *Journal of Plankton Research* 25: 1331–1346. https://doi.org/10.1093/plankt/fbg096.

Sylvan, J. B., A. Quigg, S. Tozzi, J. W., Ammerman. 2007. Eutrophication-induced phosphorus limitation in the Mississippi River plume: Evidence from fast repetition rate fluorometry. *Limnology and Oceanography* 52:2679-2685.

Turner, E. L., B. Paudel, and P. A. Montagna. 2015. Baseline nutrient dynamics in shallow well mixed coastal lagoon with seasonal harmful algal blooms and hypoxia formation. *Marine Pollution Bulletin* 96. Elsevier Ltd: 456–462. https://doi.org/10.1016/j.marpolbul.2015.05.005.

Walsh, J. J., R. H. Weisberg, J. M. Lenes, F. R. Chen, D. A. Dieterle, L. Zheng, K. L. Carder, et al. 2009. Isotopic evidence for dead fish maintenance of Florida red tides, with implications for coastal fisheries over both source regions of the West Florida shelf and within downstream waters of the South Atlantic Bight. *Progress in Oceanography* 80. Elsevier Ltd: 51–73. https://doi.org/10.1016/j.pocean.2008.12.005.

Wetz, M. S., K. C. Hayes, K. V. B. Fisher, L. Price, and B. Sterba-Boatwright. 2016. Water quality dynamics in an urbanizing subtropical estuary(Oso Bay, Texas). *Marine Pollution Bulletin* 104. Elsevier Ltd: 44–53. https://doi.org/10.1016/j.marpolbul.2016.02.013.

Worden, Alexandra Z., J. K. Nolan, B. Palenik. 2004. Assessing the dynamics and ecology of marine picophytoplankton: The importance of the eukaryotic component. *Limnology and Oceanography* 49:168-179.

Yang, Y. Y., and G. S. Toor. 2016. δ15N and δ18O Reveal the Sources of Nitrate-Nitrogen in Urban Residential Stormwater Runoff. *Environmental Science and Technology* 50: 2881–2889. https://doi.org/10.1021/acs.est.5b05353.

Zhang, X., Z. Shi, Q. Liu, F. Ye, L. Tian, X. Huang. 2013. Spatial and temporal variations of picoplankton in three contrasting periods in the Pearl River Estuary, South China. *Continental Shelf Research* 56:1-12. doi: 10.1016/j.csr.2013.01.015.

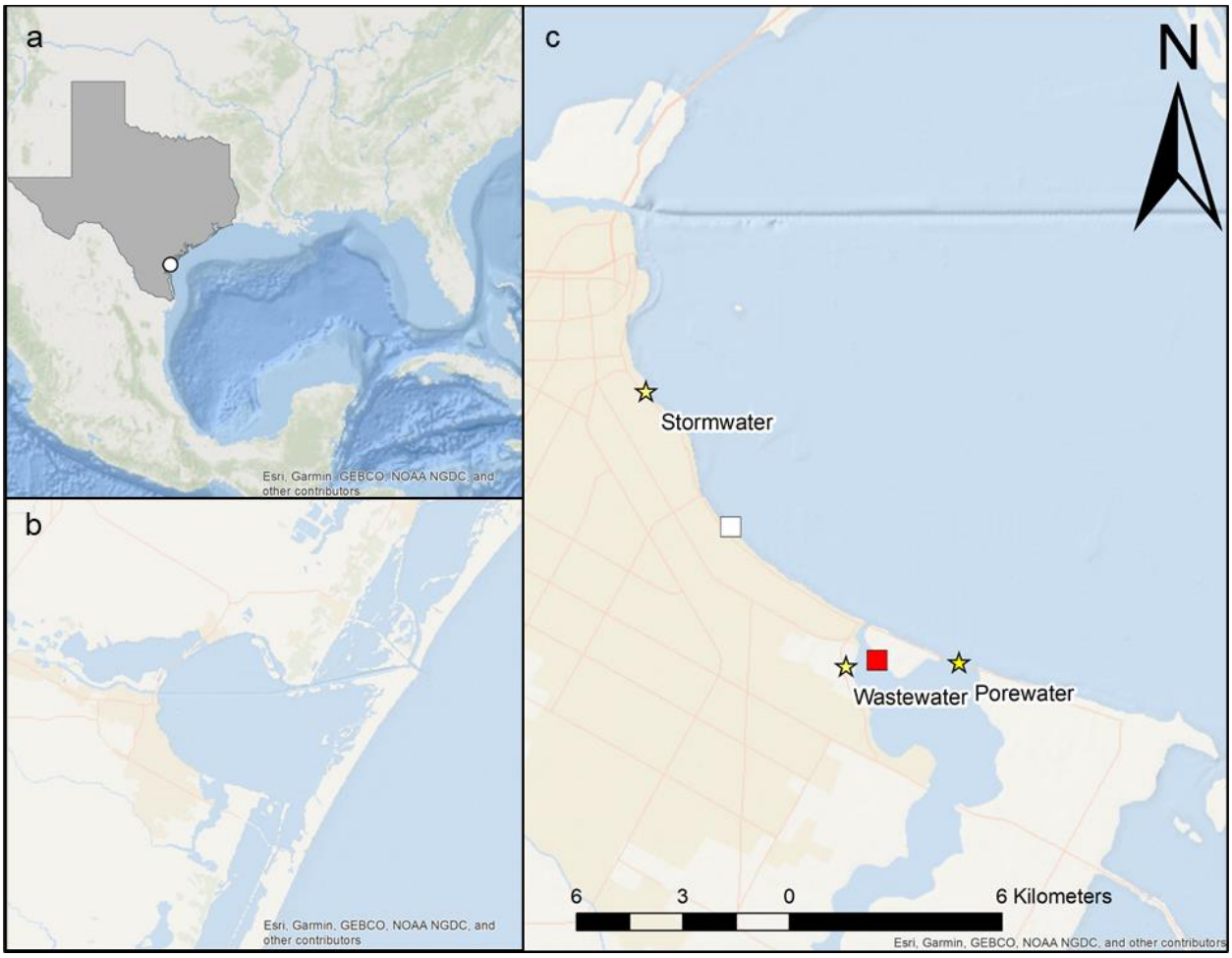

Fig. 2.1 Relative position of Corpus Christi Bay on the Texas coast (a), full view of the Corpus Christi Bay system (b). Site of water collection for bioassays (white square), *in situ* incubation (red square), and locations of nutrient source collections (yellow stars).

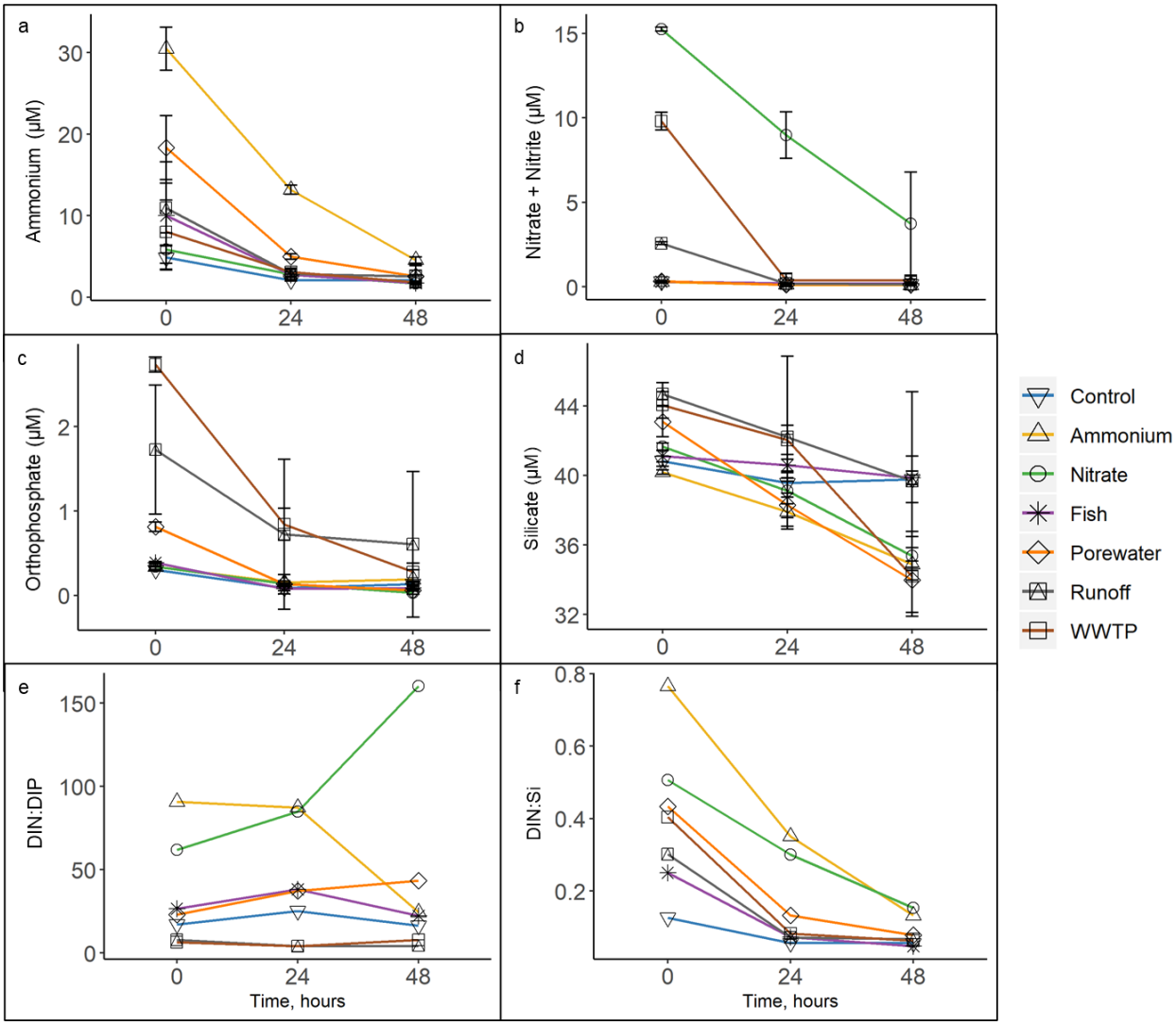

Fig. 2.2 Inorganic nutrient concentrations and ratios over the course of the summer experiment.

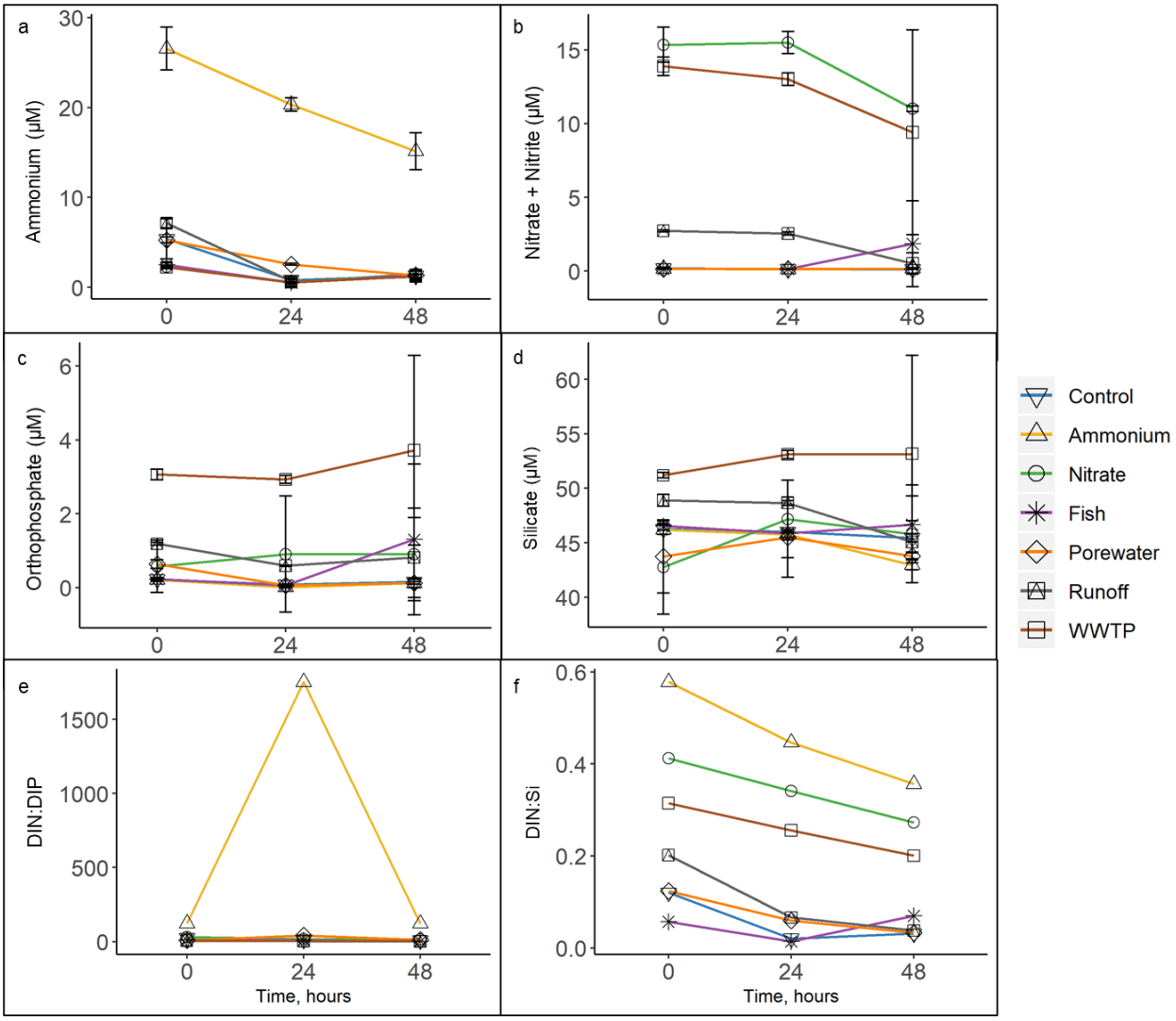

Fig. 2.3 Inorganic nutrient concentrations and ratios over the course of the fall experiment.

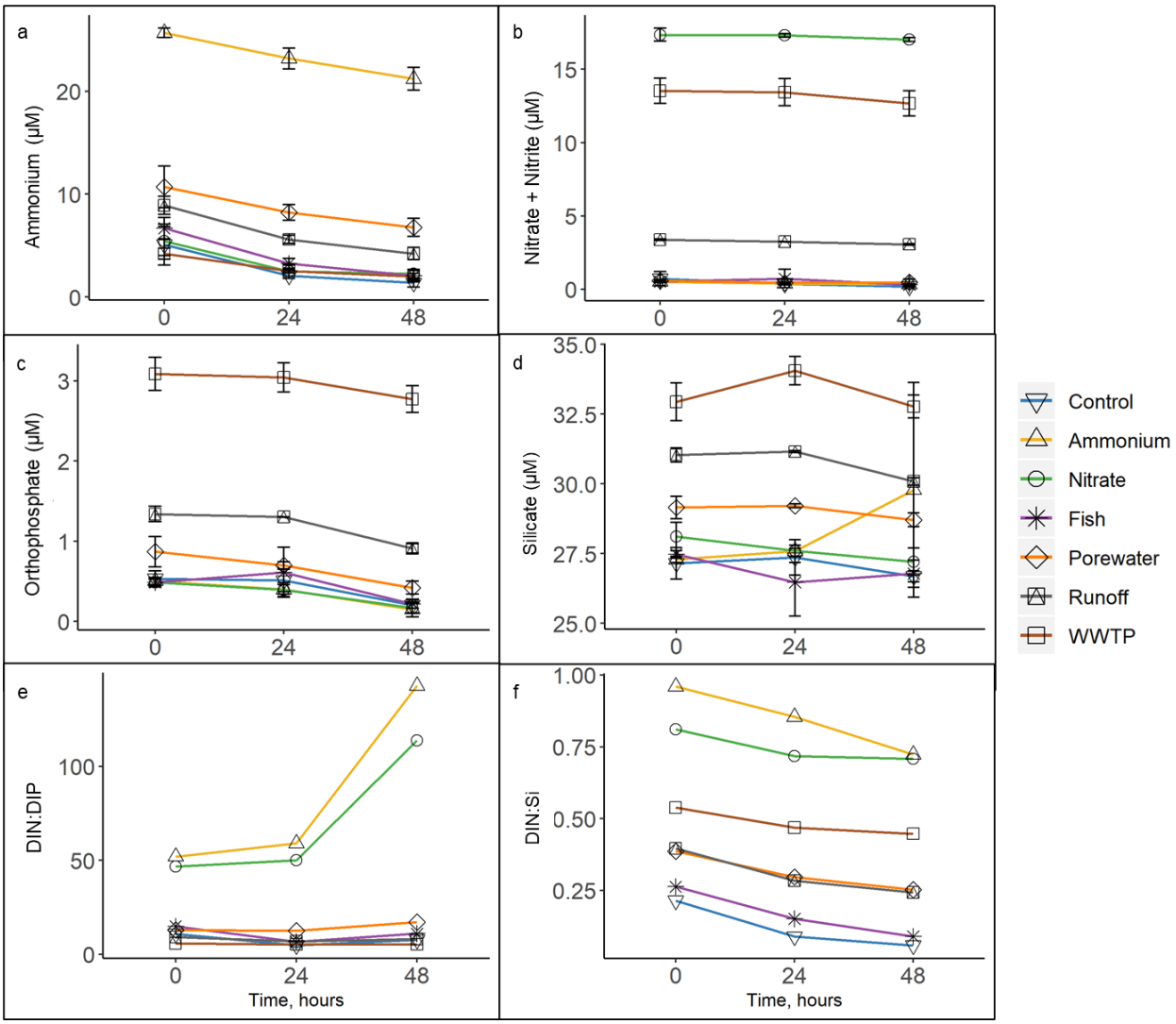

Fig. 2.4 Inorganic nutrient concentrations and ratios over the course of the winter experiment.

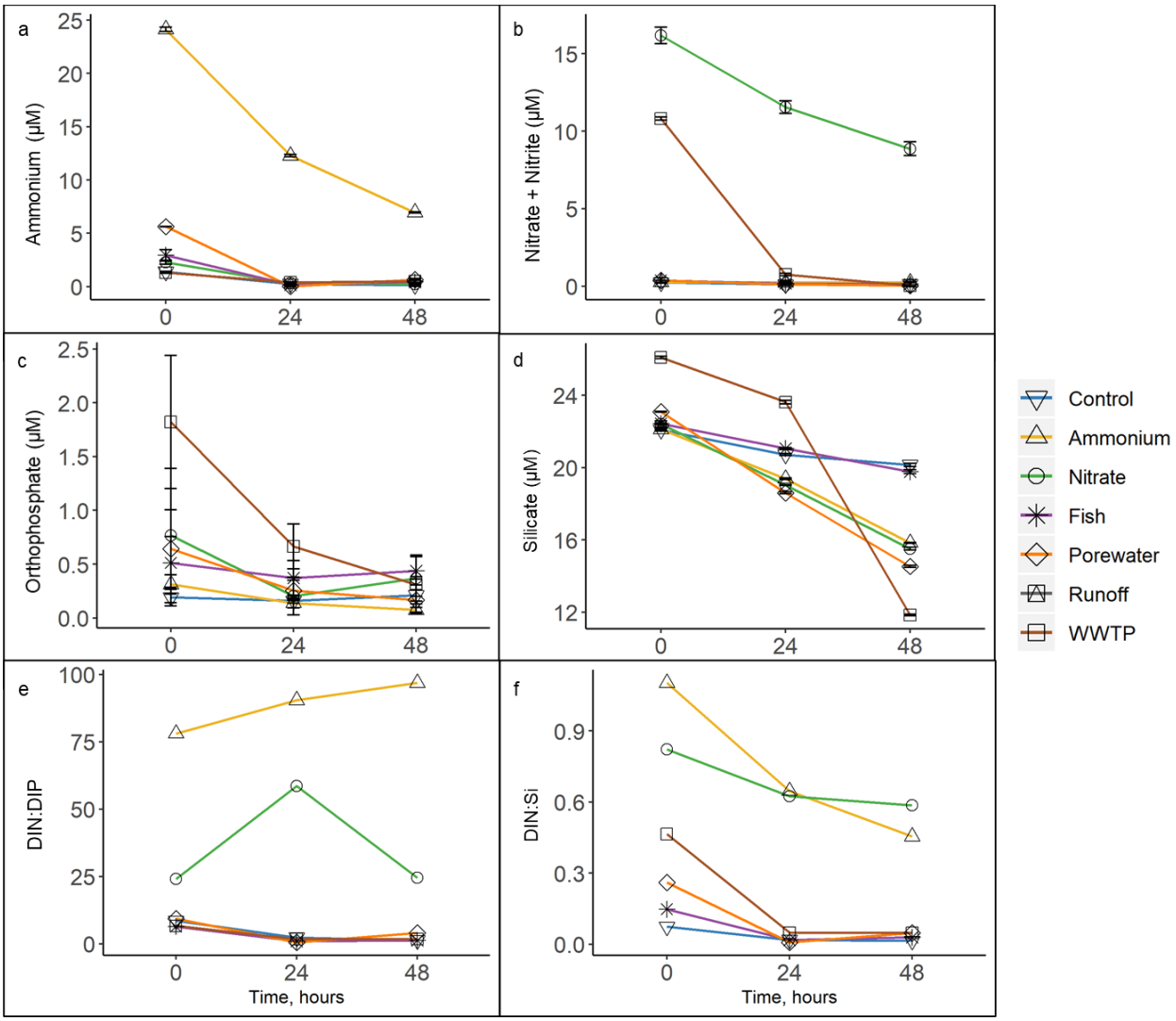

Fig. 2.5 Inorganic nutrient concentrations and ratios over the course of the spring experiment.

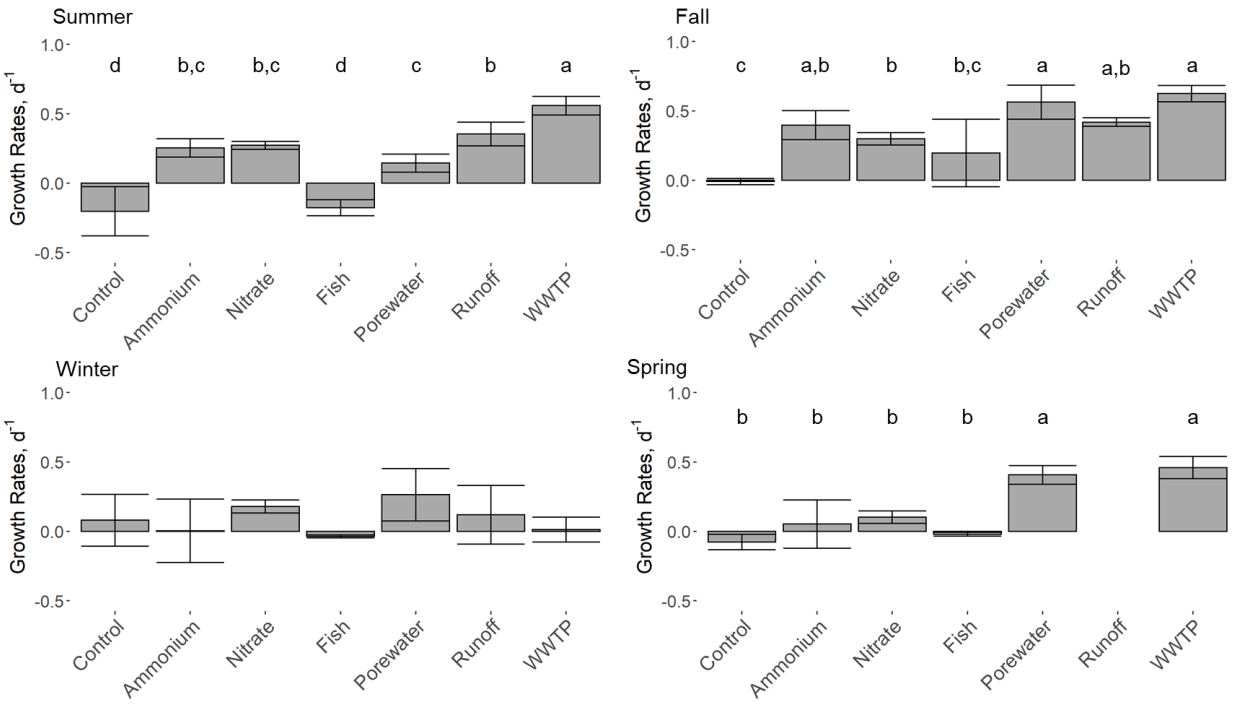

Fig. 2.6 Growth rates calculated from T0 to T48 using community biovolume (μm^3 mL^{-1}) as the response metric. Lowercase letters indicate results from multiple comparison procedures with treatments with different letters indicating significant differences.

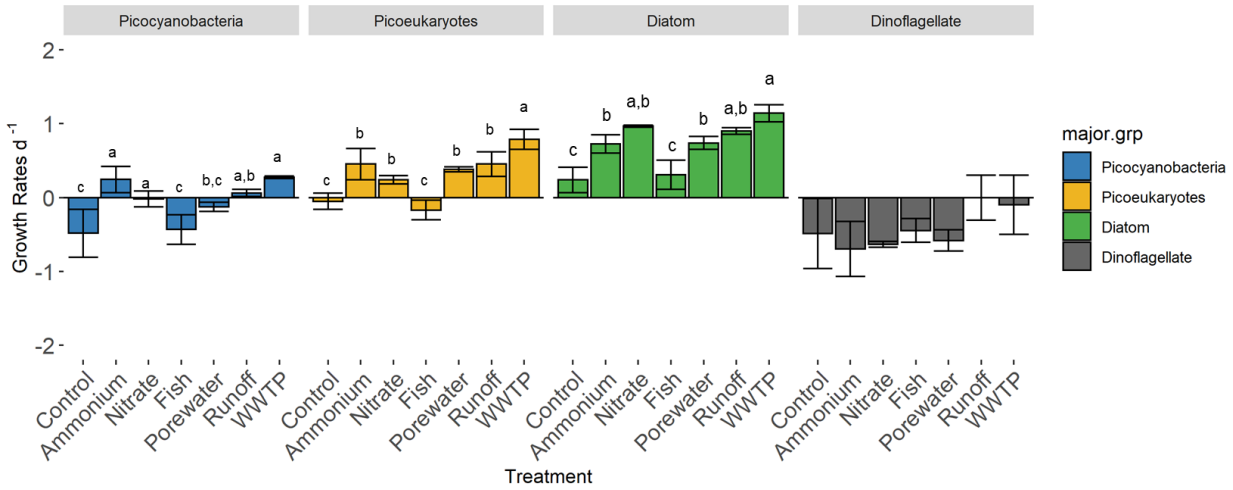

Fig. 2.7 Growth rates calculated from T0 to T48 during the summer bioassay for each major taxonomic group using biovolume (μm^3 mL^{-1}) as the response metric.

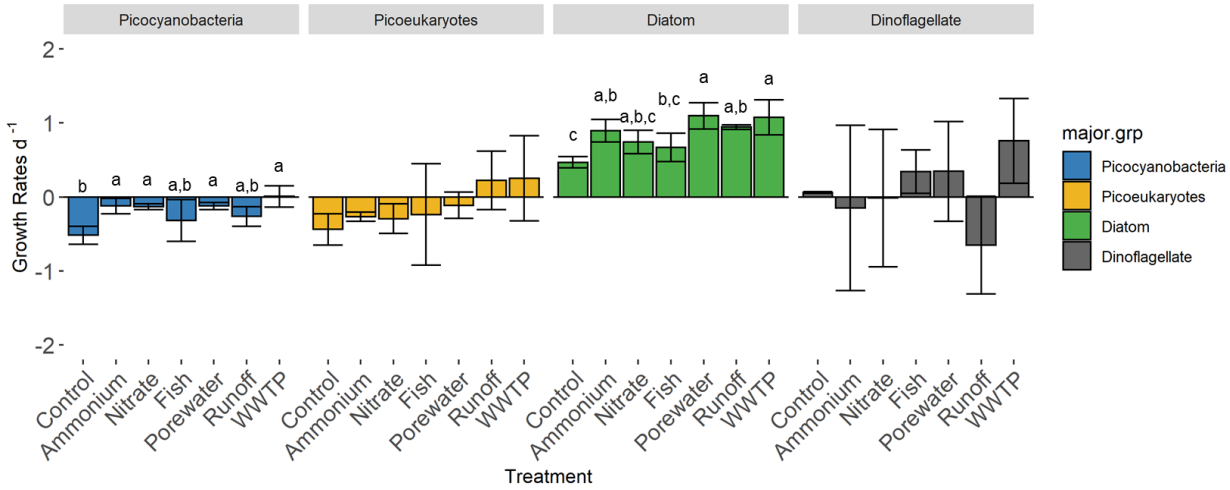

Fig. 2.8 Growth rates calculated from T0 to T48 during the fall bioassay for each major taxonomic group using biovolume (μm^3 mL^{-1}) as the response metric.

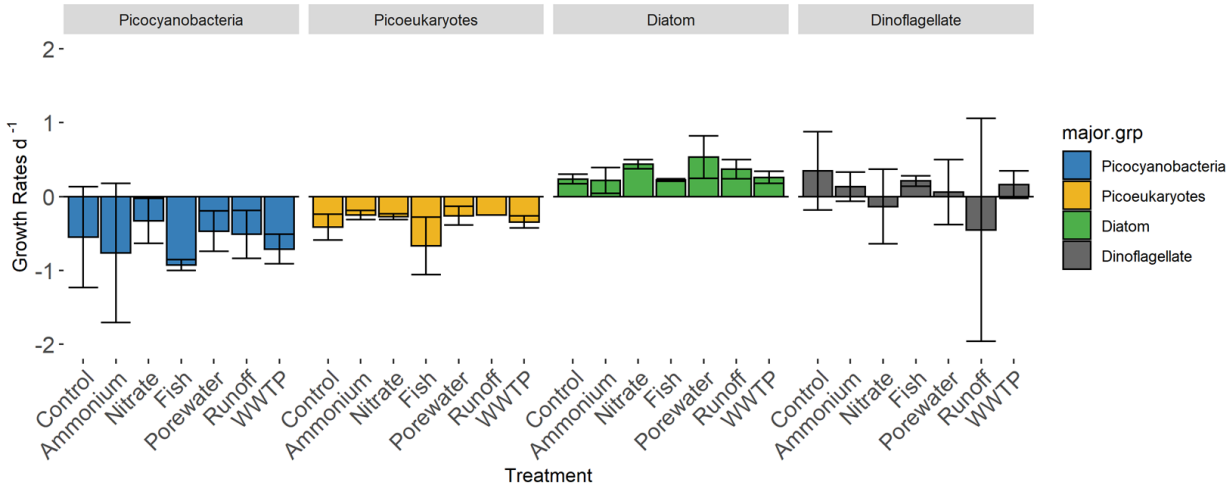

Fig. 2.9 Growth rates calculated from T0 to T48 during the winter bioassay for each major taxonomic group using biovolume (μm^3 mL^{-1}) as the response metric.

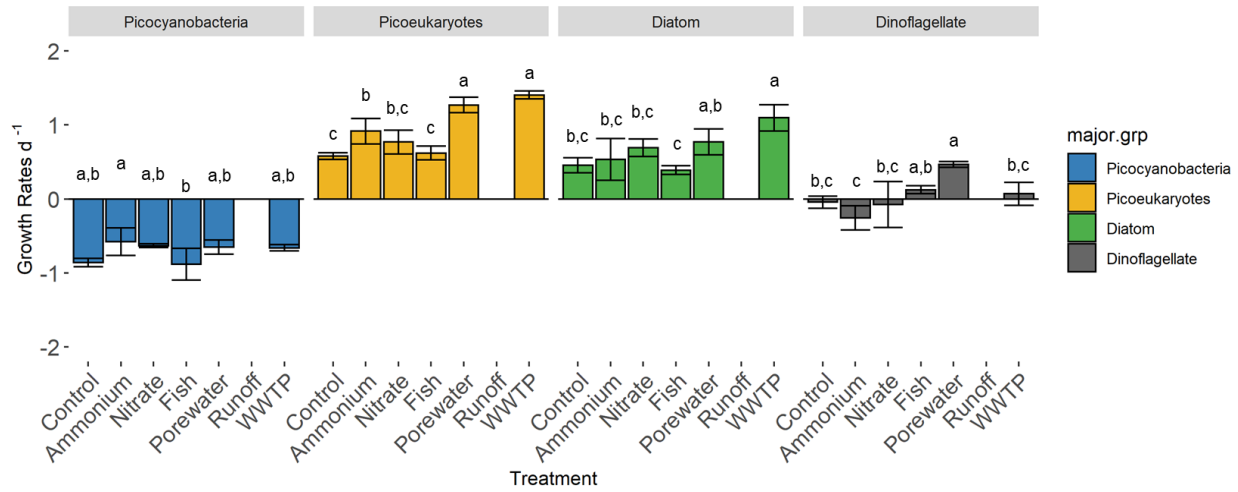

Fig. 2.10 Growth rates calculated from T0 to T48 during the spring bioassay for each major taxonomic group using biovolume (μm^3 mL^{-1}) as the response metric. The runoff treatment was not applied during the spring bioassay.

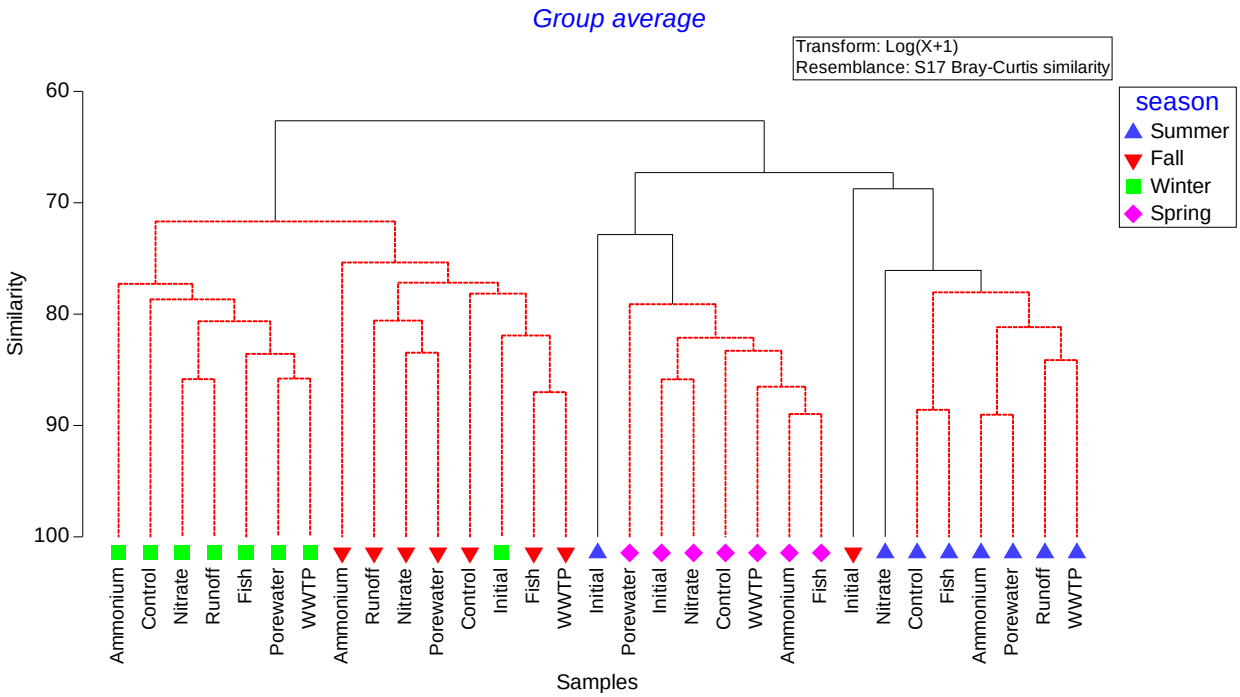

Fig. 2.11 Hierarchical clustering (group-average) analysis with biovolume-based community composition across all seasons. Red lines indicate no significant difference between communities (SIMPROF, Primer v7).

Table 2.1 Site conditions at time of collection.

	Summer	Fall	Winter	Spring
Temperature (°C)	31.3	22.2	6.8	30.2
Salinity	34.30	28.65	29.82	35.05
Secchi depth (m)	0.5	0.8	0.4	0.6
Chlorophyll *a* (μg L^{-1})	7.79 ± 0.18	4.36 ± 0.04	6.71 ± 0.03	3.82 ± 0.32

Table 2.2 Nutrient concentrations at T0 following nutrient additions. NH_4^+ and NOx represent ammonium and nitrate plus nitrite, DIN in the sum of NH_4^+ and NOx, DIP is orthophosphate (PO_4), Si is silicate, and all are in µmol L^{-1}. N added was calculated by mean T0 TDN - mean Initial TDN for each treatment individually.

	Treatment	NH_4^+	NOx	PO_4	Si	DON	DIN:DIP	DIN:Si	N Added
Summer	Initial	4.48 ± 2.09	BDL	0.41 ± 0.03	40.2 ± 0.21	26.86 ± 1.7	10.88	0.11	-
	Control	4.85 ± 1.52	0.31 ± 0.01	0.30 ± 0.01	40.82 ± 0.30	27.43 ± 2.55	17.12	0.13	1.24
	Ammonium	30.47 ± 2.62	0.29 ± 0.04	0.34 ± 0.04	40.18 ± 0.12	20.16 ± 1.35	90.73	0.77	19.56
	Nitrate	5.83 ± 0.43	15.26 ± 0.11	0.34 ± 0.01	41.65 ± 0.22	22.98 ± 1.04	61.85	0.51	12.71
	Fish	10.01 ± 6.58	0.30 ± 0.08	0.39 ± 0.01	41.11 ± 0.35	28.52 ± 0.21	26.52	0.25	7.47
	Porewater	18.35 ± 3.92	0.33 ± 0.02	0.81 ± 0.05	43.09 ± 0.87	30.71 ± 5.51	22.97	0.43	18.03
	Runoff	10.92 ± 3.06	2.57 ± 0.08	1.73 ± 0.76	44.67 ± 0.65	42.61 ± 5.47	7.81	0.3	24.75
	WWTP	8.01 ± 3.87	9.81 ± 0.52	2.74 ± 0.09	44.04 ± 0.77	30.06 ± 4.97	6.51	0.4	16.52
Fall	Initial	0.39 ± 0.1	0.14 ± 0.01	0.2 ± 0.03	47.19 ± 0.1	30.83 ± 7.23	2.68	0.01	-
	Control	5.37 ± 2.23	0.19 ± 0.06	0.22 ± 0.06	46.26 ± 0.51	26.8 ± 3.51	24.87	0.12	1.01
	Ammonium	26.56 ± 2.38	0.16 ± 0.02	0.22 ± 0.03	46.21 ± 0.44	32.88 ± 8.05	123.5	0.58	28.25
	Nitrate	2.29 ± 0.14	15.34 ± 1.19	0.58 ± 0.71	42.78 ± 4.33	20.35 ± 1.61	30.44	0.41	6.63
	Fish	2.51 ± 0.22	0.14 ± 0.01	0.24 ± 0.02	46.56 ± 0.42	23.81 ± 2.85	11.19	0.06	-4.89
	Porewater	5.28 ± 0.32	0.15 ± 0.01	0.64 ± 0.12	43.73 ± 3.33	44.62 ± 3.78	8.51	0.12	18.69
	Runoff	7.13 ± 0.52	2.73 ± 0.07	1.19 ± 0.04	48.89 ± 0.54	37.27 ± 0.34	8.29	0.2	15.78
	WWTP	2.23 ± 0.15	13.89 ± 0.62	3.06 ± 0.14	51.2 ± 0.25	38.92 ± 1.98	5.26	0.31	23.69

Table 2.2 cont'd. Nutrient concentrations at T0 following nutrient additions. NH_4^+ and NOx represent ammonium and nitrate plus nitrite, DIN in the sum of NH_4^+ and NOx, DIP is orthophosphate (PO_4), Si is silicate, and all are in µmol L^{-1}.

	Treatment	NH_4^+	NOx	PO_4	Si	DON	DIN:DIP	DIN:Si	N Added
Winter	Initial	1.98 ± 0.25	0.41 ± 0.03	0.9 ± 0.35	24.8 ± 1.71	20.22 ± 4.92	2.66	0.1	-
	Control	5.09 ± 1.98	0.73 ± 0.48	0.53 ± 0.10	27.15 ± 0.57	15.89 ± 3.48	10.92	0.21	0.05
	Ammonium	25.67 ± 0.45	0.52 ± 0.05	0.5 ± 0.04	27.29 ± 0.11	21.71 ± 2.2	51.96	0.96	16.1
	Nitrate	5.43 ± 1.4	17.36 ± 0.44	0.49 ± 0.04	28.11 ± 0.51	35.33 ± 4.49	46.8	0.81	18.51
	Fish	6.7 ± 1.03	0.53 ± 0.07	0.49 ± 0.06	27.48 ± 0.12	31.96 ± 3.63	14.83	0.26	16.57
	Porewater	10.7 ± 2.02	0.58 ± 0.1	0.87 ± 0.19	29.15 ± 0.41	53.05 ± 3.51	12.98	0.39	17.26
	Runoff	8.92 ± 0.88	3.38 ± 0.04	1.34 ± 0.09	31.04 ± 0.25	26.39 ± 2.71	9.19	0.4	39.37
	WWTP	4.21 ± 0.54	13.54 ± 0.86	3.09 ± 0.2	32.94 ± 0.67	18.3 ± 1.08	5.75	0.54	18.16
Spring	Initial	0.08 ± 0.08	0.19 ± 0.1	0.49 ± 0.06	18.5 ± 0.16	35.12 ± 0.98	0.55	0.01	-
	Control	1.40 ± 0.04	0.24 ± 0.00	0.19 ± 0.08	22.08 ± 0.06	29.85 ± 1.95	8.58	0.07	-3.90
	Ammonium	24.14 ± 0.19	0.25 ± 0.01	0.31 ± 0.09	22.12 ± 0.05	35.44 ± 1.01	78.09	1.1	24.44
	Nitrate	2.28 ± 0.18	16.17 ± 0.54	0.77 ± 0.62	22.41 ± 0.18	36.79 ± 2.21	24.08	0.82	19.84
	Fish	2.94 ± 0.53	0.39 ± 0.18	0.51 ± 0.24	22.43 ± 0.05	27.75 ± 2.05	6.49	0.15	-4.32
	Porewater	5.63 ± 0.02	0.38 ± 0.01	0.64 ± 0.36	23.07 ± 0.02	37.08 ± 0.85	9.34	0.26	7.69
	Runoff	-	-	-	-	-	-	-	-
	WWTP	1.31 ± 0.07	10.82 ± 0.1	1.82 ± 0.62	26.08 ± 0.06	38.75 ± 8.69	6.66	0.46	15.48

Table 2.3 Initial phytoplankton biovolume ($\mu m^3 L^{-1} \times 10^6$) and (percent contribution) of each major taxonomic group counted. The (-) indicates non-detect.

	Summer	Fall	Winter	Spring
Total Biovolume	2,473	1,192	2,165	1,529
Picocyanobacteria	809 (32.73)	682 (57.18)	833 (38.48)	752 (49.17)
Picoeukaryotes	248 (10.03)	113 (9.51)	110 (5.08)	78 (5.10)
Diatom	387 (15.64)	306 (25.62)	937 (43.26)	173 (11.28)
Dinoflagellate	933 (37.71)	56 (4.67)	221 (10.19)	500 (32.69)
Flagellate	31 (1.25)	2 (0.13)	24 (1.11)	20 (1.3)
Cryptophyte	29 (1.18)	12 (1.00)	41 (1.88)	7 (0.43)
Euglenoid	-	6 (0.48)	-	-
Chlorophyte	2 (0.10)	-	-	1 (0.02)
Raphidophyte	34 (1.36)	17 (1.41)	-	-

CHAPTER III: AN ASSESSMENT OF TRENDS IN THE FREQUENCY AND DURATION OF *KARENIA BREVIS* RED TIDE BLOOMS ON THE SOUTH TEXAS COAST

Abstract

Limited data coverage on harmful algal blooms (HABs) in some regions makes assessment of long-term trends difficult, and also impedes understanding of bloom ecology. Here, observations reported in a local newspaper were combined with cell count and environmental data from resource management agencies to assess trends in *Karenia brevis* "red tide" frequency and duration in the Nueces Estuary (Texas) and adjacent coastal waters, and to determine relationships with environmental factors. Based on these analyses, the Coastal Bend region of the Texas coast has experienced a significant increase in the frequency of red tide blooms since the mid-1990s. Salinity was positively correlated with red tide occurrence in the Nueces Estuary, and a documented long-term increase in salinity of the Nueces Estuary may be a major factor in the long-term increase in bloom frequency. This suggests that freshwater inflow management efforts in Texas should consider impacts on red tide habitat suitability (i.e., salinity regime) in downstream estuaries. Natural climate variability such as the El Niño-Southern Oscillation, which is strongly related to rainfall and salinity in Central and South Texas, was also an influential predictor of red tide presence/absence. Though no significant change in the duration of blooms was detected, there was a negative correlation between duration and temperature. Specifically, summer-like temperatures were not favorable to *K. brevis* bloom development. The relationships found here between red tide frequency/duration and environmental drivers present a new avenue of research that will aid in refining monitoring and forecasting efforts for red tides on the Texas coast and elsewhere. Findings also highlight the

importance of factors (i.e., salinity, temperature) that are likely to be altered in the future due to both population growth in coastal watersheds and anthropogenic climate change.

Introduction

Red tides formed by the marine dinoflagellate *Karenia brevis* have affected Gulf of Mexico coastlines for centuries (Magaña et al. 2003; Brand and Compton 2007), typically during late summer-fall. The most notable effects are fish kills, shellfisheries closures, marine mammal and seabird mortality, and respiratory and digestive distress in humans (Baden and Mende 1979; Kirkpatrick et al. 2004; Brand et al. 2012). In the United States, the West Florida and Texas coastlines are most commonly affected, with Florida historically suffering the most damage (Tester and Steidinger 1997; Magaña et al. 2003; Stumpf et al. 2008; Brand et al. 2012). An analysis of trends in *K. brevis* red tide occurrence was conducted for Florida coastal waters and indicated that frequency of occurrence, intensity, and duration were higher in the years 1994-2002 compared to 1954-1963 (Brand and Compton 2007). Magaña et al. (2003) reported that the frequency of red tides on the Texas coast increased over the period of 1996-2000 compared to earlier years. In both instances, availability of historical data limited the scope of inferences that could be drawn from study findings (Schrope 2008; Vargo 2009; Heil et al. 2014).

Eutrophication is often cited as the cause of increases in harmful algal blooms (HABs) globally (Anderson 1989; Bricker et al. 2008; Davidson et al. 2014). In the case of *K. brevis* however, its ability to use nutrients from a wide variety of sources has called into question the role of eutrophication as the main factor causing increased bloom frequency and intensity (Vargo 2009; Dixon et al. 2014; Heil et al. 2014). In Florida for example, studies suggest that a complex suite of environmental conditions determine bloom formation. Briefly, downwelling conditions followed by upwelling concentrates *K. brevis* and subsequently transports it shoreward (Tester

and Steidinger 1997; Weisberg et al. 2016; Weisberg et al. 2019) (Rounsefell and Nelson 1967; Steidinger and Ingle 1972; Landsberg and Steidinger 1988; Steidinger 2009). During transport, *K. brevis* is thought to acquire nutrients from sediment porewater (directly or via benthic flux), zooplankton excretions, bacterial remineralization, upwelled deep-water nutrients, and "leaky" *Trichodesmium* blooms in an otherwise oligotrophic environment (Vargo 2009; Dixon et al. 2014; Heil et al. 2014). It is only in the nearshore and estuarine environments where blooms come into contact with relatively high nutrient waters (Vargo 2009; Dixon et al. 2014; Heil et al. 2014).

In Texas, physical concentration and advection of cells is also important in the initiation of red tides. Recent modeling work suggests a southern origin of red tides and a general transport pattern of: 1) summer upcoast winds carry seed populations from the southern Gulf of Mexico to the Texas coast, and 2) a switch to downcoast winds from summer to fall that produce Ekman transport towards the coast, delivering *K. brevis* to the near-shore environment (Hetland and Campbell 2007; Thyng et al. 2013; Henrichs et al. 2015). Though physical mechanisms are critical in the development/transport of *K. brevis* in West Florida and Texas blooms, environmental conditions in coastal waters must also be suitable. Field and laboratory studies have consistently demonstrated strong relationships between *K. brevis* and salinity and temperature, with higher salinities (20 - 40) and low to moderate temperatures (7°C - 32°C) related to greater *K. brevis* success (Rounsefell and Nelson 1967; Steidinger 2009; Dixon et al. 2014). Blooms in Texas are frequently transported into estuaries (Buskey 1996), and there is also anecdotal evidence of blooms developing within the estuary as opposed to coastal waters (Tester et al. 2002). Unfortunately, there have been no studies to date on *K. brevis* population dynamics in Texas estuaries. Additionally, despite occurrences of *K. brevis* red tides in Florida estuaries on

the Gulf and Atlantic Coasts (Flaherty and Landsberg 2011; McHugh et al. 2011; Walters et al. 2013; Hart et al. 2015; Harris et al. 2020), few have addressed questions regarding *K. brevis* ecology in an estuarine setting (Steidinger and Ingle 1972; Landsberg and Steidinger 1988; Steidinger 2009), highlighting a critical gap in our knowledge.

A major challenge for assessing trends in the environmental sciences is the lack of long-term data (Anderson et al. 2002; Davidson et al. 2014). Nonetheless, since the early 2000's significant advances have been made by utilizing non-traditional data sources, resulting in emergence of a new field, marine historical ecology (Kittinger et al. 2014; Engelhard et al. 2016). Successful case studies have used newspaper articles, diaries, correspondence, photographs, and maps to reconstruct historical fisheries populations and ranges, assess loss of historical ecosystem services, and set ecosystem restoration targets (Kittinger et al. 2014; Engelhard et al. 2016). Here we combined information on red tide occurrences from local news articles with cell count data from resource management agencies to assess long-term trends in red tide frequency and duration in the Nueces Estuary (Texas) and adjacent coastal waters. The goals of this study were to: 1) extend the temporal record of red tides in a portion of the Texas Coastal Bend using validated newspaper accounts, 2) quantitatively assess trends in red tide frequency in a data poor region (estuarine/nearshore waters of the South Texas coast) and environmental factors associated with red tide occurrence, and 3) use these data to increase understanding of *K. brevis* red tide dynamics in an estuarine setting. This is important because estuaries of the South-Central Texas coast are undergoing significant environmental change due to rapid population growth and climate change (Bugica et al. 2020). Furthermore, climate scenarios suggest that the region will become hotter and drier in the future (Pachauri et al. 2014; Nielsen-Gammon et al. 2020). Results from this study offer insight into the utility of non-

traditional data for detection of long-term trends and red tide population dynamics in a data poor region (Texas coast). Additionally, these results can be used to inform monitoring programs, improve predictive capabilities, and to develop targeted studies to address key questions regarding *K. brevis* ecology.

Methods

Daily newspaper articles from *Corpus Christi Caller Times* from 1955 through 2016 were obtained and read for relevant articles on red tide. Information from the newspaper articles was then aggregated into yearly presence/absence and duration (days) datasets for each of two segments, the Nueces Estuary and the coastal zone from Port O'Connor to Land Cut (Fig. 3.1). In cases when a single red tide spanned two calendar years, its presence and total duration would only be recorded in the first year. For example, if a bloom began in September of Year 1 and ended in January of Year 2 the total duration in days across both years was recorded as the duration for year 1. Cell counts of *K. brevis* were obtained from the NOAA repository (2005-2013; (NOAA National Centers for Environmental Information 2014) and the Texas Department of Health Division of Seafood Safety (1996-2016; TXHD). Each cell count record was converted to categorical presence/absence. A comparison between the newspaper and agency presence/absence and duration data was conducted using three cell count thresholds from the agency data: 5,000 cells L^{-1} (shellfisheries closures), 10,000 cells L^{-1} (fish killing levels), and 100,000 cells L^{-1} (visual detection likely) (Tester and Steidinger 1997; Steidinger 2009).

Accessory Data Collection

Bay-wide salinity and temperature data (monthly) were obtained from the Texas Parks & Wildlife trawl sampling dataset (Table 3.1). Monthly climate indices for the El Niño Southern Oscillation (ENSO), the Pacific Decadal Oscillation (PDO), and the North Atlantic Oscillation

(NAO) were accessed through NOAA's National Climatic Data Center (https://www.ncdc.noaa.gov). Daily meteorological data were also accessed through NOAA's National Climatic Data Center, using a weather station located at the Naval Air Station, Corpus Christi (Fig. 3.1). Average daily air temperature, precipitation, and wind speed were chosen as the variables of interest because of known linkages between these indicators and *K. brevis* (Tester and Steidinger 1997; Magaña and Villareal 2006; Vargo 2009). Air temperature was used as a proxy for water temperature due to relatively short and intermittent water temperature record (1995-1996; 2006-present) available for the study area. Air and water temperature showed a strong linear relationship, though at air temperature <15^{o}C the relationship was not as strong (Fig. 3.2). However, these cooler temperatures are outside the typical seasonal window for *K. brevis* in Texas.

Statistical Analysis

The following analyses were conducted in R v 3.6.2. The associated code can be found in the GRIID-C data repository at http://doi.org/ 10.7266/7VRN6BXA.

Trends in Bloom Presence/Absence & Relationship with Environmental Factors

Logistic regression (LogisticDx v 0.2) (Dardis 2015) was used to explore trends in red tide occurrence, and relationships with environmental variables. Year was used as the sole explanatory variable to assess changes in the frequency of red tide occurrence for the Nueces Estuary and adjacent Coastal Zone. To better understand any changes detected with the year-only logistic regression, non-parametric change point detection was performed using Pettitt's Test for both locations (trend v. 1.2.2) (Pettitt 1979; Pohlert 2020). Yearly averages of ENSO, NAO, PDO, and fall (Aug-Nov) averages of water temperature and salinity were used, in addition to year, to assess the influence of environmental variability on red tide occurrence in the Nueces

Estuary and the Coastal Zone. No collinearity was detected among the regressors, and all variables were used in creation of the initial full model. Dredge and a summary of model averages (MuMIn v 1.43.6) (Barton 2020) were used to determine the importance of each explanatory variable and the best models were built. The models were compared for relative quality using Akaike's Information Criterion (AICc) and assessed for goodness of fit using the Hosmer-Lemeshow test (LogisticDx v 0.2) (Dardis 2015). The year-only and final explanatory models were compared to the null model (only presence/absence and the intercept included) as a final check for model suitability. Nagelkerke pseudo R^2 values (pscl v 1.5.2) (Jackman 2020) were also calculated to assess the variability explained by each of the models and can be interpreted similarly to a traditional R^2 value (Smith and McKenna 2013; Walker and Smith 2016). Finally, the odds ratios for each variable in the year-only and final explanatory model were calculated to aid in the interpretation of the influence of each variable. For the year-only model, the odds ratio is interpreted as the probability of a red tide occurring for each step forward in time, e.g. an odds ratio of 1.17 indicates that there is a 17% increase in the probability of a red tide occurring with each passing year. For the explanatory models, the odds ratio is not interpreted in the same way due to differing scales among the explanatory variables, optimum temperature and salinity ranges of red tide growth/survival, and the multivariate nature of the models. Instead, the odds ratios are presented in the results section as a metric to aid in the full appreciation of the model output. For multivariate models, the odds ratio is interpreted as the likelihood of a red tide occurring due to a change in one variable with all other variables held constant, e.g. an odds ratio of 1.17 for variable a indicates that, with all else held constant, there is a 17% increase in the probability of a red tide occurring with each 1 unit increase in variable a.

If model fit, pseudo R^2, AICc, and/or comparison to the null model was not acceptable, the analysis concluded with the year-only model.

Trends in bloom duration & relationship with environmental factors

Linear regression was used to explore trends in *K. brevis* red tide duration in the Nueces Estuary and adjacent Coastal Zone with year as the only explanatory variable. To explore relationships between environmental parameters and red tide duration, models with water temperature, salinity, NAO, PDO, and ENSO (described in section 2.1) were used to create an initial full linear regression model. Dredge and a summary of model averages (MuMIn v 1.43.6) (Barton 2020) were used to determine the importance of each explanatory variable and the best models were built. The models were compared for relative quality using AICc and assessed for goodness of fit. The final model was compared to the null model (only duration and the intercept) as a check of model suitability. If model fit, pseudo R^2, AICc, and/or comparison to the null model was not acceptable, the analysis concluded with the year-only model.

Environmental conditions associated with bloom stages

In a given year, each day that red tide was present was assigned a "1" and a two-week (14 days) buffer of "0s" was assigned before the red tide was detected (as reported in news articles) and after detection ceased. These three periods were coded as before bloom (B), during bloomo (D), and after bloom (A) stages. As a part of initial data exploration, ANOVAs were used to compare average daily air temperature, precipitation, and wind speed among the three bloom stages. To account for interannual variation and seasonal variation, year and month were included as random factors. A total of three datasets were used in the following analyses: the original daily presence/absence containing all three stages, daily presence/absence dataset containing only B and D stages, and daily presence/absence dataset containing only D and A

stages. Following this, generalized linear mixed-effects logistic regression (lme4 v 1.1-20) (Bates et al. 2015) was used to model daily red tide presence/absence on the three datasets. Dredge and a summary of model averages (MuMIn v 1.43.6) (Barton 2020) were used to determine the importance of each variable. The best models were built and compared for relative quality using AICc and assessed for goodness of fit. The final model chosen for each dataset was compared to the null model (only presence/absence and the intercept included) as a final check for model suitability. Additionally, Nagelkerke pseudo R^2 values were calculated for each of the three models to assess the variability explained.

Results

Validation of the Corpus Christi Caller Times Dataset

Qualitative analysis of the newspaper and agency-derived cell count datasets provided evidence that the newspaper reports were a reliable source of information on the occurrence and duration of red tides in the Texas Coastal Bend. Beginning with the time frame covered by NOAA (2005-2013) and/or TXHD (1996-2016) cell counts, there was near perfect corroboration of annual red tide occurrence reported in the newspaper (Table 3.2). For the Nueces Estuary, there was one instance (2012) of a red tide being reported in the newspaper that was not in either of the agency records. The newspaper article describing the 2012 red tide does, however, quote Texas Parks and Wildlife scientists on the location of the red tide "drifting in Corpus Christi Bay through the Port Aransas Jetties" lending support to it being a real occurrence that was not documented by agency-based sampling. There were no instances of red tides reported in the agency record that were missed by the newspaper. In the Coastal Zone there were two instances (2000, 2012) of a red tide being reported in the newspaper that did not appear in the TXHD or NOAA records. The red tide occurrence in 2000 is, however, corroborated by a study by Cheng

et al. (2005), while the single day event reported in the coastal zone in September 2012 is from the same article mentioned above where observations were corroborated by state resource managers. There was also one instance of a red tide reported in the scientific record but not in the newspaper (2013) for the coastal zone during this time.

Prior to 1996, there is not a unified agency database for comparison. Five of the eight red tides that were reported in the newspaper to have occurred between 1955 and 1995 along the Texas coast were, however, captured in the literature (Table 3.3) (Wilson and Ray 1956; Trebatoski 1988; Buskey 1996; Magaña et al. 2003; Cheng et al. 2005). Qualitative assessment of these articles suggests that reporters were generally aware of red tides. For example, in the newspaper articles prior to 1996, 11 articles describe a red tide occurring elsewhere, regardless of the state of red tides in Texas coastal waters. Furthermore, a majority (75%) of the articles prior to 1996 referenced interviews with local, state, and/or academic scientists, strengthening the veracity of the reports. The 25% that did not cite someone from the scientific community tended to consist of articles mentioning red tide in another context (e.g. tourism dollars lost, efforts to help the economy, town festivals). There were also two occasions when red tide reports indicated that the causative agent was an organism other than *K. brevis* and one occasion where discolored water was found to be an oil drilling fluid spill.

When comparing the duration data derived from the newspaper to the duration as derived from the NOAA and TXHD records at three abundance thresholds, it was apparent that the publishing cycle and/or the occurrence of other newsworthy events were not likely to limit reporting of red tides. In the Nueces Estuary at the 5,000 cells L^{-1} and 10,000 cells L^{-1} thresholds, the duration tended to be shorter based on newspaper articles than based on cell counts (46.46 ± 40.94 vs 65.83 ± 40.75 and 62.75 ± 38.43; Table 3.2). When duration was compared using the

100,000 cells L^{-1} threshold, the duration was more similar between the two records (46.46 ± 40.94 vs 46.17 ± 32.90; Table 3.2). This suggests that duration may be underestimated for the Nueces Estuary in the newspaper data at low cell abundances (<100,000 cells L^{-1}). In the Coastal Zone duration tended to be longer on average based on newspaper articles than based on cell counts at all thresholds compared (29.00 ± 21.29 vs 24.55 ± 31.79, 25.8 ± 31.82, 12.50 ± 24.53; Table 3.2). In the Nueces Estuary, this may be indicative of remnant populations persisting in localized, poorly flushed regions of the estuary as has been hypothesized by others (2020).

The duration estimates reported in newspapers may differ from those from agency-based data because of different response triggers. TXHD sampling efforts are initiated in response to red tide sightings and are concentrated in areas of shellfisheries whereas the NOAA dataset was a compilation of multiple sources (Pennock et al. 2004), likely with different research objectives goals (i.e. toxin production, life cycle, ecophysiology). This is reflected by the fact that the NOAA dataset is more frequently the source of corroborating data in the Coastal Zone where TXHD is more frequently the corroborating source in the Nueces Estuary. Since agency-based sampling occurred in response to red tide sightings (Pennock et al. 2004) the newspaper was likely to report a similar or earlier start date, as was observed in 7 out of 11 occurrences in Nueces Estuary and 6 out of 10 in the Coastal Zone. The 2009 red tide provides an example of the effects of differing temporal and spatial sampling efforts. The duration derived from the TXHD record is longer than that derived from the NOAA dataset in the Nueces Estuary, but the reverse is true in the adjacent Coastal Zone (Table 3.2).

Trends in bloom presence/absence

Results showed a statistically significant increase in the frequency of red tides for the Nueces Estuary and the Coastal Zone (Table 3.4). Explanation of the Odds Ratio and Nagelkerke

pseudo R^2 value can be found in the Methods section. Additionally, Pettitt's test revealed a significant change in red tide frequency occurring around 1995 in the Nueces Estuary and the Coastal Zone (Table 3.5). For the coastal zone segment, there were no explanatory models that performed better than the year-only model and the analysis concluded there. The explanatory model for the Nueces Estuary included salinity, ENSO, and NAO (Table 3.6). ENSO and NAO were negatively related to red tide occurrence while salinity was positively related, indicating that higher salinity, negative ENSO phase, and negative NAO phase are more likely to correspond with red tide presence. The models presented above met all quality controls.

Trends in bloom duration

The year-only linear regression models (year vs. red tide duration) for the Nueces Estuary and Coastal Zone were not significant, indicating that there was no change in red tide duration over time. The duration of red tides in the Nueces Estuary ranged from 1 to 127 days, with an average of 42 days and a median of 25 days. For the Coastal Zone segment, the duration of red tides ranged from 1 to 71 days, with an average and median of 24 days. For the Nueces Estuary, an explanatory model including temperature indicated a significant negative relationship between red tide duration and temperature (Fig. 3.3). This model had an acceptable fit, was significantly different than the null model ($\alpha = 0.05$, $p = 0.03$), and had an R^2 of 0.34. For the Coastal Zone segment there were no explanatory models that passed quality control.

Environmental conditions associated with bloom stages

For the full dataset with all stages, the final logistic regression model included average daily temperature and average daily wind speed with year and month as random factors. The model was significantly different than the null model ($\alpha = 0.01$, $p = < 0.001$) and had a Nagelkerke's pseudo R^2 of 0.46 (Table 3.7). The explanatory model for the dataset that included

B and D stages had daily average temperature with year and month as random factors. The model was significantly different than the null model ($\alpha = 0.01$, $p = < 0.001$) and had a Nagelkerke's pseudo R^2 of 0.75. The explanatory model for the dataset with D and A stages included average daily wind speed with year and month as random factors. The model was significantly different than the null model ($\alpha = 0.01$, $p = < 0.001$) and had a Nagelkerke's pseudo R^2 of 0.64.

Discussion

HABs are influenced by human activity as well as natural climate oscillations and longer-term anthropogenic climate change (Brand et al. 2012; Davidson et al. 2014; Davidson et al. 2016). One of the challenges in understanding long-term trends in a HAB of interest is the availability of data documenting its occurrence and duration, and that of key environmental drivers (Anderson et al. 2002; Davidson et al. 2014). The field of marine historical ecology has provided strong evidence for the use of non-traditional data sources in the assessment of historical conditions and trends (Kittinger et al. 2014; Engelhard et al. 2016). Here, datasets of red tide presence/absence and duration were generated using archived newspaper articles from the *Corpus Christi Caller Times*. Quantitative comparisons with modern (1996-2016) agency-based cell counts, as well as a qualitative assessment of the early record (1955-1996), provided ample support for the use of this source. A bias evident in many long-term datasets, especially those from non-traditional sources, is increased reporting due to increased awareness rather than true increases in the occurrence of events, HAB or otherwise. Articles from the early record (1955-1996) that referenced red tides from other geographical areas, listed warning signs and potential impacts of red tides, provided follow-up reports when discolored water was something other than *K. brevis*, and continued coverage on damages sustained during a previous red tide,

are an indication of general awareness of red tides and interest in them by the news media. The advantages of using this non-traditional data source were two-fold: 1) it allowed for a quantitative assessment of trends in red tide occurrence from a data poor region (Texas coast, western Gulf of Mexico), and 2) it allowed us to identify climatological drivers (i.e. ENSO) as well as local environmental factors that are important for bloom initiation and demise in an estuarine setting, representing one of the first studies to do so.

The Nueces Estuary and adjacent Coastal Zone appear to have experienced a significant increase in the frequency of red tides between 1955 and 2016. In both locations, change point analysis indicated that the change from less to more frequent red tides occurred in approximately 1995. These findings agree with previous qualitative discussion of increases in red tide frequency in western Gulf of Mexico coastal waters (Tester et al. 2002; Magaña et al. 2003). The assessment of the newspaper record leads us to conclude that these observed increases are not attributable to increased reporting in the recent record due to increased awareness. Five of the eight red tides reported in the newspaper prior to 1996 were corroborated by scientific publications and 75% of the articles written during this time referenced interviews with scientists suggesting consistent awareness of red tides among two time periods. This study examined the factors driving observed increases in red tide frequency and used that information to develop testable hypotheses with a goal of refining monitoring and forecasting approaches for *Karenia brevis* red tides

In the Coastal Zone adjacent to the Nueces Estuary, explanatory modeling indicated that no combination of the environmental variables could explain red tide occurrence better than year alone. The finding that neither large-scale climate variability nor local conditions were important in explaining red tide occurrence aligns well with what is known about transport induced bloom

initiation. For example, Thyng et al. (2013) describe the importance of downcoast winds in determining whether cells are transported from offshore to the Texas coast, and suggest that interannual variability in wind speed/direction are important considerations in whether a bloom will develop or not in a given year.

Within the Nueces Estuary, salinity (positive), ENSO (negative), and NAO (negative) were important for explaining red tide occurrence, with a pseudo R^2 of 0.50. The positive relationship between red tide occurrences and salinity is consistent with prior laboratory work on the physiological tolerances of *K. brevis*, which showed maximum growth rates at salinities of ~30-35, and decreasing growth rates at lower salinities (Aldrich and Wilson 1960; Magaña and Villareal 2006). Additionally, analysis of long-term field data in Florida coastal waters indicated that only 3% of samples that were "positive" for *K. brevis* had salinity ≤ 24 (Dixon et al. 2014). Bugica et al. (2020) recently demonstrated significant increases in salinity in the Nueces Estuary and other Texas Coastal Bend estuaries over the past 20-30 years due to damming and increased human demands on water resources. This trend is likely to continue with projected population growth in Texas coastal counties (Texas State Data Center, http://txsdc.utsa.edu/Data/TPEPP/Projections/Index.aspx) and warmer and drier conditions expected in the western Gulf of Mexico under changing climate pressures (Pachauri et al. 2014; Nielsen-Gammon et al. 2020). Understanding how anthropogenic activities are affecting salinity regimes in these estuarine systems will be critical for assessing potential future frequency of red tides.

Positive ENSO phase is associated with increased rainfall on the Texas coast, as are lower salinities in estuaries (Tolan 2007). This relationship between ENSO, rainfall, and salinity on the Texas coast explains the negative relationship between ENSO and red tide occurrence in

the Nueces Estuary, with El Niño (positive ENSO) events leading to lower salinities that are not ideal for *K. brevis*. Aside from ENSO, the NAO was also related to red tides, exhibiting a negative relationship with red tide occurrence in the Nueces Estuary. A study by Parazoo et al. (2015) examined precipitation extremes and documented that periods of strongly negative NAO amplified drought conditions in Texas, which would lead to higher salinities in estuaries and conceivably be favorable to *K. brevis*. This is consistent with our findings of a negative relationship between NAO and red tide occurrence in the Nueces Estuary. In other words, the negative phase of the NAO (drought, high salinity) would equate to greater likelihood of red tide occurrence.

A final consideration for the relationship between climate variability and red tide occurrence is the global regime shift that occurred in the mid-1990s and involved the NAO, the Atlantic Meridional Overturning Circulation, the Subpolar Gyre, the Atlantic Multidecadal Oscillation, and the Pacific Decadal Oscillation (Chikamoto et al. 2012; Alheit et al. 2019). The change point analysis conducted here coincides with this global regime shift, suggesting that either the relationship between NAO and red tide is merely coincidental, or that there are as yet unknown teleconnections between Atlantic modes of climate variability and the western Gulf of Mexico. Further work to understand how and at what time scale(s) these modes of climate variability individually and collectively influence circulation, temperature, and precipitation in this region is warranted.

Tester et al. (2002) suggest that while circulation and transport are critical for bloom development along the Texas coast, conditions within estuaries (poorly flushed, high salinity) may maintain seed or remnant populations of *K. brevis* prolonging bloom conditions in estuaries. Therefore, understanding factors influencing bloom dynamics in the estuary will be critical in

assessing risk to coastal waters of the western Gulf of Mexico now and in the future. No significant change in the duration of red tides was detected in the Nueces Estuary though temperature was negatively correlated with the duration of red tides ($\alpha = 0.05$; $p = 0.058$). The relationship between temperature and red tide duration may be related to the physiological requirements of *K. brevis*, which has an optimum temperature range between 22°C and 28°C (Vargo 2009). Magaña and Villareal (2006) demonstrated highest *K. brevis* growth rates in cultures at salinities of 30 and 35 and temperatures of 20 and 25°C. They also found that their *K. brevis* cultures (native to S. Texas) could not be acclimated to temperatures greater than 30°C. Errera et al. (2014) also demonstrated significantly lower growth rates of *K. brevis* cultures at 30°C relative to 25°C. Despite the borderline significance seen here, our results offer further support for the role of temperature in the daily red tide presence/absence analyses.

To investigate climatic conditions that are associated with the time periods preceding and following a bloom relative to those during a bloom, daily red tide presence/absence was modeled using daily weather conditions. The results presented and conclusions drawn here should be considered a first step towards furthering understanding of factors that facilitate bloom demise in estuarine waters. Starting with the model for all three stages (before, during, and after), air temperature and wind speed were negatively related to red tide presence. In the before bloom/during bloom model, air temperature was also negatively related to red tide presence and the effect was much larger than in the "all stages" model. This indicates that high (i.e., summer-like) temperatures are detrimental to red tides, specifically to the timing of their initiation. This finding is also consistent with knowledge on the seasonality of red tides in Texas. Not only is regional circulation conducive to transport of *K. brevis* biomass from offshore to in- and nearshore during the fall in Texas (Hetland and Campbell 2007; Thyng et al. 2013; Henrichs et

al. 2015) but fall water temperature is typically well within the physiological optimum range of *K. brevis* (24°C – 28°C). For example, the average summer water temperature in the Nueces Estuary during the period of 1982-2015 (this study) was 29.3 ± 1.2 while the average fall water temperature was 25.8 ± 1.2. This lends further support to the hypothesis that cooler temperatures in fall are important in supporting red tide initiation and maintenance.

The only environmental variable of importance in the during bloom/after bloom model was wind speed, which was negatively related to red tide presence and accounted for greater than half (pseudo $R^2 = 0.64$) of the variation between red tide presence and absence. Abrupt decreases in temperature and high turbulence associated with the passage of cold fronts have been suggested to be important in bloom decline based on anecdotal accounts of bloom dissipation, experimental evidence of decreased growth at sub-optimal temperatures, and field observations of lysed cells and aerosolized brevetoxin due to crashing waves (Tester and Steidinger 1997; Magaña and Villareal 2006; Vargo 2009). Our finding agrees with the hypothesis that frontal passages and associated increased wind speeds and turbulence are likely critical in ending a red tide. However, they do not support a role for water temperature in bloom decline. The correlation with decreasing temperatures at the start of a bloom but lack of correlation with temperature at the end of blooms suggests that *K. brevis* may be better equipped to handle physiological stress from temperatures lower than optimum rather than higher. Culture and field studies have shown tolerance of *K. brevis* to temperatures much lower than optimum (~7°C vs. ~20°C/22°C) whereas the difference between highest temperature tolerated and the upper limit optimum (~32°C vs. ~ 23°C/28°C) is much smaller (Steidinger 2009). This supports our conclusion that *K. brevis* may handle low temperature stress more effectively than high temperature stress. When considered along with findings from laboratory-based studies on *K. brevis* temperature optima,

results presented here suggest that future increases in summer-fall temperatures associated with anthropogenic climate change have the potential to delay the initiation of red tides, while increases in winter temperatures may act to delay the demise. Assuming that other environmental conditions (i.e. light, wind, salinity) are adequate for survival and growth of red tides this could lead to scenarios where the window for red tides is shortened (if starting later in year), stays the same (if starting later but ending later), or lengthened (if starting later but extending much longer than normal).

Conclusion

Results show that red tides have been increasing in frequency on the Texas coast over the past 60 years, necessitating a better understanding of the environmental factors driving red tide occurrence. A recent assessment of water quality trends on the Texas coast only found clear signatures of eutrophication (high and/or increasing chlorophyll, nutrients) in two estuarine complexes (Baffin Bay-Upper Laguna Madre, Galveston Bay), although some evidence of eutrophication was found in smaller sub-estuaries and isolated regions of the larger estuaries (Bugica et al. 2020). In the Nueces Estuary, Bugica et al. (2020) found increasing orthophosphate concentrations at five of the nine sites in the system, but both ammonium and nitrate showed long-term decrease throughout the estuary, and three of nine study sites showed decreasing chlorophyll levels. The lack of evidence for eutrophication argues against the hypothesis that it is a leading cause of increases in the frequency of red tides in the Nueces Estuary.

In contrast to the general lack of evidence for widespread eutrophication in the Nueces Estuary, Bugica et al. (2020) found that salinity increased over time at all nine study sties in the system. The strong relationship between salinity and increasing frequency of red tides in the

Nueces Estuary highlights the need to better understand the role of large-scale hydrologic forcing (rainfall, river discharge) on habitat suitability for *K. brevis* in Texas estuaries and nearshore coastal waters. Although not reported here, we also found evidence of increases in red tide frequency in other central Texas coast estuaries where long-term increases in salinity were also observed (Tominack et al. unpubl. data) (Bugica et al. 2020). Long-term increases in salinity are linked to damming and growing human water demands in coastal watersheds over the past ~50 years (Nielsen-Gammon et al. 2020). Population and climate projections suggest that over the coming century, Texas will see additional increases in population and water demands, as well as a warmer and drier climate (Pachauri et al. 2014; Nielsen-Gammon et al. 2020). This will likely lead to further increases in salinity in Texas estuaries, leading to conditions that are more similar to seawater and thus more hospitable to *K. brevis* (Montagna et al. 2002). Though freshwater inflow management in Texas has changed from resource- to ecosystem-based following the introduction of Senate Bill 3 in 2007 (https://www.twdb.texas.gov/surfacewater/flows/freshwater/index.asp), implications of freshwater inflow management have not considered red tide habitat suitability to date.

An additional implication of this study's findings pertains to efforts aimed at forecasting red tide blooms. Early warning detection (days to weeks lead time) of red tide in the western Gulf of Mexico is already being done through automated cell imaging and counting (Campbell et al. 2013) as well as satellite remote sensing (Wynne et al. 2005; Tomlinson et al. 2009). The strong relationships between ENSO/NAO, salinity and red tide occurrence seen here offer an opportunity for even longer lead times considering that ENSO forecasts are often produced many months in advance (Barnston et al. 2019). Lastly, though it is recognized that many other factors (i.e. nutrient availability, grazing, viral lysis) may play a role in bloom demise (Paul et al. 2002;

Tester et al. 2002; Steidinger 2009; Walsh et al. 2011), our investigation offers valuable insight into factors limiting the duration of blooms. Future research in estuarine systems should consider the use of targeted monitoring programs, Lagrangian drifters, and/or modelling efforts to quantify the relative importance of environmental conditions (i.e. temperature, wind speed and direction) in determining conditions that may prolong active/remnant red tides or lead to their demise.

References

Aldrich, D. v, and W. B. Wilson. 1960. The effect of salinity on growth of Gymnodinium breve Davis. *The Biological Bulletin* 119: 57–64.

Alheit, J., J. Gröger, P. Licandro, I. H. McQuinn, T. Pohlmann, and A. C. Tsikliras. 2019. What happened in the mid-1990s? The coupled ocean-atmosphere processes behind climate-induced ecosystem changes in the Northeast Atlantic and the Mediterranean. *Deep-Sea Research Part II: Topical Studies in Oceanography* 159. Elsevier Ltd: 130–142. https://doi.org/10.1016/j.dsr2.2018.11.011.

Anderson, D. M. 1989. Toxic Alagal Blooms and Red Tides: A Global Perspective. In *Red Tides: Biology, Environmental Science, and Toxicology*, ed. Okaichi, D. M. Anderson, and Nemoto, 11–16. Elsevier Science Publishing Co., Inc.

Anderson, D. M., P. M. Glibert, and J. M. Burkholder. 2002. Harmful algal blooms and eutrophication: Nutrient Sources, Composition, and Consequences. *Estuaries* 25: 704–726.

Baden, D. G., and T. J. Mende. 1979. Amino acid utilization by Gymnodinium breve. *Phytochemistry* 18: 247–251. https://doi.org/10.1016/0031-9422(79)80063-1.

Barnston, A. G., M. K. Tippett, M. Ranganathan, and M. L. L'Heureux. 2019. Deterministic skill of ENSO predictions from the North American Multimodel Ensemble. *Climate Dynamics* 53. Springer Verlag: 7215–7234. https://doi.org/10.1007/s00382-017-3603-3.

Barton, K. 2020. MuMIn: Multi-Model Inference.

Bates, D., M. Mächler, B. Bolker, and S. Walker. 2015. Fitting Linear Mixed-Effects Models Using lme4. *Journal of Statistical Software* 67: 1–48. https://doi.org/10.18637/jss.v067.i01.

Brand, L. E., L. Campbell, and E. Bresnan. 2012. Karenia: The biology and ecology of a toxic genus. *Harmful Algae* 14. Elsevier B.V.: 156–178. https://doi.org/10.1016/j.hal.2011.10.020.

Brand, L. E., and A. Compton. 2007. Long-term increase in Karenia brevis abundance along the Southwest Florida Coast. *Harmful Algae* 6: 232–252. https://doi.org/10.1016/j.hal.2006.08.005.

Bricker, S. B., B. Longstaff, W. Dennison, A. Jones, K. Boicourt, C. Wicks, and J. Woerner. 2008. Effects of nutrient enrichment in the nation's estuaries: A decade of change. *Harmful Algae* 8: 21–32. https://doi.org/10.1016/j.hal.2008.08.028.

Bugica, K., B. Sterba-Boatwright, and M. S. Wetz. 2020. Water quality trends in Texas estuaries. *Marine Pollution Bulletin* 152. Elsevier Ltd. https://doi.org/10.1016/j.marpolbul.2020.110903.

Buskey, E. J. 1996. *Current Status and Historical Trends of Brown Tide and Red Tide Phytoplankton Blooms in the Corpus Christi Bay National Estuary Program Study Area Corpus Christi Bay National Estuary Program CCBNEP-07* •. Austin, Texas.

Campbell, L., D. W. Henrichs, R. J. Olson, and H. M. Sosik. 2013. Continuous automated imaging-in-flow cytometry for detection and early warning of Karenia brevis blooms in the Gulf of Mexico. *Environmental Science and Pollution Research* 20: 6896–6902. https://doi.org/10.1007/s11356-012-1437-4.

Cheng, Y. S., T. A. Villareal, Y. Zhou, J. Gao, R. H. Pierce, D. Wetzel, J. Naar, and D. G. Baden. 2005. Characterization of red tide aerosol on the Texas coast. *Harmful Algae* 4: 87–94. https://doi.org/10.1016/j.hal.2003.12.002.

Chikamoto, Y., M. Kimoto, M. Watanabe, M. Ishii, and T. Mochizuki. 2012. Relationship between the Pacific and Atlantic stepwise climate change during the 1990s. *Geophysical Research Letters* 39. Blackwell Publishing Ltd. https://doi.org/10.1029/2012GL053901.

Dardis, C. 2015. LogisticDx: Diagnostic Tests for Models with a Binomial Response.

Davidson, K., D. M. Anderson, M. Mateus, B. Reguera, J. Silke, M. Sourisseau, and J. Maguire. 2016. Forecasting the risk of harmful algal blooms. *Harmful Algae*. Elsevier B.V. https://doi.org/10.1016/j.hal.2015.11.005.

Davidson, K., R. J. Gowen, P. J. Harrison, L. E. Fleming, P. Hoagland, and G. Moschonas. 2014. Anthropogenic nutrients and harmful algae in coastal waters. *Journal of Environmental Management* 146. Academic Press: 206–216. https://doi.org/10.1016/j.jenvman.2014.07.002.

Dixon, L. K., G. J. Kirkpatrick, E. R. Hall, and A. Nissanka. 2014. Nitrogen, phosphorus and silica on the West Florida Shelf: Patterns and relationships with Karenia spp. occurrence. *Harmful Algae* 38. Elsevier: 8–19. https://doi.org/10.1016/j.hal.2014.07.001.

Engelhard, G. H., R. H. Thurstan, B. R. MacKenzie, H. K. Alleway, R. C. A. Bannister, M. Cardinale, M. W. Clarke, et al. 2016. ICES meets marine historical ecology: Placing the

history of fish and fisheries in current policy context. In *ICES Journal of Marine Science*, 73:1386–1403. Oxford University Press. https://doi.org/10.1093/icesjms/fsv219.

Errera, R. M., S. Yvon-Lewis, J. D. Kessler, and L. Campbell. 2014. Reponses of the dinoflagellate Karenia brevis to climate change: PCO2 and sea surface temperatures. *Harmful Algae* 37. Elsevier: 110–116. https://doi.org/10.1016/j.hal.2014.05.012.

Flaherty, K. E., and J. H. Landsberg. 2011. Effects of a Persistent Red Tide (Karenia brevis) Bloom on Community Structure and Species-Specific Relative Abundance of Nekton in a Gulf of Mexico Estuary. *Estuaries and Coasts* 34. Springer: 417–439. https://doi.org/10.1007/s12237-010-9350-x.

Harris, R. J., D. A. Arrington, D. Porter, and V. Lovko. 2020. Documenting the duration and chlorophyll pigments of an allochthonous Karenia brevis bloom in the Loxahatchee River Estuary (LRE), Florida. *Harmful Algae* 97. Elsevier B.V.: 101851. https://doi.org/10.1016/j.hal.2020.101851.

Hart, J. A., E. J. Phlips, S. Badylak, N. Dix, K. Petrinec, A. L. Mathews, W. Green, and A. Srifa. 2015. Phytoplankton biomass and composition in a well-flushed, sub-tropical estuary: The contrasting effects of hydrology, nutrient loads and allochthonous influences. *Marine Environmental Research* 112. Elsevier Ltd: 9–20. https://doi.org/10.1016/j.marenvres.2015.08.010.

Heil, C. A., L. K. Dixon, E. Hall, M. Garrett, J. M. Lenes, J. M. O'Neil, B. M. Walsh, et al. 2014. Blooms of Karenia brevis (Davis) G. Hansen & Ø. Moestrup on the West Florida Shelf: Nutrient sources and potential management strategies based on a multi-year regional study. *Harmful Algae* 38. Elsevier: 127–140. https://doi.org/10.1016/j.hal.2014.07.016.

Henrichs, D. W., R. D. Hetland, and L. Campbell. 2015. Identifying bloom origins of the toxic dinoflagellate Karenia brevis in the western Gulf of Mexico using a spatially explicit individual-based model. *Ecological Modelling* 313. Elsevier: 251–258. https://doi.org/10.1016/j.ecolmodel.2015.06.038.

Hetland, R. D., and L. Campbell. 2007. Convergent blooms of Karenia brevis along the Texas coast. *Geophysical Research Letters* 34: 1–5. https://doi.org/10.1029/2007GL030474.

Jackman, S. 2020. pscl: Classes and Methods for R Developed in the Political Science Computational Laboratory. Sydney, New South Wales, Australia.

Kirkpatrick, B., L. E. Fleming, D. Squicciarini, L. C. Backer, R. Clark, W. Abraham, J. Benson, et al. 2004. Literature review of Florida red tide: Implications for human health effects. *Harmful Algae*. Elsevier. https://doi.org/10.1016/j.hal.2003.08.005.

Kittinger, J. N., L. McClenachan, K. B. Gedan, and L. K. Blight, ed. 2014. *Marine Historical Ecology in Conservation: Applying the Past to Manage the Future*. University of California Press.

Landsberg, J. H., and K. A. Steidinger. 1988. A historical review of Gymnodinium breve red tides implicated in mass mortalities of the manatee (Trichechus manatus latirostris) in Florida, UAS. In *Harmful Algae*, 97–100. Xunta de Galicia and Intergovernmental Oceaographic Commission of UNESCO.

Magaña, H. A., C. Contreras, and T. A. Villareal. 2003. A historical assessment of Karenia brevis in the western Gulf of Mexico. *Harmful Algae* 2: 163–171. https://doi.org/10.1016/S1568-9883(03)00026-X.

Magaña, H. A., and T. A. Villareal. 2006. The effect of environmental factors on the growth rate of Karenia brevis (Davis) G. Hansen and Moestrup. *Harmful Algae* 5: 192–198. https://doi.org/10.1016/j.hal.2005.07.003.

McHugh, K. A., J. B. Allen, A. A. Barleycorn, and R. S. Wells. 2011. Severe Karenia brevis red tides influence juvenile bottlenose dolphin (Tursiops truncatus) behavior in Sarasota Bay, Florida. *Marine Mammal Science* 27. John Wiley & Sons, Ltd: 622–643. https://doi.org/10.1111/j.1748-7692.2010.00428.x.

Nielsen-Gammon, J., J. Banner, B. Cook, D. Tremaine, C. Wong, R. Mace, H. Gao, et al. 2020. Unprecedented drought challenges for Texas water resources in a changing climate: what do researchers and stakeholders need to know? *Earth's Future* 8. John Wiley & Sons, Ltd. https://doi.org/10.1029/2020EF001552.

Parazoo, N. C., E. Barnes, J. Worden, A. B. Harper, K. B. Bowman, C. Frankenberg, S. Wolf, M. Litvak, and T. F. Keenan. 2015. Global Biogeochemical Cycles in the Texas-northern Mexico region. *Global Biogeochemical Cycles* 29: 1–19. https://doi.org/10.1002/2015GB005125.Received.

Pachauri, R. K., Allen, M. R., Barros, V. R., Broome, J., Cramer, W., Christ, R., Church, J. A., Clarke, L., Dahe, Q., Dasgupta, P., Dubash, N. K., Edenhofer, O., Elgizouli, I., Field, C. B., Forster, P., Friedlingstein, P., Fuglestvedt, J., Gomez-Echeverri, L., Hallegatte, S., … van Ypserle, J.-P. (2014). *Climate Change 2014: Synthesis Report. Contribution of Working Groups I, II and III to the Fifth Assessment Report of the Intergovernmental Panel on Climate Change* (R. K. Pachauri & L. Meyer, Eds.). IPCC.

Paul, J. H., L. Houchin, D. Griffin, T. Slifko, M. Guo, B. Richardson, and K. Steidinger. 2002. A filterable lytic agent obtained from a red tide bloom that caused lysis of Karenia brevis

(Gymnodinum breve) cultures. *Aquatic Microbial Ecology* 27: 21–27. https://doi.org/10.3354/ame027021.

Pennock, J. R., R. Greene, W. Fisher, T. Villareal, J. Simons, Q. Dortch, C. Moncrieff, et al. 2004. HABSOS: An Integrated Case Study for the Gulf of Mexico: Final Report. *Dauphin Island Sea Lab. Dauphin Island, Alabama*.

Pettitt, A. N. 1979. A Non-Parametric Approach to the Change-Point Problem Published by : Wiley for the Royal Statistical Society A Non-parametric Approach to the Change-point Problem. *Journal of the Royal Statistical Society. Series C (Applied Statistics)* 28: 126–135.

Pohlert, T. 2020. trend: Non-Parametric Trend Tests and Change-Point Detection.

Rounsefell, G. A., and W. R. Nelson. 1967. *Red-Tide Research Summarized to 1964 Including an Annotated Bibliography*. Washington, D.C.

Schrope, M. 2008. Oceanography: Red tide rising. *Nature* 452. American Association for the Advancement of Science (AAAS): 24–26. https://doi.org/10.1038/452024a.

Smith, T. J., and C. M. McKenna. 2013. A Comparison of Logistic Regression pseudo R2 indices. *Multiple Linear Regression Viewpoints* 39: 17–26.

Steidinger, K. A. 2009. Historical perspective on Karenia brevis red tide research in the Gulf of Mexico. *Harmful Algae* 8: 549–561. https://doi.org/10.1016/j.hal.2008.11.009.

Steidinger, K. A., and R. M. Ingle. 1972. Observations on the 1971 summer red tide in Tampa Bay, Florida. *Environmental Letters* 3: 271–278.

Stumpf, R. P., R. W. Litaker, L. Lanerolle, and P. A. Tester. 2008. Hydrodynamic accumulation of Karenia off the west coast of Florida. *Continental Shelf Research* 28: 189–213. https://doi.org/10.1016/j.csr.2007.04.017.

Tester, P. A., and K. A. Steidinger. 1997. Gymnodinium breve red tide blooms: Initiation, transport, and consequences of surface circulation. *Limnology and Oceanography* 42. Wiley-Blackwell: 1039–1051. https://doi.org/10.4319/lo.1997.42.5_part_2.1039.

Tester, P. A., K. Wiles, S. M. Varnam, G. V. Ortega, A. M. Dubois, and V. A. Fuentes. 2002. Harmful algal blooms in the western Gulf of Mexico: Karenia brevis is messin'with Texas and Mexico. *Harmful Algae*: 41–43.

Thyng, K. M., R. D. Hetland, M. T. Ogle, X. Zhang, F. Chen, and L. Campbell. 2013. Origins of Karenia brevis harmful algal blooms along the Texas coast . *Limnology and Oceanography: Fluids and Environments* 3. Wiley-Blackwell: 269–278. https://doi.org/10.1215/21573689-2417719.

Tolan, J. M. 2007. El Niño-Southern Oscillation impacts translated to the watershed scale: Estuarine salinity patterns along the Texas Gulf Coast, 1982 to 2004. *Estuarine, Coastal and Shelf Science* 72: 247–260. https://doi.org/10.1016/j.ecss.2006.10.018.

Tomlinson, M. C., T. T. Wynne, and R. P. Stumpf. 2009. An evaluation of remote sensing techniques for enhanced detection of the toxic dinoflagellate, Karenia brevis. *Remote Sensing of Environment* 113: 598–609. https://doi.org/10.1016/j.rse.2008.11.003.

Trebatoski, B. 1988. Observations on the 1986-1987 Texas Red Tide (Ptychodiscus brevis). *Texas Water Comission*. Austin, Texas: Texas Water Commission.

US DOC; NOAA; NESDIS; National Oceanographic Data Center; National Coastal Data Development Center; 2014 [cited 2018 Feb 5]. Database: Physical and biological data collected along the Texas, Mississippi, and Florida Gulf coasts in the Gulf of Mexico as part of the Harmful Algal BloomS Observing System from 19 Aug 1953 to 11 July 2014 (NODC Accession 0120767). Version 1.1. National Oceanographic Data Center, NOAA.

Dataset. Available from: https://data.nodc.noaa.gov/cgi-bin/iso?id=gov.noaa.nodc:0120767.

Vargo, G. A. 2009. A brief summary of the physiology and ecology of Karenia brevis Davis (G. Hansen and Moestrup comb. nov.) red tides on the West Florida Shelf and of hypotheses posed for their initiation, growth, maintenance, and termination. *Harmful Algae* 8: 573–584. https://doi.org/10.1016/j.hal.2008.11.002.

Walker, D. A., and T. J. Smith. 2016. JMASM algorithms and code nine pseudo R2 indices for binary logistic regression models. *Journal of Modern Applied Statistical Methods* 15. Wayne State University Library System: 848–854. https://doi.org/10.22237/jmasm/1462077720.

Walters, S., S. Lowerre-Barbieri, J. Bickford, J. Tustison, and J. H. Landsberg. 2013. Effects of Karenia brevis red tide on the spatial distribution of spawning aggregations of sand seatrout Cynoscion arenarius in Tampa Bay, Florida. *Marine Ecology Progress Series* 479: 191–202. https://doi.org/10.3354/meps10219.

Weisberg, R. H., Y. Liu, C. Lembke, C. Hu, K. Hubbard, and M. Garrett. 2019. The Coastal Ocean Circulation Influence on the 2018 West Florida Shelf K. brevis Red Tide Bloom. *Journal of Geophysical Research: Oceans* 124: 2501–2512. https://doi.org/10.1029/2018JC014887.

Weisberg, R. H., L. Zheng, Y. Liu, A. A. Corcoran, C. Lembke, C. Hu, J. M. Lenes, and J. J. Walsh. 2016. Karenia brevis blooms on the West Florida Shelf: A comparative study of the robust 2012 bloom and the nearly null 2013 event. *Continental Shelf Research* 120. Elsevier: 106–121. https://doi.org/10.1016/j.csr.2016.03.011.

Wynne, T. T., R. P. Stumpf, M. C. Tomlinson, V. Ransibrahmanakul, and T. A. Villareal. 2005. Detecting Karenia brevis blooms and algal resuspension in the western Gulf of Mexico with satellite ocean color imagery. *Harmful Algae* 4: 992–1003. https://doi.org/10.1016/j.hal.2005.02.004.

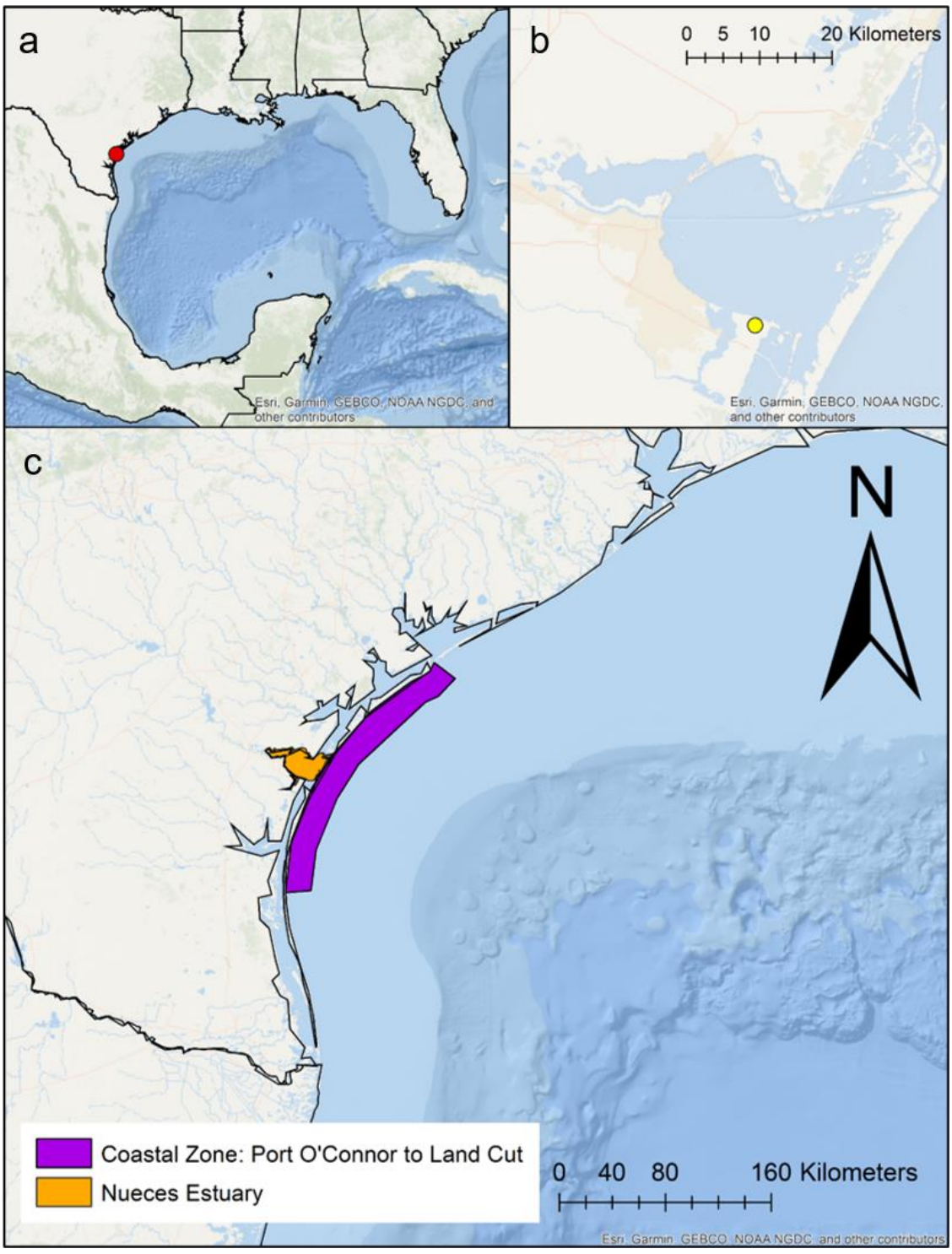

Fig. 3.1 Map of study areas on Texas Gulf of Mexico coastline. (A) location of Nueces Estuary in the Gulf of Mexico (red circle), (B) zoomed in view of the Nueces Estuary and the location of Naval Air Station Corpus Christi (yellow circle), and (C) location of the Nueces Estuary relative to the adjacent coastal zone. The coastal zone segment (purple) extends from the Land Cut in the south to Port O'Connor in the north.

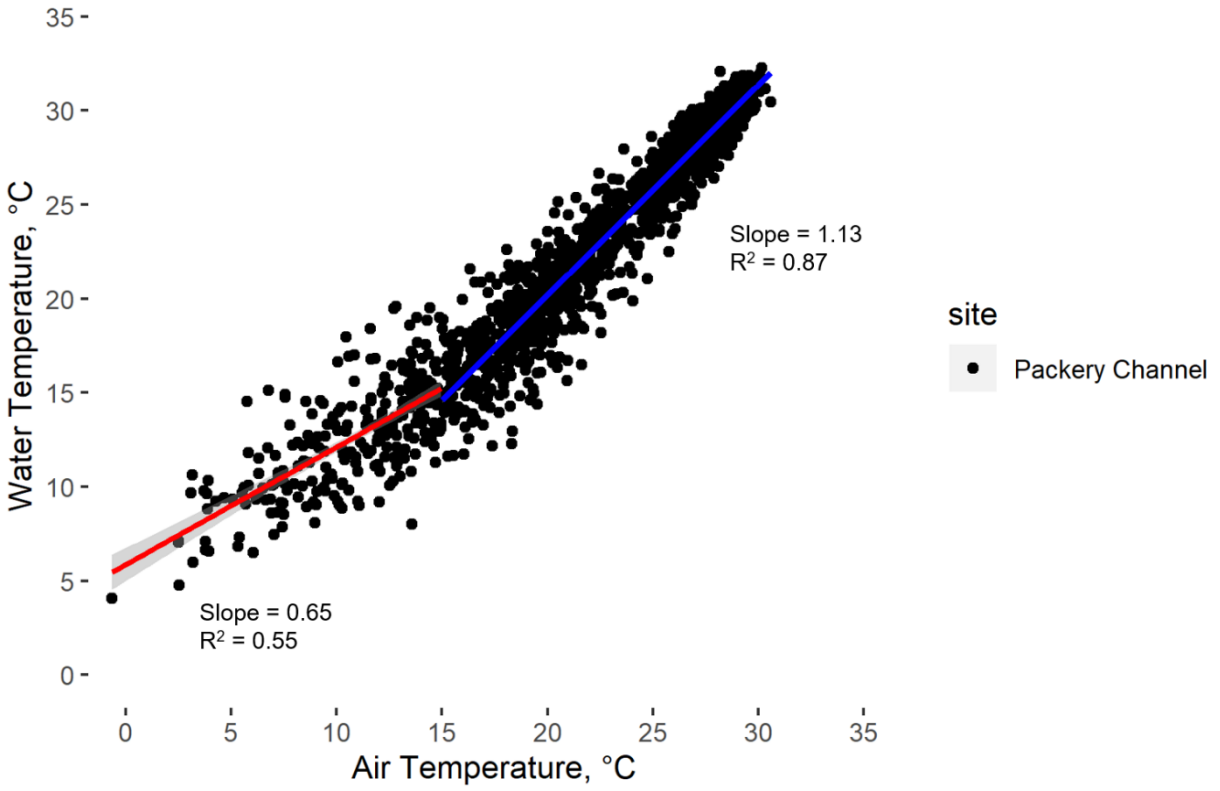

Fig. 3.2 Comparison of air and water temperature (°C) at Packery Channel in the Nueces Estuary. Data were obtained from https://tidesandcurrents.noaa.gov, station number 8775792, for the time period of August 2012 thru October 2018.

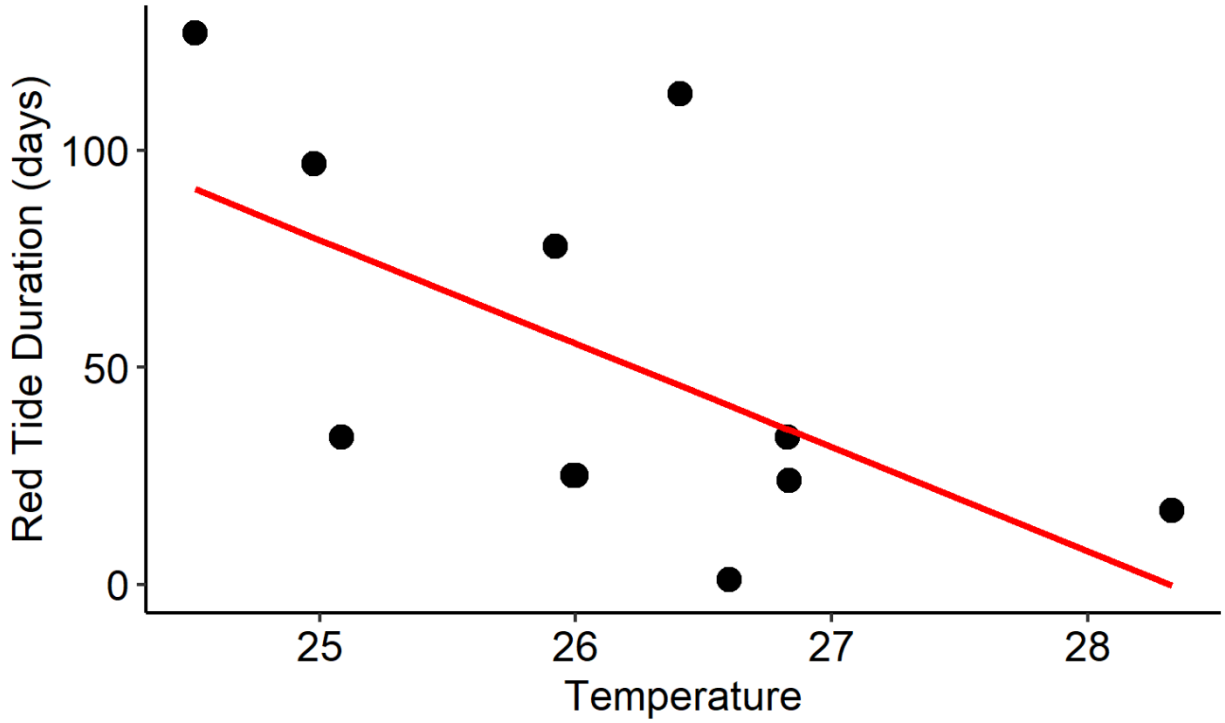

Fig. 3.3 Red tide duration in the Nueces Estuary plotted against average Fall temperatures (°C). Fall temperatures were calculated as the average of all temperatures recorded in the Texas Parks and Wildlife trawl dataset in the Nueces Estuary from August through November of each year (1982-2015). The red line represents the linear regression model fit.

Table 3.1 Fall seasonal average water temperature (°C) ± standard deviation, salinity ± standard deviation, and number of observations for Texas Parks and Wildlife trawl dataset. Seasonal averages are comprised of values from August thru November of each year.

Year	Nueces Estuary			Coastal Zone Port O'Connor to Land Cut		
	Temperature (°C)	Salinity	No. Observations	Temperature (°C)	Salinity	No. Observations
1982	25.61 ± 4.86	33.46 ± 2.27	116			
1983	26.2 ± 3.31	28.73 ± 2.39	114			
1984	24.53 ± 4.44	34.69 ± 4	114			
1985	26.59 ± 3.61	32.95 ± 4.23	80	26.64 ± 2.62	31.96 ± 2.55	64
1986	24.98 ± 6.2	35.95 ± 6.36	80	25.67 ± 2.97	32.82 ± 3.71	64
1987	24.72 ± 4.47	32.59 ± 4.2	80	25.18 ± 2.95	36.71 ± 2.11	64
1988	26.6 ± 3.62	36.67 ± 2.16	80	26.45 ± 3	33.93 ± 2.72	64
1989	25.82 ± 3.31	36.44 ± 5.03	80	25.88 ± 3.38	30.62 ± 3.91	64
1990	26.04 ± 4.01	33.93 ± 5.87	80	26.9 ± 2.8	33.73 ± 1.67	64
1991	25.06 ± 5.83	33.6 ± 3.92	80	25.26 ± 4	34.15 ± 3.32	64
1992	23.79 ± 3.97	30.24 ± 2.95	104	25.7 ± 3.1	33.98 ± 4.45	64
1993	25.16 ± 4.85	33.49 ± 3.41	104	24.95 ± 3.93	35.32 ± 3.91	64
1994	26.42 ± 2.65	33.91 ± 3.46	104	26.28 ± 2.76	32.01 ± 3.42	64
1995	26.31 ± 4.64	33.24 ± 3.12	104	26.12 ± 4.17	31.58 ± 1.61	56
1996	25.98 ± 3.35	38.06 ± 3.12	80	25.75 ± 3.02	34.39 ± 3.13	64
1997	24.51 ± 5.57	30.19 ± 5.4	80	24.73 ± 4.52	32.82 ± 2.92	64
1998	26.37 ± 3.58	31.46 ± 8.59	80	26.11 ± 3.12	32.62 ± 4.03	64
1999	26.33 ± 3.57	31.71 ± 2.91	80	26.64 ± 2.76	33.93 ± 2	64
2000	25.08 ± 5.43	37.31 ± 3.04	80	24.17 ± 3.25	33.87 ± 1.85	64

Table 3.1 cont'd

Year	Nueces Estuary			Coastal Zone Port O'Connor to Land Cut		
	Temperature (°C)	Salinity	No. Observations	Temperature (°C)	Salinity	No. Observations
2001	26.82 ± 3.3	33.9 ± 5.24	80	26.45 ± 2.69	33.39 ± 3.28	64
2002	26.16 ± 4.12	19.02 ± 7.72	80	26.35 ± 3.15	30.65 ± 3.97	64
2003	26.89 ± 3.53	27 ± 7.69	80	26.65 ± 1.83	32.6 ± 3.66	64
2004	26.72 ± 3.77	27.68 ± 3.66	80	27.85 ± 2.76	32.97 ± 2.5	64
2005	26.83 ± 4.51	34.21 ± 2.36	80	27.43 ± 3.53	32.18 ± 2.2	64
2006	26 ± 3.5	35.45 ± 2.91	80	26.98 ± 2.47	34.48 ± 1.5	64
2007	25.62 ± 5.51	20.38 ± 4.93	80	27.62 ± 2.82	30.27 ± 2.57	64
2008	25.85 ± 3.45	33.4 ± 1.89	80	25.16 ± 2.34	32.18 ± 2.88	64
2009	25.92 ± 4.08	35.45 ± 2.83	80	26.19 ± 2.74	31.58 ± 2.63	64
2010	26.14 ± 4.68	27.9 ± 4.63	80	27.23 ± 2.52	31.99 ± 2.37	64
2011	26.4 ± 3.32	39.51 ± 2.1	80	26.93 ± 2.57	35.16 ± 1.94	64
2012	26.6 ± 4.37	39.58 ± 2.49	60	26.16 ± 3.22	34.08 ± 3.02	48
2013	21.26 ± 1.87	33.6 ± 1.96	20	21.61 ± 0.46	30.3 ± 1.92	16
2014	25.86 ± 5.49	38.84 ± 2.31	80	26.14 ± 3.71	35.05 ± 1.86	64
2015	28.32 ± 1.75	31.77 ± 3.57	60	27.87 ± 1.85	31.83 ± 3.32	48

Table 3.2 Comparison of red tide duration (days) from newspaper reports with cell counts data from the Texas Health Department (TXHD) and NOAA Harmful Algal Bloom Observation Study (HABSOS) (NOAA National Centers for Environmental Information 2014). A 2000 red tide in the Coastal Zone during the same period as in the newspaper accounts was confirmed by Magaña et al. (2003) and Cheng et al. (2005).

Nueces Estuary					
Year	Newspaper	5,000 cells L^{-1}	10,000 cells L^{-1}	100,000 cells L^{-1}	Scientific Record
1996	25	43	43	15	TXHD
1997	127	40	40	40	TXHD
1998					
1999					
2000	34	25	25	25	TXHD
2001	34	109	101	101	TXHD
2002					
2003					
2004					
2005	24	77	60	60	TXHD
2006	25	65; 37	65; 37	17; 17	TXHD; HABSOS
2007					
2008					
2009	78	153; 84	147; 78	85; 64	TXHD; HABSOS
2010					
2011	113	87	87	87	HABSOS
2012	1				
2013					
2014					
2015	17	69	69	42	TXHD
2016	33	1	1	1	TXHD
Mean ± Standard Deviation	46.46 ± 40.94	65.83 ± 40.75	62.75 ± 38.43	46.17 ± 32.90	

Table 3.2 cont'd

Coastal Zone from Port O'Connor to Land Cut					
Year	Newspaper	5,000 cells L-1	10,000 cells L^{-1}	100,000 cells L^{-1}	Scientific Record
1996	37	2	2	2	TXHD
1997	20	20	20		TXHD
1998					
1999					
2000	31				Magaña et al. [1]; Cheng et al. [47]
2001					
2002					
2003					
2004					
2005	1	8	2		HABSOS
2006	17	20	20	10	HABSOS
2007					
2008					
2009	71	1; 78	78		TXHD; HABSOS
2010					
2011	49	93	88	62	HABSOS
2012	1				
2013		20	20	1	HABSOS
2014					
2015	27	27	27	1	TXHD
2016	36	1	1	1	TXHD
Mean ± Standard Deviation	29.00 ± 21.29	24.55 ± 31.79	25.80 ± 31.82	12.50 ± 24.53	

Table 3.3. Summary of *Corpus Christi Caller Times* articles. References for published work that corroborates occurrence of red tides prior to 1996 appear in the 'Notes' column along with any unique features of the reporting.

Year	No. Articles	Region Affected	Start- Nueces	End- Nueces	Start- Coastal Zone	End- Coastal Zone	Notes
1955	1	Texas coast near Mexico border	NA	NA	NA	NA	Wilson and Ray (Anderson et al. 2002; Davidson et al. 2014)
1957	1	Tampico, Mexico	NA	NA	NA	NA	Discusses current diatom bloom in Coastal Bend and work by US Fish and Wildlife Service
1963	2	West Florida	NA	NA	NA	NA	Discusses current scientific knowledge of red tides and previous occurrences in Texas
1970	3	Nueces Estuary	7/6/1970	7/10/1970	NA	NA	
1972	2	Coastal Bend	NA	NA	10/25/1972	NA	Description of red tide in New England; Texas Parks and Wildlife in Magaña et al. (Kittinger et al. 2014; Engelhard et al. 2016)
1973	4	Coastal Bend	5/4/1973	5/4/1973	5/4/1973	5/4/1973	
1974	4	Mexico	NA	NA	NA	NA	Describes wind as potential factor for red tide to move north and work in Florida to predict red tides; Texas Parks and Wildlife in Magaña et al. (Tester et al. 2002; Magaña et al. 2003)
1975	5	Nueces Estuary	8/6/1975	8/9/1975	NA	NA	Latter three articles describe other red tide on Upper Texas Coast not attributed to *K. brevis*

Table 3.3 cont'd.

Year	No. Articles	Region Affected	Start- Nueces	End- Nueces	Start- Coastal Zone	End- Coastal Zone	Notes
1980	2	Nueces and Lavaca-Colorado Estuaries	NA	NA	NA	NA	Describes discolored water and fish kills attributed to a chemical spill and an organism other than *K. brevis*, respectively
1986	71	Texas coast	10/8/1986	1/12/1987	9/7/1986	10/25/1986	Trebatoski (2013)
1987	13	NA	NA	NA	NA	NA	Describes the effects of the red tide from the previous year and potential disaster relief funding
1988	2	Puget Sound, Washington, USA	NA	NA	NA	NA	Describes red tides in general, the last time one was seen in Texas, and a red tide occurring in Puget Sound
1990	4	Mission Aransas Estuary	NA	NA	NA	NA	Buskey et al. (Aldrich and Wilson 1960; Magaña and Villareal 2006)
1991	1	Lower Laguna Madre	NA	NA	NA	NA	Describes possible red tide; controls and a small persistent patch in a ship channel; Buskey et al. (Dixon et al. 2014)
1996	21	Texas coast south of Galveston to Mexico border	9/28/1996	10/22/1996	9/12/1996	10/18/1996	
1997	11	Texas coast south of Galveston to Mexico border	9/25/1997	1/29/1998	9/18/1997	10/8/1997	

Table 3.3 cont'd.

Year	No. Articles	Region Affected	Start- Nueces	End- Nueces	Start- Coastal Zone	End- Coastal Zone	Notes
1998	2	NA	NA	NA	NA	NA	Description of a red tide conference and potential effects of red tide on National Seashore visitor attendance
2000	12	Texas coast south of Galveston to Mexico border	9/21/2000	10/24/2000	9/24/2000	10/24/2000	
2001	2	Nueces Estuary	12/20/2001	1/22/2002	NA	NA	
2002	1	NA	NA	NA	NA	NA	History of Corpus Christi that includes red tide of 1996
2005	8	Texas Coastal Bend and south	10/4/2005	12/19/2005	9/16/2005	9/16/2005	
2006	8	Texas Coastal Bend and south	10/2/2006	12/5/2006	10/3/2006	10/19/2006	
2009	15	Texas Coastal Bend and south	10/15/2009	12/31/2009	10/10/2009	12/19/2009	
2010	1	NA	NA	NA	NA	NA	Single article describing a *Dinophysis* bloom
2011	11	Texas Coast	10/7/2011	1/27/2012	10/7/2011	11/24/2011	
2012	4	Texas Coast	9/26/2012	9/26/2012	9/26/2012	9/26/2012	

Table 3.3 cont'd

Year	No. Articles	Region Affected	Start- Nueces	End- Nueces	Start- Coastal Zone	End- Coastal Zone	Notes
2015	7	Texas Coast	10/2/2015	10/18/2015	9/6/2015	10/2/2015	Mentions co-occurring *Trichodesmium* bloom and how it may relate to red tide
2016	3	Texas Coastal Bend and south	9/10/2016	10/12/2016	9/7/2016	10/12/2016	Two articles earlier in the year mention previous red tides in another context

Table 3.4 Summary information for the logistic regression of red tide occurrence vs year (year-only model) for each region.

Geographic Area	Estimate	Estimate Standard Error	95% Confidence Intervals	p-value	Odds Ratio	Nagelkerke Pseudo-R^2
Nueces Estuary	0.06	0.02	0.02, 0.10	0.003	1.06	0.24
Coastal Zone from Port O'Connor to Land Cut	0.07	0.02	0.02, 0.12	0.002	1.08	0.29

Table 3.5 Results of change point analysis (Pettitt's Test), where $p \leq 0.5$ is significant.

Geographic Area	Time Point	K_T Statistic	p-value
Nueces Estuary	41 (1995)	387	0.049
Coastal Zone from Port O'Connor to Land Cut	41 (1995)	347	0.101

Table 3.6 Results from final logistic regression model explaining red tide occurrence chosen for the Nueces Estuary.

Geographic Area	Explanatory Variables	Estimates	Estimate Standard Error	95% Confidence Interval	Odds Ratio	Nagelkerke Pseudo-R^2
Nueces Estuary	ENSO	-1.52	0.91	-3.56, -0.11	0.22	0.50
	NAO	-3.54	1.58	-7.28, -0.83	0.03	
	salinity	0.54	0.24	0.17, 1.14	1.72	

Table 3.7 Summary information for the final three logistic regression models chosen to explain daily presence/absence of *K. brevis* red tides in Nueces Estuary.

Dataset	Explanatory Variables	Estimates	Estimate Standard Error	95% Confidence Interval	Odds Ratio	Nagelkerke Pseudo-R^2
All Stages; B, D, A[a]	Temperature	-0.12	0.03	-0.19, -0.06	0.88	0.46
	Wind Speed	-0.12	0.07	-0.25, 0.01	0.89	
Stages B and D	Temperature	-0.52	0.09	-0.74, -0.34	0.59	0.75
Stages D and A	Wind Speed	-0.30	0.11	-0.53, -0.09	0.74	0.64

[a] Stage B indicates the period of 14 days before a red tide, D indicates the period of red tide presence, and A indicates the period of 14 days after a red tide.

CONCLUDING SUMMARY

Estuaries provide innumerable services to local ecosystems and economies. Over the past half century, however, they have become increasingly impacted by anthropogenic activities (i.e., urbanization, agriculturalization, increased demand for wastewater treatment, damming of rivers), often resulting in decreased freshwater inflows, increased nutrient loading, and changes in nutrient composition. These altered hydrologic and nutrient dynamics have been implicated in declining water quality and eutrophication across many estuarine systems. Corpus Christi Bay, Texas is a shallow, low inflow estuary that has experienced rapid population growth and urbanization. In contrast to other estuarine systems that are experiencing rapid urbanization, there is no evidence of widespread symptoms of eutrophication in Corpus Christi Bay. Low inflow conditions and a relatively small area of developed land compared to regions with larger river systems and more sprawling urban environments (i.e., Chesapeake Bay, Neuse River Estuary watersheds) may help explain this apparent contradiction. Regardless of the mechanism, projections of further population growth and a warmer, drier climate in the region, necessitates a comprehensive understanding of nutrient-phytoplankton dynamics in this system. This dissertation constitutes the first in depth study of phytoplankton dynamics in the system and provides critical information to resource managers. The main goals of this work were to 1) quantify phytoplankton biovolume, community composition, and environmental drivers across an estuarine-nutrient gradient, 2) quantify phytoplankton response to pulsed nutrient inputs, and 3) quantify trends in the occurrence of *K. brevis* red tides and environmental drivers.

A 27-month field study revealed that phytoplankton biovolume correlated with nutrients, precipitation, salinity, and temperature. During spring and summer months, phytoplankton biovolume was controlled primarily by the availability of nutrients, as evidenced by inverse

relationships with nutrients and increased biovolume following precipitation-driven nutrient inputs. Fall and winter phytoplankton biovolume, however, was primarily controlled by hydraulic flushing, temperature, and the availability of light. Spatially, phytoplankton biovolume was also predominantly constrained by the availability of nutrients, though proximity to point sources of freshwater inflows was negatively related to phytoplankton biovolume, perhaps due to flushing effects. A combination of nutrient and physical conditions also structured phytoplankton community composition. Diatoms were dominant in the winter and spring when nutrients were elevated and temperatures were cooler, whereas dinoflagellates were dominant when nutrients were lower and temperatures were warmer. Picocyanobacteria and picoeukaryotes were important in spring and summer, with the former also playing an important role during the fall. The prevalence of dinoflagellates and both picophytoplankton groups were also higher in sites where nutrient concentrations were elevated and water circulation was restricted. Given future projections for a warmer, drier climate and increased urbanization, and the increased prevalence of dinoflagellates and picophytoplankton under warmer, low flow conditions, it is possible that these groups will become more dominant in the future. Diatom dominated communities are known to support short, efficient food webs, whereas communities dominated by picocyanobacteria are known to favor carbon cycling through the microbial loop and longer less efficient food webs. Therefore, a shift in community composition has the potential to impact ecosystem function and productivity.

This study also addressed the role of nutrient limitation in driving phytoplankton dynamics experimentally. Seasonal nutrient addition bioassays revealed that nitrogen was the most frequently limiting nutrient. During the winter, phytoplankton growth was not nutrient limited. These findings highlight the potential for season-dependent increased phytoplankton

biovolume and symptoms of eutrophication as anthropogenic activities continue to alter land use patterns and nutrient inputs and the climate continues to warm. Results from the investigation of growth rate responses of different major taxonomic groups also highlight the need to further explore the difference between pulsed and chronic nutrient inputs. Diatom growth rates were consistently stimulated by pulsed nutrient inputs, whereas the responses of picocyanobacteria, picoeukaryotes, and dinoflagellates were more variable. Assessment of the role chronic sources of nutrients, such as wastewater treatment plant effluent and internal cycling of nutrients in benthic environments that may be enhanced under warmer conditions, is necessary to fully describe nutrient-phytoplankton dynamics in Corpus Christi Bay.

Due to the near annual occurrence of *K. brevis* red tides in Corpus Christi Bay, this study quantified trends in the frequency of occurrence, duration, and environmental drivers of red tides. Findings revealed that there has been a significant increase in the occurrence of red tides in the Nueces Estuary since the mid-1990s, though no change in the duration of red tides was detected. Results indicated that blooms of *K. brevis* were favored under high salinity conditions compared to low salinity conditions, non-El Niño conditions, and during the negate phase of the North Atlantic Oscillation. Non-El Niño conditions are associated with decreased precipitation and increased salinity on the south Texas Coast, with the negative phase of the North Atlantic Oscillation amplifying drought conditions. These findings highlight the importance of considering large-scale decadal and multidecadal climatological patterns in driving local scale in the study of harmful algal bloom dynamics. Increasing duration of red tides was associated with cooler temperatures, in line with known temperature tolerance ranges of *K. brevis*. Additionally, modeling efforts at the daily level of resolution supported the role of fall-like temperatures in supporting the initiation of red tides in the Nueces Estuary and increasing wind speeds in

eliciting the demise of a red tide. Taken together these results indicate that under future climate scenarios for a warmer and drier climate red tide phenology has the potential to shift to later in the year or for blooms to become longer (i.e., lasting later into winter). Given the use of water management strategies on the Texas coast it is imperative to conduct further studies on active red tides to better understand the role of freshwater inflows in supporting red tides in the Nueces Estuary and along the Texas coast as a whole.

Overall, results from this dissertation improve our understanding of phytoplankton dynamics in an urbanizing, low-inflow estuary. Results here indicate that under future conditions there is potential for increased phytoplankton biomass, increased occurrence of sporadic high biomass blooms, and increased prevalence of less desirable taxa (i.e., dinoflagellates, picophytoplankton), with the potential to disrupt the food web and biogeochemical cycling within the system. Increased occurrence of high biomass blooms has the potential to exacerbate the annual hypoxic zone in the southwest of Corpus Christi Bay by increasing microbial degradation of labile phytoplankton detritus and oxygen drawdown. Additionally, fish kills caused by increasing occurrences of *K. brevis* red tides have the potential to diminish recreation and tourism industries as well as disrupt local fisheries and increase symptoms of eutrophication by negatively impacting benthic communities. This research lays the groundwork for more targeted studies aimed at addressing these and other questions in the Corpus Christi Bay system, as well as in other systems that are expected to become drier and warmer in the future.

APPENDIX 1

CHAPTER I SUPPLEMENTAL DATA

The following table provides a summary of the shapes assigned to each genus observed during a 27-month field study in Corpus Christi Bay. Where a genus or group of unknowns (i.e., unknown dinoflagellates) was comprised of taxa with different shapes, that genus or group of unknowns is listed for all of the shapes used. For chain-forming organisms, each individual cell was counted and measured for abundance and biovolume calculations. The shape and formula designations were based on Sun and Liu (2003). For the formulas below, a.dim represents the cross-section when it is the only dimension in a formula, a.dim represents length of a cell when there are other dimensions in the formula, and b.dim represents the width of a cell. Other dimensions were specific to shape and are described in the Notes and Formula Adjustments column.

Table S1.1 Shapes and formulas used to estimate cell specific biovolume at the Genus level. For unknown organisms regardless of major taxonomic group, shape was estimated based on sketches. For further analyses, unknowns within each major taxonomic group were grouped together following abundance and biovolume calculations.

Shape	Genera	Formula	Notes and Formula Adjustments
Cone	Small flagellate, Pyramimonas-like, Unknown Dinoflagellate	$Pi/12 * a.dim * b.dim^2$	No adjustments necessary
Cone with a halfsphere	Chatonella, Chroomonas, Small flagellate, Prorocentrum micans, Scripsiella	$Pi/4 * a.dim * b.dim^2$	No adjustments necessary

Table S1.1 cont'd.

Shape	Genera	Formula	Notes and Formula Adjustments
Cone with a halfsphere and a cylinder	Euglenoids	$Pi/3 * (a.dim_1 + a.dim_2) * b.dim_1^2 + pi/4 * (a.dim_2 + b.dim_2) * b_2^2 + pi/12 * a.dim_2 * b.dim_1 * b.dim_2$	This is euglenoids, which I noted were not as tapered as one might think. I assumed the following: $b.dim_1 = 0.8*b.dim$; $a.dim_1 = 0.8*a.dim$; $a.dim_2 = 0.1*a.dim$ Updated formula= $Pi/3*(0.8*a.dim + 0.1*a.dim)*(0.8*b.dim)^2 + pi/4 * (0.1*a.dim + b.dim) * b.dim^2 + pi/12*0.1*a.dim*0.8*b.dim*b.dim)$
Cylinder	Auliscus, Unknown Centric Diatom, Coscinodiscus, Cyclotella, Paralia, Thalassiosira	$Pi/4 * a.dim^2 * c.dim$	Average c.dim for all cylinder taxa was ~0.5*a.dim, but I made some taxa specific adjustments based on where I had c.dim measurements. Coscinodiscus was always 20 when measured; Paralia was always 15 when measured; Thalassiosira I could always measure; Auliscus c.dim == 0.5*a.dim
Cylinder girdle view	Bacteriastrum, Unknown Diatom, Guinardia, Oscillatoria-like, Rhizosolenia, Leptocylindrus	$Pi/4 * b.dim^2 * a.dim$	No adjustments necessary
Cylinder with 2 halfspheres	Corethron, Skeletonema	$Pi * b.dim^2 * ((a.dim/4)-(b.dim/12))$	No adjustments necessary

Table S1.1 cont'd.

Shape	Genera	Formula	Notes and Formula Adjustments
Cylinder with a cone	Asterionella, Unknown Dinoflagellate, Katodinium	Cylinder volume from above + cone volume from above	For Asterionella, assumed that the height of the cone was the same as the width (b.dim measured). b.dim for the spine (cylinder calc) was always 2 and the height of the spine was a.dim (total height measured) – b.dim. No other assumptions for Asterionella. Updated formula = $Pi/4 * 2^2 *$ (a.dim – b.dim) + $pi/12 * b.dim * b.dim^2$ For Katodinium and an unknown dinoflagellate I assumed that the height of the cone was half of the width (measured as b.dim) and that the cylinder = total length (measured as a.dim) – 0.5*b.dim Updated formula = $Pi/4*(a.dim-(0.5*b.dim))*b.dim^2) + pi/12*(0.5*b.dim)*b.dim^2$
Cymbelloid	Cymbella	$2/3 * a.dim * c.dim^2 *$ arcsin(b.dim/2c.dim)	Needed to assume c.dim → assumed c.dim = 0.5*b.dim Updated formula = $2/3 * a.dim * (0.5*b.dim)^2 *$ arcsin(b.dim/b.dim)
Double cone	Unknown Dinoflagellate, Gonyaulax, Gyrodinium, Hermesium, Heterocapsa, Oxyphysis, Protoperidinium, Unknown Silicoflagellate	$Pi/12 * a.dim * b.dim^2$	No adjustments necessary
Double sphere	Unknown Dinoflagellate	2 * sphere from below	No adjustments necessary

Table S1.1 cont'd.

Shape	Genera	Formula	Notes and Formula Adjustments
Ellipsoid with 2 cones and a cylinder	Ceratium	$Pi/4 * a.dim_2 * b.dim_2^2 + pi/12 *(a.dim_3 + a.dim_4) * b.dim_2^2 + pi/6 * a.dim_1 * b.dim_1 * b.dim_2$	Assuming that the ratios between the one set of b and c measurements that I took and the total length and width hold true: # a.dim == total length and bottom spines are ~= to the "body" then the top spine (d.dim) == 0.5*a.dim and c.dim and e.dim == 0.25*a.dim # to determine the width of the top spine, assume that the total width (measured as b.dim here) is == width of bottom spines + width of top spine. # following the assumption for cone calculations, width of bottom spines == 0.5*e.dim so f.dim==b.dim - e.dim Updated formula = $Pi/4*(0.5*a.dim)*(b.dim-(0.25*a.dim))^2 + p12*(0.25*a.dim + 0.25*a.dim)*(b.dim-(0.25*a.dim))^2 + p6 *(0.25*a.dim)*b.dim*(b.dim-(0.25*a.dim))$
Elliptic prism	Caloneis, Unknown Cryptophyte, Cymatosira, Unknown Diatom, Naviculoid, Pleurosigma, Surirella, Unknown Organism, Amphiprora, Amphora, Diploneis, Chaetoceros, Eucampia, Fragilaria-like, Odontella	Pi/4 * a.dim * b.dim * c.dim	Needed to assume c.dim → based on Emily's calculations c.dim = 0.2*a.dim Updated formula = Pi/4 * a.dim * b.dim * (0.2*a.dim)

Table S1.1 cont'd.

Shape	Genera	Formula	Notes and Formula Adjustments
Gomphonemoid	Licmorpha	(a.dim * b.dim)/4 * [a.dim + (pi/4 -1) * b.dim] * arcsin(c.dim/2a.dim)	Needed to estimate c.dim → I assumed that c.dim = b.dim Updated formula = (a.dim * b.dim)/4 * [a.dim + (pi/4 -1) * b.dim] * arcsin(b.dim/2a.dim)
Parallelogram prism	Unknown Diatom	½ * a.dim * b.dim * c.dim	Needed to estimate c.dim → only one unknown diatom here. Very general assumption that c.dim = 0.25*b.dim Updated formula = ½ * a.dim * b.dim * 0.25*b.dim
Prism triangle	Ditylum	Sqrt(3)/4 * c.dim * $a.dim^2$	No adjustments necessary
Prolate spheroid	Small Flagellate, Fibrocapsa, Oxyrrhis, Unknown Raphidophyte, Scenedesmus-like, Cochlodinium	Pi/6 * $b.dim^2$ * a.dim	No adjustments necessary
Rectangular box	Bacillaria, Unknown Diatom, Nitzschia, Psuedonitzschia, Striatella, Tabelaria-like, Thalassionema, Thalassiothrix	a.dim * b.dim *c.dim	Needed to assume c.dim → made c.dim = 0.5*b.dim Updated formula = a.dim * b.dim * (0.5*b.dim)

Table S1.1 cont'd.

Shape	Genera	Formula	Notes and Formula Adjustments
Prolate spheroid with 2 cylinders	Ceratium fusus, Cylindrotheca	Prolate spheroid from above + 2 * cylinder girdle view from above	This was taxa specific with C. fusus and C. Closterium the only taxa in this shape class. For cylindrotheca I measured the dimensions of the spheroid portion a couple of times and estimate that the a.dim for calculating the prolate spheroid (c.dim) is 0.25*(a.dim*b.dim) as they were measured. The length (d.dim) for each cylinder should then be (a.dim-c.dim)/2, and the b.dim for each cylinder (e.dim) should be 1. # For C. fusus the width of prolate spheroid portion and total length were measured. Following previous assumptions about cylindrotheca, (the prolate spheroid a.dim) c.dim == a.dim*0.2 and the width of the cylinders, e.dim == b.dim*0.2. The length of each cylinder is equal to total length (a.dim-c.dim)/2
Sphere	Chroococcus, Picocyanobacteria, Picoeukaryotes	Pi/6 * a.dim	No adjustments necessary
Triple sphere	Small flagellate	3 * sphere from above	No adjustments necessary